Universidade de Aveiro
Ano 2020
Departamento de Ciências Médicas

JOANA SOFIA LOPES FERREIRA

CARACTERIZAÇÃO DOS NÍVEIS DE PROTEÍNA E TRANSCRIÇÃO DE COMPONENTES DA SINAPSE EM MURGANHOS MUTANTES DE AMISINA

CHARACTERIZATION OF PROTEIN AND TRANSCRIPT LEVELS IN AMISYN MUTANT MICE

Universidade de Aveiro
Ano 2020

Departamento de Ciências Médicas

JOANA SOFIA LOPES FERREIRA

CARACTERIZAÇÃO DOS NÍVEIS DE PROTEÍNA E TRANSCRIÇÃO DE COMPONENTES DA SINAPSE EM MURGANHOS MUTANTES DE AMISINA

CHARACTERIZATION OF PROTEIN AND TRANSCRIPT LEVELS IN AMISYN MUTANT MICE

Dissertação apresentada à Universidade de Aveiro para cumprimento dos requisitos necessários à obtenção do grau de Mestre em Biomedicina Molecular, realizada sob a orientação científica da Doutora Ira Milosevic, Professora Auxiliar Convidada do Departamento de Ciências Médicas da Universidade de Aveiro.

Thesis submitted to University of Aveiro to fulfil the requirements to obtain the Master's degree in Molecular Biomedicine held under the scientific guidance of Dr. Ira Milosevic, Invited Assistant Professor at the Department of Medical Sciences of the University of Aveiro.

This work was supported by Schram-Stiftung T287/25457 and Deutsche Forschungsgemeinschaft (Emmy Noether Young Investigator Award MI-1702/1) to Ira Milosevic.

This work was supported by an Erasmus+ grant provided in the context of the mobility Eramus+ program.

Dedico este trabalho aos meus pais que sempre me apoiaram e me deram força ao longo desta grande jornada.

o júri

Presidente	Professor Doutor Ramiro Daniel Carvalho de Almeida professor auxiliar do Departamento de Ciências Médicas da Universidade de Aveiro
Arguente	Doutor Paulo Pinheiro assistente da Universidade de Coimbra
Orientador	Doutora Ira Milosevic professora auxiliar convidada do Departamento de Ciências Médica da Universidade de Aveiro

acknowledgments

I would like to thank to Dr. Ira Milosevic and Dr. Nuno Raimundo for the great opportunity provided and for all the knowledge they helped me gain during this journey.

To the Synaptic Vesicle Dynamics group (Dirk, Sindhu, Uhdaya, Jialin) and to the Mitochondrial Signaling group (Kasia, King) members for all the patience when teaching new techniques.

To Jialin Jin for all the help, guidance, teachings and patience.

To Joana Pires, Joana Moreira and Mariana Moreira for all the friendship and support even in the most difficult days.

To my parents and brother for all the support, even from far away.

palavras-chave

Amisina, exocitose, vesícula sináptica, regulação negativa.

resumo

A amisina é uma proteína SNARE de 24 kDa especifica de vertebrados, cujas interações com proteínas exocíticas chave sintaxina1A, sintaxina4, SNAP25 e fosfolípido $PI(4,5)P_2$ são conhecidas. Baseado em publicações recentes em células neuroendócrinas e na elevada expressão de amisina no tecido cerebral, formulámos a hipótese de que esta proteína tem um papel na regulação negativa da exocitose de vesiculas sinápticas. Mutações na amisina (nome do gene: STXBP6) foram reportadas no contexto de algumas doenças, como TEA (transtorno do espetro autista), cancro e diabetes, o que enfatiza a importância da realização de mais estudos.

Nesta dissertação, várias abordagens experimentais foram realizadas, como expressão de proteína recombinante, ensaio de co-sedimentação de lipossomas, Western Blot e análise de PCR quantitativo, para avançar a caracterização da proteína amisina e das suas possíveis funções.

O ensaio de co-sedimentação de lipossomas revelou que a amisina requere o fosfolípido $PI(4,5)P_2$ para se ligar a membranas através do seu domínio PH. Mutações no domínio PH da amisina aboliram a interação desta proteína com a membrana. Para além disso, observámos que os murganhos knock-out (KO) de amisina são viáveis, e realizámos uma análise sistemática dos níveis de proteína e de transcrição de várias proteínas relacionadas com o processo de neurotransmissão. Esta análise revelou que a falta de amisina leva a um decréscimo dos níveis das proteínas VAMP2 e PSD95 e a um aumento dos níveis das proteínas Rab3A e α-sinucleína. Também foi descoberto que os níveis de transcrição relativos à EndoA1, PSD95, RhoA e CAMKIV diminuíram e que os níveis de transcrição de Rab7 aumentaram quando a amisina não estava presente. Estudos adicionais são necessários para compreender completamente as funções desta pequena proteína SNARE.

keywords Amisyn, exocytosis, synaptic vesicle, negative regulation.

abstract

Amisyn is a 24 kDa protein vertebrate-specific SNARE protein known to interact with key exocytic proteins syntaxin1A, syntaxin4, SNAP25 and phospholipid $PI(4,5)P_2$. Based on the recently published work in neuroendocrine cells and amisyn's high expression in brain tissue, we hypothesize that this protein has a role in the negative regulation of synaptic vesicle exocytosis. Mutations in amisyn (gene name: STXBP6) have been reported in the context of several diseases like ASD (autism spectrum disorders), cancer and diabetes, which emphasized the importance of further studies.

In this thesis, various experimental approaches were performed such as recombinant protein expression, liposome co-sedimentation assay, Western Blot, and quantitative PCR analyses, to advance the characterization of the amisyn protein and its possible functions.

Liposome co-sedimentation assay revealed that amisyn requires phospholipid $PI(4,5)P_2$ to bind to the membranes through its PH domain. Mutations in the amisyn's PH domain abolished protein's interactions with the membrane. Further, we observed that amisyn knock-out (KO) mice are viable, and we preformed systematic analysis of protein and transcript levels of various proteins related to the process of neurotransmission. This analysis revealed that the lack of amisyn leads to a decrease in VAMP2 and PSD95 protein levels and to an increase in Rab3A and α-synuclein protein levels. It was also found that the transcript levels of EndoA1, PSD95, RhoA and CAMKIV decreased and the transcript levels of Rab7 increased when amisyn was not present. Further studies are needed to fully comprehend the functions of this small SNARE protein.

Table of contents

I. Abbreviation list

ASD	Autism spectrum disorders
ATP	Adenosine triphosphate
CDK5	Cyclin-dependent kinase 5
CGN	*cis*-Golgi network
ER	Endoplasmic reticulum
IPTG	Isopropyl β-D-1-thiogalactopyranoside
KO	Knock-out
LTP	Long-term potentiation
NSF	N-ethylmaleimide sensitive fusion protein
ON	Overnight
PH	Pleckstrin homology
PI(4,5)P_2	Phosphatidylinositol 4,5-biphosphate
qPCR	Quantitative Real-time polymerase chain reaction
ResP	Resting pool
RRP	Readily releasable pool
SNAP25	Synaptosomal-associated protein of 25 kDa
SNARE	Soluble NSF attachment receptor
STX	Syntaxin
STXBP5	Tomosyn gene
STXBP6	Amisyn gene
SYT1	Synaptotagmin1
TGN	*trans*-Golgi network
TRP	Total recycling pool
WT	Wild-type
α-SNAP	N-ethylmaleimide-sensitive factor attachment protein alpha

II. Figure list

III. Table list

1. Introduction

1.1. Human nervous system

The nervous system can be subdivided into central nervous system (CNS), composed by the nerve tissue present in the brain and spinal cord, and peripheral nervous system (PNS), composed by all the nerve tissue outside the two aforementioned regions (National Institutes of Health (US) & Biological Sciences Curriculum Study, 2007). The PNS can be subdivided into afferent (sensory) system and efferent (motor) system, being the latter classified into somatic nervous system (skeletal muscles) and autonomic nervous system (smooth muscles and glands) (Tortora & Derrickson, 2017). The autonomic nervous system also has subdivisions, which are the parasympathetic nervous system, sympathetic nervous system, and enteric nervous system (Tortora & Derrickson, 2017). The sensory system detects an internal or external stimulus and conducts this signal to the CNS where it will be integrated (Tortora & Derrickson, 2017). After integration, the motor system can be recruited to conduct the signal to the effectors (muscles and glands) to perform an adequate response (Tortora & Derrickson, 2017).

The human brain is composed of four main parts: the brain stem, the cerebellum, the diencephalon and the cerebral hemispheres (Ludwig & Varacallo, 2020). The brain stem contains the medulla oblongata, responsible for breathing control and blood pressure maintenance, the pons, that contribute to posture and balance preservation, and the midbrain, involved mostly in eye movement (Ludwig & Varacallo, 2020). The cerebellum performs multiple functions such as planning, execution and coordination of movement, posture maintenance, and crucial participation in cognitive and sensory-motor processes (Ludwig & Varacallo, 2020). The thalamus, hypothalamus, pineal gland and part of the pituitary gland are the main constituents of the diencephalon, being the first structure responsible for processing motor and sensory impulses (Ackerman, 1992). In contrast, the hypothalamus controls autonomic stimuli (e.g., involuntary movement of the heart) and the release of hormones through interaction with the pineal and pituitary glands (Ackerman, 1992). The two aforementioned glands have different functions, the first one is responsible for producing melatonin, while the last one produces several hormones, many of which regulate other glands (Ackerman, 1992). The principal structures present within the cerebral hemispheres are cerebral cortex (grey matter), white matter, ventricular system, basal ganglia and limbic system (Ackerman, 1992). The main cerebral cortex functions are conscious movement of the body and receiving and consciously understanding sensory information (Ackerman, 1992). The white matter, a region with highly myelinated neurons, is known by its ability of critical impulse conduction between different areas of the CNS (Sorond & Gorelick, 2019) and the ventricular system, that is filled with cerebrospinal fluid (CSF), is thought to transport nutrients to the brain and protect it from trauma (Lowery & Sive, 2009). Basal ganglia receive information from almost all the cortical areas being a part of the movement regulation mechanism (Ludwig & Varacallo, 2020). The limbic system has many functional regions, two of which are the hippocampus, mainly responsible for memory formation, and the amygdala, involved in processing emotional information (Ludwig & Varacallo, 2020).

1.2. Comparison between human and mouse brain

Although mammals have brains with a typical structural organization, and similar neural structures and neural circuits within and between them (e.g., hippocampus and amygdala), there

are some differences between the mouse and human brains (Cryan & Holmes, 2005). The human brain has a cerebral cortex with much more prominent folds and much bigger in mass when compared to the mouse model (**Figure 1**), which can be responsible for the human capacity of processing complex psychological information (Cryan & Holmes, 2005). Another cortical difference lies in gene expression between homologous cell types, being the serotonin receptors family one of the most divergent (Hodge et al., 2019).

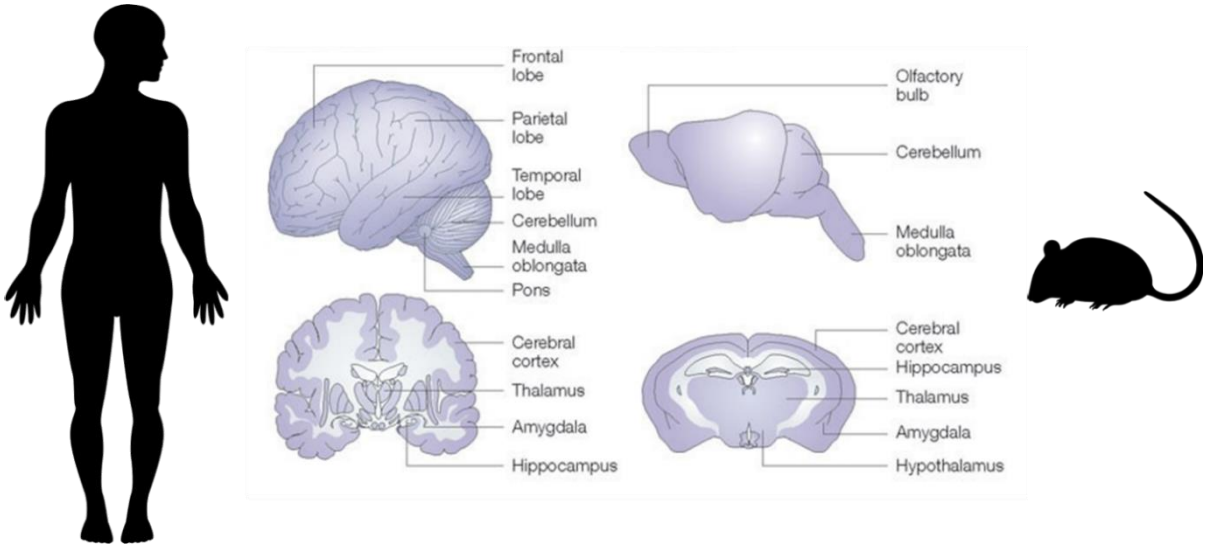

Figure 1- Comparison between the human and mouse brain. It is adapted from: (Cryan & Holmes, 2005).

1.3. Two main types of brain cells: Neurons and Neuroglia

Two types of cells compose the nervous tissue, neuroglia, and neurons (Tortora & Derrickson, 2017). The neuroglia compresses six different types of cells, being four present in the CNS and two in the PNS (Tortora & Derrickson, 2017). In the CNS, there are astrocytes, oligodendrocytes, microglia, and ependymal cells (Tortora & Derrickson, 2017). Astrocytes subdivide into two categories, protoplasmic astrocytes, present in gray matter, and fibrous astrocytes, present in white matter (Tortora & Derrickson, 2017). Astrocytes in general play a neuron support role while maintaining an appropriate chemical environment, that allows the transmission of nervous impulses, and preserving the blood-brain barrier (Tortora & Derrickson, 2017). Oligodendrocytes are involved in the formation and maintenance of the myelin sheaths present in the CNS neuronal axons, where one of these cells can myelinate several axons (Tortora & Derrickson, 2017). Microglia has functions similar to phagocytes, removing cellular debris, and phagocytizing damaged tissue and microbes (Tortora & Derrickson, 2017). The ependymal cells are present in the brain ventricles and the spinal cord, with the function of producing, protecting, and assisting the circulation of the CSF (Tortora & Derrickson, 2017). In the PNS, the Schwann cells have the role of myelination, where one of these cells forms sheaths around a single axon, and axon regeneration (Tortora & Derrickson, 2017). Satellite cells are mainly needed for structural support and substance exchange regulation between the interstitial fluid and the cell body (Tortora & Derrickson, 2017).

In the human body, three different types of neurons are present according to their structure (Tortora & Derrickson, 2017). Multipolar neurons have multiple dendrites and one axon, being the

most common in the CNS and efferent system (Tortora & Derrickson, 2017). The bipolar neurons have one main dendrite and one axon, existing only in the retina, inner ear, and olfactory area (Tortora & Derrickson, 2017). The pseudo-unipolar neurons have one process that branches into the peripheral process, which terminates with dendrites, and the central process, which ends with axon termini, being the primary function of this latter neuron type to receive sensory information (Tortora & Derrickson, 2017). The neurons can also be classified regarding their role in sensory neurons, interneurons and motor neurons (Tortora & Derrickson, 2017). The sensory neurons can contain sensory receptors in their dendrites or be next to a specialized receptor cell and convey an action potential, initiated after a sensory stimulus, to the CNS (Tortora & Derrickson, 2017). The interneurons are mostly contained in the CNS between sensory and motor neurons, and their function is to integrate sensory information and transmit the adequate signal to the motor neurons, which convey the action potential to the effectors (Tortora & Derrickson, 2017).

Although neurons have different morphologies and functions, these cells have four regions in common, which are the following: cell body, dendrites, axon, and axon terminals (Lodish et al., 2000b). The cell body is where the nucleus is located and where most of the proteins and membranes required for the renewal of cell structures are synthesized and assembled into multiprotein particles and membranous vesicles, respectively (Lodish et al., 2000b). To lead the produced molecules to the axon or axon termini, sites where there is no such production, it is necessary to resort to anterograde transport, which uses the axon microtubules until the molecules are incorporated in the plasma membrane or other organelles (Lodish et al., 2000b). The opposite process is called retrograde transport and is responsible for moving damaged structures or organelles resorting to axon microtubules from the axon or axon termini to the cell body, only location where there are lysosomes (organelles with a degradative function) (Lodish et al., 2000b). The dendrites can also produce some proteins, although their main function is receiving signals from the axon termini of other neurons and transmitting an electrical impulse in the direction of the cell body (Lodish et al., 2000b). The axon is in communication with the cell body through the axon hillock, which is followed by the initial segment (Tortora & Derrickson, 2017). In the majority of neurons, when nerve impulses reach the trigger zone, a region between the axon hillock and the initial segment, the decision of firing or not an action potential takes place (Tortora & Derrickson, 2017). If this impulse is strong enough, the formation of an action potential takes place (Lodish et al., 2000b). That signal will be conducted through the axon in the direction of the axon terminus until the synapse is reached (Lodish et al., 2000b). The active zone of a presynaptic terminal is a specific region that does the interface between the plasma membrane and synaptic cleft where the exocytosis of most synaptic vesicles occurs (Südhof, 2012).

Some neurons are covered by myelin sheaths, which are coverings composed of lipids and proteins that provide insulation to the axon (Tortora & Derrickson, 2017). These coverings are the processes that arise from an oligodendrocyte or a Schwann cell, depending on where the neuron is located (CNS or PNS, respectively) (Tortora & Derrickson, 2017). In the PNS, there is a cytoplasmic layer that contains the cell nucleus denominated neurolemma, which is thought to take part in the regeneration of the sheaths and their gaps (Tortora & Derrickson, 2017). The gaps between each myelin sheath are called nodes of Ranvier, which are regions of the axon membrane rich in voltage-gated channels, an important characteristic for the action potential propagation and maintenance (Tortora & Derrickson, 2017).

All the neurons have ion channels present in their membrane however, the type of channels may vary between neurons and locations within a neuron (Tortora & Derrickson, 2017). Leak channels are present in all neurons (dendrites, cell bodies, and axons), being opened and closed in a random way (Tortora & Derrickson, 2017). The ligand-gated channels respond to the binding of a specific ligand, appearing only in the dendrites and cell body (Tortora & Derrickson, 2017). Voltage-gated channels are essential for action potential generation and conduction through the axons, responding to changes in the membrane potential (Tortora & Derrickson, 2017). There are also channels that open or close in response to mechanical stimuli (e.g., vibration, pressure) called mechanically gated channels that are present for example in auditory or pressure receptors (Tortora & Derrickson, 2017).

1.4. Neurons are excitable cells

When a neuron is at rest, i.e., not sending any signal, the extracellular concentration of the sodium ion (Na^+) and the chloride ion (Cl^-) are higher than in the cytosol with the opposite being verified in regards to the potassium ion (K^+) concentrations (Tortora & Derrickson, 2017). In a neuron, more leak K^+ channels are found in the plasma membrane in comparison to leak Na^+ channels and the negative charges in the cytosol are attached to large molecules (ATP and proteins), which prevents their diffusion to the extracellular fluid (ECF) (Tortora & Derrickson, 2017). The Na^+/K^+-ATPase removes more positive charges from the cytosol than it imports (three Na^+ leave and two K^+ enter), with leads to a negative resting membrane potential, that is around -70 millivolts (mV) (Tortora & Derrickson, 2017).

A variable increase (depolarization) or decrease (hyperpolarization) of the resting membrane potential is called a graded potential (Tortora & Derrickson, 2017). These potentials are events that occur when mechanically gated or ligand-gated channels are opened or closed in response to a stimulus (Tortora & Derrickson, 2017). There are various types of graded potentials; there are postsynaptic potentials if the neuron ligand-gated channels respond to neurotransmitters, however if they occur in sensory receptors, they are denominated receptor potentials (Tortora & Derrickson, 2017). These potentials usually happen in neuronal dendrites and cell body, since these are the typical locations of the previously mentioned channels (Tortora & Derrickson, 2017). The amplitude of these electric signals is dependent on stimulus strength, which influences the quantity and for how long the channels remain opened or closed (Tortora & Derrickson, 2017). These structural changes in the ion channels cause a brief and localized current flow that spreads for the nearby regions and decays over time and distance (decremental conduction) because the leak channels allow a loss of charges through the membrane (Tortora & Derrickson, 2017). When graded potentials are added (summation), they can complement or cancel each other (Tortora & Derrickson, 2017). In the case of two depolarizing graded potentials or two hyperpolarizing graded potentials, the resulting signal would be a stronger depolarizing or hyperpolarizing graded signal, respectively (Tortora & Derrickson, 2017). But if the two graded potentials where the same amplitude but opposite, they would cancel each other having no effect on the membrane potential (Tortora & Derrickson, 2017). This summation process can allow the formation of stronger signals with better chances of arriving at the trigger zone, increasing or decreasing the probability of reaching the threshold potential, which would enable the neuron to fire an action potential (Tortora & Derrickson, 2017). The threshold is a membrane potential value that varies between neurons but usually remains equal in the same neuron, being in many cases -55 mV (Tortora & Derrickson, 2017).

When the membrane potential is depolarized to threshold in the trigger zone, the activation gate, present in voltage-gated Na^+ channels, opens allowing the influx of these ions (Tortora & Derrickson, 2017). The entry of Na^+ increases the membrane potential (depolarization) until the overshoot is reached (about +30 mV) and activates other nearby Na^+ channels (Tortora & Derrickson, 2017). After this, the inactivation gate in Na^+ channels closes and the voltage-gated K^+ channels open, allowing the efflux of K^+, which initiates the repolarizing phase (until -70 mV) (Tortora & Derrickson, 2017). Since the K^+ channels have a slower close ability, there is the possibility that the resting membrane potential may be overpast (hyperpolarization), a situation that is resolved as the channels close and the Na^+/K^+-ATPase functions (Tortora & Derrickson, 2017). It is important to note that action potentials are all-or-none events, in which a subthreshold stimulus (depolarization below the threshold) will not generate any action potential, whereas a threshold stimulus (depolarization just until the threshold) will (Tortora & Derrickson, 2017). A supra-threshold stimulus (depolarization over the threshold) will cause action potentials with the same amplitude but with higher frequency in comparison to a threshold stimulus (Tortora & Derrickson, 2017).

After an action potential, there is an interval of time, when it is not possible to occur another action potential because the voltage-gated Na^+ channels are either already activated or inactivated until the resting membrane potential is reached (Tortora & Derrickson, 2017). This time frame is called an absolute refractory period (Tortora & Derrickson, 2017). There is also a relative refractory period, a period when the voltage-gated Na^+ channels are returning to their resting state (activation gate closed and inactivation gate open), and the voltage-gated K^+ channels are still open (Tortora & Derrickson, 2017). In this time frame, there is the possibility to generate a new action potential but the stimulus will have to be larger than the one that fired the previous action potential for it to happen (Tortora & Derrickson, 2017).

The action potential conduction is dependent on positive feedback, where the influx of sodium ions through voltage-gated Na^+ channels leads to the opening of other voltage-gated Na^+ channels in nearby regions (Tortora & Derrickson, 2017). Because of this propagation mechanism where the action potential is regenerated along the axon, there is no loss of signal strength (Tortora & Derrickson, 2017). Action potentials can only travel from the trigger zone until the axon terminals, being impossible to propagate in the opposite direction due to the absolute refractory period (Tortora & Derrickson, 2017). There are two types of propagation, depending on the type of neuron that experiences the action potential (Tortora & Derrickson, 2017). In unmyelinated neurons, there is a continuous propagation of the action potentials, where a depolarization and repolarization occur in sequential order from the trigger zone until the axon terminal (Tortora & Derrickson, 2017). In myelinated neurons, the propagation is saltatory because the action potential generated in the first node of Ranvier (region rich in voltage-gated Na^+ channels) creates an ionic flow inside and outside the neuron (Tortora & Derrickson, 2017). This ionic current can open the voltage-gated Na^+ channels in the second node, through the depolarization of the membrane to threshold (new action potential) (Tortora & Derrickson, 2017). This latter propagation mode has the advantages of being faster and more efficient in terms of energy when compared to continuous propagation (Tortora & Derrickson, 2017).

1.4.1. Synapses

A synapse is a region where the presynaptic neuron and postsynaptic neuron or effector cell communicate with each other (Tortora & Derrickson, 2017). The presynaptic neuron is the cell that conducts the electrical impulse until the synaptic end bulb is reached, and the postsynaptic cell (postsynaptic neuron or effector cell) is the one that receives the signal (Tortora & Derrickson, 2017).

There are two types of synapses, the electrical synapses (rare) and the chemical synapses (Lodish et al., 2000a). In the electrical synapses, a gap junction that contains pores composed of two aligned channels links the membranes of the pre and postsynaptic neurons (Purves et al., 2001). These synapses work by permitting the passive flow of ionic current through its pores (Purves et al., 2001). Besides ions, these structures also allow the diffusion of ATP, second messengers and other intracellular metabolites between the two neurons (Purves et al., 2001). This type of synapses has the advantage of transmitting the signal virtually in an instantaneous way, being useful for electrical activity synchronization among populations of neurons and coordination of intracellular signaling and metabolism between neurons (Purves et al., 2001).

In chemical synapses, the pre and postsynaptic cells are separated by a synaptic cleft, that is filled with interstitial fluid (Tortora & Derrickson, 2017). This fluid does not allow the passage of the electrical impulse, which obligates the conversion of the ion current into a chemical signal (Tortora & Derrickson, 2017). When the action potential reaches the synaptic end bulb, the voltage-gated channels open (due to the membrane depolarization) which allows the influx of calcium ions (Ca^{2+}) (Tortora & Derrickson, 2017). The increase of Ca^{2+} signals for the exocytosis of synaptic vesicles, releasing neurotransmitters to the synaptic cleft (Tortora & Derrickson, 2017). As neurotransmitters bind to ligand-gated channels, more channels are stimulated allowing specific ions to flow through the membrane, which can generate a hyperpolarizing or a depolarizing postsynaptic potential (Tortora & Derrickson, 2017). The time spent in this signal transmission process is denominated synaptic delay (Tortora & Derrickson, 2017).

1.4.2. Neurotransmitters and synaptic vesicles

There are two types of neurotransmitters in regards to their size, neuropeptides, and small-molecule neurotransmitters (that include low molecular weight and gas neurotransmitters) (Mason, 2017c; Tortora & Derrickson, 2017). Some examples of neuropeptides are endorphins, substance P and neuropeptide Y, while acetylcholine, excitatory amino acids (e.g., glutamate), inhibitory amino acids (e.g., glycine), biogenic amines, nucleotides (e.g., ATP), nitric oxide and carbon monoxide are examples of small-molecule neurotransmitters (Mason, 2017c; Tortora & Derrickson, 2017).

While the translation of the pre-propeptide takes place (on the ribosome), this protein is targeted to the lumen of the endoplasmic reticulum (ER) by a specific amino-terminal sequence (Brady et al., 2012b). Inside the ER, the peptides lose their signal sequence and go through oligomerization and folding processes (Brady et al., 2012b; Purves et al., 2018b). After this, propeptides leave the ER in transport vesicles coated with coat protein complex II (COPII) (Brady et al., 2012b). The COPII-coated vesicles lose their coats and merge, forming a *cis*-Golgi network (CGN), which is associated with the Golgi apparatus' *cis* face (Brady et al., 2012b). In the CGN occurs the

protein sorting process that determines which proteins are retrieved to the ER and which proceed to the *cis* face of the Golgi apparatus, through the several cisternae of the aforementioned organelle until reaching its *trans* face (Brady et al., 2012b). In this process, the proteins get gradually modified as they progress through the organelle (Brady et al., 2012b). In the TGN, proteins start the maturation process (Brady et al., 2012b). They are sorted accordingly with their target destination (lysosomes or plasma membrane), after which the precursor synaptic vesicles bud off from this organelle (Brady et al., 2012b). The newly formed vesicles are transported through the axon until they reach the presynaptic terminal, while the propeptides become mature (formation of neuropeptides) (Brady et al., 2012b; Purves et al., 2018b). In the presynaptic terminal, the already mature vesicles (large dense-core vesicles) are dispersed throughout the terminal, requiring a high-frequency series of action potentials to be released (Brady et al., 2012b; Mason, 2017a). This kind of vesicles is not recycled, which means that to replace them, the synthesis process needs to begin again from the first step (Mason, 2017a).

Low molecular weight neurotransmitters are mainly synthesized in the presynaptic terminals (Purves et al., 2018d). Dopamine beta-hydroxylase (DBH) is an enzyme, thought to be associated with secretory vesicles, responsible for converting dopamine into noradrenaline, contributing for the presynaptic synthesis of this neurotransmitter (Lamouroux et al., 1987). The synthesis process is facilitated by the transport of the precursor molecules from the extracellular space into the cytoplasm, through transmembrane transporter proteins, and by the presence of specific enzymes in the terminals, which are responsible for converting the precursor molecules into neurotransmitters (Purves et al., 2018d). After synthesis, the low molecular weight neurotransmitters are loaded into recycling vesicles (normally forming small clear-core vesicles) by vesicular transporters that take advantage of the proton gradient present in the vesicular membrane for this transport (Mason, 2017c). The proton-electrochemical gradient is possible due to the presence of H^+-ATPases in the membrane of the synaptic vesicle, which generates a higher concentration of protons inside the vesicle when compared with the concentration in the cytosol (Brady et al., 2012d; Mason, 2017c). The originated small clear-core vesicles are transported to the active zone where they are ready to be docked, fused in response to a single action potential, and recycled by an endocytic process (Mason, 2017a).

Gas neurotransmitters are synthesized and directly released into the cytosol, many times of the neuronal dendrites (Mason, 2017c). Since these molecules have a short lifetime and diffuse through membranes, they are produced when needed and not stored (Mason, 2017c). When the neuron is triggered and the release of this type of neurotransmitters takes place, these gaseous molecules diffuse away in all directions, even retrogradely which can convey helpful information about the state of the postsynaptic terminal to the presynaptic terminal (Mason, 2017c).

1.4.3. Synaptic vesicle trafficking, exocytosis, and endocytosis

It is thought that synaptic vesicles are kept tethered within the reserve pool by synapsin, being mobilized when this protein is phosphorylated (Purves et al., 2018d). The phosphorylation is often catalyzed by the Ca^{2+}/Calmodulin-dependent protein kinase type II (CaMKII), which allows the dissociation of the synapsin from the synaptic vesicles (Purves et al., 2018d). Then, these vesicles are guided to the active zone by bassoon and piccolo proteins, and it is thought that docking regulation is made by rabphilin3 (targeted to the vesicle membrane by Rab3 and Rab27) in

interaction with SNAP25 (Ferrer-Orta et al., 2017; Südhof, 2012). In the active zone, the vesicles are primed, by the formation of a complex between two vesicle membrane proteins (Rab3 and Rab27) and two proteins present in the plasma membrane (RIM - Rab interacting molecule - and Munc13) (Jahn & Fasshauer, 2012; Mason, 2017a; Shin, 2014). The formation of a SNAREpin takes place, which is a coiled-coil structure that involves the interaction between one R-SNARE protein (synaptobrevin/VAMP2) and two Q-SNARE proteins (SNAP25 - 25 kDa synaptosomal associated protein - and syntaxin1) (Mason, 2017a). An R-SNARE protein and a Q-SNARE protein are soluble NSF (N-ethylmaleimide sensitive fusion protein) attachment receptor peptides that contribute with arginine (R) and glutamate (Q) to the ionic 0 layer, respectively (Fasshauer et al., 1998; Z.-W. Wang, 2008). The aforementioned ionic layer is the core of the SNARE complex, where ionic interactions between R and Q residues occur (Fasshauer et al., 1998; Z.-W. Wang, 2008). The three SNARE proteins begin zippering up, which transforms the *trans*-SNARE complex into a *cis*-SNARE, bringing the membranes closer together (Mason, 2017a). The two membranes do not fuse until an action potential arrives, because of the preventing action of synaptotagmin (whose expression and trafficking are regulated by SV2A) and complexin, that clamp down spontaneous synaptic release (Madeo et al., 2014; Mason, 2017a). When an action potential reaches the active zone, the voltage-gated Ca^{2+} channels open, allowing the influx of calcium ions that will bind to synaptotagmin (Mason, 2017a). This latter protein will interact with the SM (Sec1/Munc18) protein complex and the SNAREpin, finishing its configuration change, which results in membrane fusion and expansion of the fusion pore, by a facilitated lipid mixing process (SM activity) (Mason, 2017a). The merge of the two membranes allows the free diffusion of the neurotransmitters in the synaptic cleft, which after some time will bind to the corresponding receptors, be enzymatically degraded or diffuse away from the postsynaptic receptors and suffer reuptake into nerve terminals or glial cells (exclusive of low molecular weight neurotransmitters) (Mason, 2017a, 2017c; Purves et al., 2018d). In this exocytosis process, some proteins participate in multiple phases, such as α-synuclein that has an essential role in the docking, priming, and fusion steps, probably aiding SNARE complex assembly (Huang et al., 2019). Syntaxin2 is also involved in exocytic processes, but constitutively (van den Bogaart et al., 2013).

After exocytosis, α-SNAP primes the SNARE complex allowing the binding of NSF to the newly formed SNARE-SNAP complex (Cipriano et al., 2013). Then NSF hydrolyzes ATP, which results in a conformational change of this protein that drives the threading of SNAP25 (N-terminal) into the NSF pore (Cipriano et al., 2013). The hydrolysis of ATP results in residue translocation, which destabilizes the SNARE core (Cipriano et al., 2013). α-SNAP, syntaxin, and VAMP disassemble, followed by the dissociation of SNAP25 and from NSF (Cipriano et al., 2013).

Also, after exocytosis, there is a need for recovering the vesicle membrane to the cytoplasm (Kandel et al., 2013b). There are three mechanisms possible for this recovery: reversible fusion pore, clathrin-mediated recycling, and bulk retrieval pathways (Kandel et al., 2013b). The first pathway is the fastest because the formation of the fusion pore is reversible, which means there is an incomplete fusion with the membrane (Kandel et al., 2013b). There are two types of reversible fusion pore pathway: *kiss-and-stay*, that happens when the synaptic vesicle persists in the active zone after the closing of the pore, and *kiss-and-run*, when the vesicle leaves the active zone (Kandel et al., 2013b). When the frequency of stimulation is higher, the second pathway is recruited (Kandel et al., 2013b). In the clathrin-mediated pathway, the vesicle membrane is retrieved by clathrin into a clathrin-coated vesicle, that will then be recycled in an early endosomal compartment so that it can be reused (Kandel et al., 2013b). Bulk retrieval pathway happens when high-frequency

stimulation is durable, occurring, in the presynaptic terminal, large invaginations of the membrane (Kandel et al., 2013b).

In the clathrin-mediated pathway, when several synaptic vesicles fuse with the plasma membrane, there is an increase of concentration of proteins present in these vesicles, which allows the occurrence of the sorting process by diffusion facilitated by the interaction between synaptophysin and cholesterol (Rizzoli, 2014; Shin, 2014). The presence of these vesicle proteins in the plasma membrane leads to the accumulation of their interactors (e.g., AP2 and AP180) (Rizzoli, 2014). Some cofactors, like endophilin, can be responsible for the formation of curvature in the membrane, which is followed by the coating of the vesicle being formed with clathrin (Rizzoli, 2014). Endocytosis is thought to be triggered by the influx of extracellular Ca^{2+}, due to the possibility of calcineurin activation, and consequent dephosphorylation of various endocytosis cofactors (such as AP180 or dynamin) (Rizzoli, 2014). These proteins are later phosphorylated by protein kinases, such as Cyclin-Dependent Kinase 5 (CDK5), a process that may also play a role in endocytosis triggering (Rizzoli, 2014). Endophilin and intersectin recruit dynamin, a GTPase, to the endocytosing vesicle pinching site, where this protein forms a ring-like structure, that disconnects the vesicle from the plasma membrane (Rizzoli, 2014). The newly endocytic vesicle associates with polymerizing actin that seems to propel vesicles into the synapse, when the polymerization stops the depolymerization begins, leading to the disassociation of actin from the vesicle (Rizzoli, 2014). After budding, the dynamin pinching site is exposed and free of clathrin, which allows the recognition of this site by auxilin (Hsc70 cofactor) and Hsc70, which have the capability of binding and destabilizing the clathrin molecules (Rizzoli, 2014). It is thought that the uncoated vesicle may produce PI(3)P in its membrane, which recruits its binding proteins (such as PI(3) kinases) and sva (membrane organizer protein, that associates with EEA1) (Rizzoli, 2014). When PI(3) kinases interact with Rab5, the recruitment of several endosomal cofactors takes place which allows the transformation of the vesicles into endosome-like organelles that are capable of fusing with pre-existing early endosomes (EEs) or of homotypic fusing to form new EEs (Müsch, 2014; Rizzoli, 2014). Endosomes preform sorting of the molecules for recycling into their tubular regions and then bud the vesicles (Müsch, 2014; Rizzoli, 2014). This budding process may be due to the recruitment of AP3 (that forms a coat around the vesicle) by probably ARF1 (ADP ribosylation factor 1) (Rizzoli, 2014). The vesicles are filled with neurotransmitters, as described in 1.4.2. section and terminate the recycling process in the reserve pool (Purves et al., 2018d; Rizzoli, 2014).

Endocytic processes can also have a degradative purpose (Müsch, 2014). In this case, the EEs maintain the molecules to be degraded in their vesicular portion and start their maturation process (Brady et al., 2012b). This maturation involves a bidirectional exchange of lipids and proteins between the endosome and the TGN (transport mediated by syntaxin6 and 16) (Brady et al., 2012b; Chen et al., 2010; Jung et al., 2012; Müsch, 2014). EE recruits Rab7 through Rab5-GTP, which is transformed into Rab5-GDP, resulting in its dissociation from the endosome (Huotari & Helenius, 2011). After this, the formation of endosomal membrane invaginations, and the consequent formation of cargo-containing intraluminal vesicles (ILVs), takes place (Scott et al., 2014). When the vesicular regions that contain ILVs are budded off from the endosome, they become multivesicular bodies (MVBs) that will maturate and fuse with other late endosomes (LEs) (Scott et al., 2014). The mature LEs fuse with lysosomes forming endolysosomes, that, after the completion of their degradative activity, are transformed into lysosomes (Müsch, 2014).

1.4.4. Regulation of neurotransmission: Positive and negative regulators

The neurotransmission process is a mechanism that requires a tight regulation (Brady et al., 2012e). One of the most common forms of regulation of a cell is protein phosphorylation (Brady et al., 2012e). This process induces conformational changes in the substrate by the addition of a γ-phosphate group (from ATP) in a residue (Serine/Ser, Threonine/Thr, or Tyrosine/Tyr) of the target molecule (Brady et al., 2012e). The introduced conformational changes have the capability of changing the biochemical and cellular functions of the target protein (Brady et al., 2012e). It is important to note that phosphorylation is a post-translational process that is reversible (by the action of phosphatases), and that requires energy expense (Brady et al., 2012e). To minimize the energy expenditure, most of the protein kinases are inactive when the cell is in its basal state, requiring their activation when needed (Brady et al., 2012e). The activation of protein kinases/phosphatases can be induced directly or indirectly by extracellular signals (Brady et al., 2012e). In the case of direct activation, the extracellular molecules bind to plasma membrane receptors that suffer conformational change, which allows the activation of intrinsic phosphorylation/dephosphorylation activity (Brady et al., 2012e). This type occurs mainly with kinases that phosphorylate Tyrosine residues, although this mechanism regulates CDK5, a Ser/Thr kinase. In indirect activation, the extracellular molecules bind to receptors present in the plasma membrane (Brady et al., 2012e). The change in the intracellular concentration of second messengers (e.g., Ca^{2+}, DAG and cAMP), regulated by the activated receptors, activates protein kinases/phosphatases (that commonly act upon Serine or Threonine residues), such as PKA (cAMP-dependent protein kinase), PKC (protein kinase C), and CAMKII (Brady et al., 2012e). The phosphorylation activity activated by both mechanisms triggers a change in the phosphorylation state of the target phosphoproteins, which will enable a signaling cascade and evoke a physiological response (Brady et al., 2012e).

Specifically in the neurotransmission process, many proteins are regulated by phosphorylation: enzymes that regulate neurotransmitter synthesis, ion channels (e.g., voltage-gated Ca^{2+} channels) that allow a response to action potentials, proteins associated with synaptic vesicles (e.g., synapsin-I and synapsin-II) that contribute for vesicle cycling, and SNARE proteins (e.g., VAMP2) that are responsible for priming, docking, and fusion (Brady et al., 2012e).

There are two types of exocytic regulators, positive and negative (M. Takahashi & Ohnishi, 2002). The negative regulators inhibit or suppress neurotransmitter release, while positive regulators enhance neurotransmission (M. Takahashi & Ohnishi, 2002). Many positive regulation events occur through the action of receptor Tyrosine kinases, which regulate MAP Kinase and PLC pathways (M. Takahashi & Ohnishi, 2002). Negative regulation, on the other hand, can be associated with non-receptor Tyrosine kinases (M. Takahashi & Ohnishi, 2002).

1.4.5. Amisyn and tomosyn as negative regulators of exocytosis

Negative regulation is a mechanism that responds to the need of synaptic depression, and that has an important role in neuroprotection (M. Takahashi & Ohnishi, 2002). When a stimulus is presented in a repeated manner, the strength of the behavioural response decreases (habituation), and it is observed a decrease in neurotransmitter release (M. Takahashi & Ohnishi, 2002).

There is evidence that supports the existence of silent synapses, and synaptic plasticity can be associated with the transition between active and silent synapses (M. Takahashi & Ohnishi, 2002). There are two ways for a synapse to be silent, lack of neurotransmitter release, or lack of sensitivity to neurotransmitters (M. Takahashi & Ohnishi, 2002).

1.4.5.1. Tomosyn/STXBP5

Tomosyn-1 (STXBP5) is 130 kDa protein (Fujita et al., 1998) that regulates the release of neurotransmitters by exocytosis inhibition (Geerts et al., 2017). This protein contains an R-SNARE domain in the C-terminal, WD40 repeats in its N-terminus, and a hypervariable linker domain (Ashery et al., 2009). The WD40 repeats allow the binding of tomosyn to synaptotagmin in a Ca^{2+}-dependent manner (Mochida, 2015). This interaction leads to an impaired catalytic activity of synaptotagmin, which may negatively regulate the exocytosis steps that require this enzyme (Mochida, 2015). The R-SNARE domain is responsible for competing with Munc18 and VAMP2 to bind to syntaxin1 and SNAP25, which inhibits the formation of the SNARE complex (Cazares et al., 2016; Shen et al., 2020), and consequently inhibits transmitter release from the RRP (readily releasable pool) (Cazares et al., 2016) (**Figure 2**). However, data show that vesicles associated with tomosyn in high concentrations might have the capacity to fuse, which might indicate that this protein blocks Q-SNARE membrane protein in excess (Trexler et al., 2016). There is also data pointing out to potential competition between a tomosyn-syntaxin1A-SNAP25 pathway and the Munc18-Munc13 pathway, since both Munc18 and tomosyn can partially rescue a Munc13 phenotype (Park et al., 2017).

This protein is a substrate of CDK5, which can phosphorylate proteins in an activity-dependent way (Cazares et al., 2016). Tomosyn also interacts with Rab3A-GTP, which allows the formation of a complex between those two proteins and synapsin1, being this complex sensitive to the phosphorylation state of tomosyn (Cazares et al., 2016). Tomosyn mediates the transition between the resting pool (ResP) and the total recycling pool (TRP) (constituted by the recycling pool and the RRP), being possible that the complex tomosyn-Rab3A-synapsin1 might explain the association of this mechanism with CDK5 (Cazares et al., 2016). In mast cells, the dissociation of syntaxin4 and the association to syntaxin3 was promoted by inhibition of tomosyn phosphorylation or by the absence of PKCδ, being possible that syntaxin4-tomosyn inhibits exocytosis (Madera-Salcedo et al., 2018). When phosphorylated, this blockade may be relieved, followed by the gradual imposition of a new block regulated by the redistribution of tomosyn to syntaxin3 (Madera-Salcedo et al., 2018). It is also known that phosphorylation of tomosyn in S724 by PKA reduces binding to syntaxin1 and that phosphorylation by Akt in S783 causes the inability to bind to syntaxin4 (Madera-Salcedo et al., 2018).

Besides phosphorylation, tomosyn has been reported to be regulated by other post-translational modifications, such as SUMOylation and ubiquitylation (Ferdaoussi et al., 2017). In β-cells stimulated with glucose, it was proven that de-SUMOylation of tomosyn, reduces the interaction of this protein with syntaxin1A, that is possibly enabled to interact with SNAP25, resulting in an alleviation of the exocytosis inhibition (Ferdaoussi et al., 2017).

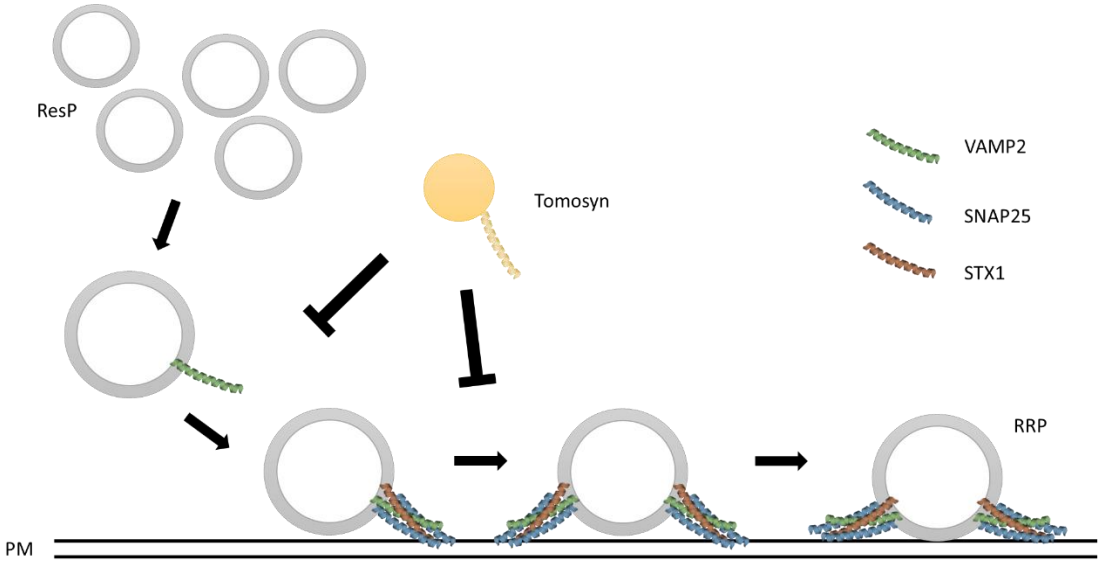

Figure 2- Negative regulation by tomosyn of the transition between the ResP and the RRP. STX1: syntaxin1; VAMP2: synaptobrevin2; ResP: resting pool; RRP: readily releasable pool. It is adapted from: (Ashery et al., 2009).

1.4.5.2. Amisyn/STXBP6

Amisyn (STXBP6) is a vertebrate-specific brain-enriched 24 kDa protein that contains a SNARE motif on its C-terminal (Scales et al., 2002) and a PH domain on its N-terminus (Kondratiuk et al., 2020) (**Figure 3**). This protein is mostly found associated with membranes in the mouse brain's nerve terminals (Kondratiuk et al., 2020). Amisyn can interact with syntaxin1A, syntaxin4, and SNAP25 (Scales et al., 2002). Its SNARE motif is mainly responsible for the interaction of amisyn with syntaxin1A and SNAP25, which leads to the formation of a ternary complex with these proteins, that is devoid of transmembrane sequence or lipidation motif (Kondratiuk et al., 2020; Scales et al., 2002) (**Figure 3**). Amisyn also interacts with $PI(4,5)P_2$, a lipid whose membrane concentration affects this protein association with the plasma membrane (Kondratiuk et al., 2020). This protein competes with VAMP2 for the SNARE complex formation (with SNAP25 and syntaxin1A) (Kondratiuk et al., 2020). It needs both its domains to be capable of interacting with the mentioned proteins, as opposed to VAMP2, that only requires its SNARE motif (Kondratiuk et al., 2020). It is thought that the formation of this amisyn containing SNARE complex is a way to control the timing of exocytosis and amount of fused vesicles (Kondratiuk et al., 2020). Even though amisyn interferes with the sizes of releasable pools and secretory vesicles docking/priming and fusion, and it negatively regulates the exocytosis events (independently of syntaxin1 binding), the properties of the fusion pore are maintained (Kondratiuk et al., 2020).

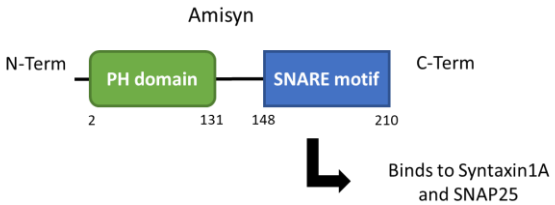

Figure 3- Diagram of the two domains present in the amisyn molecule. It is adapted from: (Kondratiuk et al., 2020).

In human insulin-secreting β-cells, it was observed that an overexpression of amisyn resulted in secretion inhibition (Collins et al., 2016) and that amisyn and dynamin1 are recruited to the exocytosis site by Epac2 (cAMP sensor), which results in a restriction of the fusion pore expansion (Guček et al., 2019). It is important to note that various diseases are associated with amisyn mutations, such as autism (Castermans et al., 2010), diabetes (Collins et al., 2016; Guček et al., 2019) and cancer (Lenka et al., 2017), which indicates the need of better understanding this protein and its associated processes.

1.4.6. Neurotransmitter receptors and synaptic transmission and plasticity

After exocytosis, neurotransmitters can bind to metabotropic and ionotropic receptors, while neuropeptides can only bind to metabotropic receptors (Mason, 2017b).

Metabotropic receptors are coupled to GTP-binding proteins (G-proteins), that when activated, act as an intermediate for regulating intracellular reactions (Purves et al., 2018d, 2018a). There are two types of G-proteins: heterotrimeric and monomeric (Purves et al., 2018a). The proteins of the first class have three subunits (α, β, and γ), the G-protein is in its inactive state when the α subunit is bond to a GDP molecule and the βγ heterodimer (Purves et al., 2018a). When an extracellular signal binds to a metabotropic receptor, the heterotrimeric G-protein binds to the receptor (Purves et al., 2018a). After this, the α subunit replaces the GDP by a GTP and the βγ subunit complex dissociates, which activates both the α subunit and the βγ heterodimer, allowing their interaction with effector molecules (Purves et al., 2018a). In the case of monomeric G-proteins, the extracellular signal allows the binding of an adaptor protein to the receptor, which interacts with GEFs (guanine nucleotide exchange factors), activating them (Purves et al., 2018a). GEFs replace the GDP present on an inactive monomeric G-protein by GTP, activating this protein (Purves et al., 2018a). Both G-protein types are inactivated by the hydrolysis of the GTP into GDP, action enhanced by GAPs (GTPase activating proteins) such as RGS (regulator of G protein signaling) proteins (Kozasa et al., 2011; Purves et al., 2018a).

There are four main types of heterotrimeric G proteins according to the kind of their α-subunit, which are: G_s, G_i/G_o, G_q/G_{11}, and G_{12}/G_{13} (Okashah et al., 2019). Upon activation of a G_s protein, the α_s subunit dissociates from the βγ-complex, which exposes the adenylyl cyclase binding site present in this subunit (Kandel et al., 2013a). The interaction of the adenylyl cyclase with the α_s subunit activates the molecule that starts producing cAMP (cyclic adenosine monophosphate) (Kandel et al., 2013a). With an increase of cAMP, the activation of a protein kinase takes place (which in most cells, the main target is the PKA) (Kandel et al., 2013a). When this enzyme is inactive the two catalytic (C) subunits are bound to two regulatory (R) subunits; however when the enzyme gets activated the C subunits dissociate, which allow the phosphorylation of the target proteins (in Serine and Threonine residues) through the transference of γ-phosphoryl from ATP to these molecules (Kandel et al., 2013a). When a G_i/G_o protein gets activated, the corresponding α subunit will have the opposite effect of the previous (G_s), which means that adenylyl cyclase will be inhibited (Kandel et al., 2013a; Purves et al., 2018a). This inhibition will cause less cAMP production, which will result in less protein phosphorylation (due to a lack of active PKA) (Kandel et al., 2013a; Purves et al., 2018a). In the case of G_q/G_{11} proteins, their activation leads to the activation of phospholipase C (PLC), one of the enzymes responsible for the hydrolysis of phospholipids (mostly phosphatidylinositol 4,5-biphosphate – $PI(4,5)P_2$) (Kandel et al., 2013a). The hydrolysis process

results in the formation of diacylglycerol (DAG) that remains in the plasma membrane, and inositol 1,4,5-triphosphate (IP_3), a cytoplasmic second messenger (Kandel et al., 2013a). DAG recruits PKC to form an active complex, that may depend on the Ca^{2+} availability, capable of phosphorylating many protein substrates (Kandel et al., 2013a). On the other hand, IP_3 can stimulate Ca^{2+} release from the stores present in the SER (smooth endoplasmic reticulum). This process is possible due to the existence of IP_3 receptors present on the SER membrane that allow the passage of Ca^{2+} to the cytoplasm (Kandel et al., 2013a). In the case of an active $G\alpha_{12/13}$ subunit, this protein interacts with the RH (RGS homology) domain of an RH-RhoGEF (RH domain-containing guanine nucleotide exchange factors for Rho) (Kozasa et al., 2011). The RH may stimulate the other two domains (DH - Dbl homology - and PH - pleckstrin homology - domains), enabling its RhoGEF activity that activates the RhoGTPases (e.g., RhoA) (Kozasa et al., 2011). These GTPases have an important role in the organization of actin and microtubules, being also involved in gene transcription, cell cycle progression, and survival/death of the cell (Stankiewicz & Linseman, 2014).

An ionotropic receptor (e.g., NMDA - N-methyl-d-aspartate - and AMPA - α-amino-3hydroxy-5-methylisoxazole-4-propionate - receptors) is a molecule composed of a neurotransmitter recognition and receptor part and an ion channel (Tortora & Derrickson, 2017). When a neurotransmitter binds to this type of receptors, the ion channel opens, allowing the passage of ions (Tortora & Derrickson, 2017). In the case of a cation channel (Ca^{2+}, Na^+, and K^+), the membrane is depolarized because the Na^+ influx outweighs the charge movement caused by the other two ions (Tortora & Derrickson, 2017). If the channel allows the passage of anions (Cl^-), the membrane is hyperpolarized, lowering the chances of firing an action potential (Tortora & Derrickson, 2017).

AMPA receptors (AMPAR) are ionotropic glutamate receptors composed of four types of subunits (GluA1, GluA2 – responsible for glutamate reception -, GluA3 and GluA4) and when bound to glutamate allow the passage of cations (Na^+ and K^+) (Purves et al., 2018b). Although NMDA receptors (NMDAR) are also glutamate ionotropic receptors, these receptors are very different from AMPAR (Purves et al., 2018b). NMDAR contain three subunit types (GluN1, GluN3 – both responsible for glycine reception - and GluN2 – responsible for glutamate reception), maintaining an Mg^{2+} blocked state in the membrane resting potential and when the synaptic transmission cannot depolarize the membrane sufficiently (Purves et al., 2018b). Only when glutamate and glycine bind to these receptors and the postsynaptic membrane is simultaneously depolarized, NMDAR can open their pores, allowing the passage of cations (Na^+, Ca^{2+}, and K^+) (Purves et al., 2018b).

Postsynaptic density (PSD) is a macromolecular signaling complex present in the postsynaptic site that seems to be involved in long-term memory formation, and that is composed of several types of proteins (Boeckers, 2006). Homer is a scaffold protein present in the PSD that interacts with metabotropic type I glutamate receptors (mGluR1 and 5), inositol 1,4,5-triphosphate receptors (IP_3R) and Shank (Tao-Cheng et al., 2014). Another PSD protein is PSD95, a molecule that belongs to the membrane-associated guanylate kinase (MAGUK) family (Vyas & Montgomery, 2016). PSD95 interacts with AMPAR and NMDAR and with transmembrane AMPAR regulatory proteins (TARPs) (Vyas & Montgomery, 2016). This interaction allows the regulation of the number of AMPAR present in the synapse (Vyas & Montgomery, 2016).

There are two types of synaptic plasticity in regards to the duration of their effects: short-term synaptic plasticity and long-term synaptic plasticity (Brady et al., 2012e). Short-term synaptic plasticity alters the strength of the synaptic connections by changing the number of

neurotransmitters liberated onto the synaptic cleft for a few minutes (Purves et al., 2018c). Long-term synaptic plasticity has similar effects, but the caused alterations can last for more extended periods, being more probable for them to be associated with learning and memory processes (Purves et al., 2018c). This long-lasting synaptic plasticity can be subdivided into two types: long-term potentiation (LTP), which increases the strength of the synapse that last a long period of time, and long-term depression (LTD), that decreases the synaptic strength, also for an extended period (Purves et al., 2018c).

LTP can be found in multiple brain regions, such as the hippocampus and cortex, and this process has mainly two phases, an early-stage (1-2h after LTP induction) and a late-stage (Purves et al., 2018c). At the beginning of the process, there is the need for a high-frequency synaptic transmission (from the presynaptic site to the postsynaptic) to relive de Mg^{2+} blockade of the NMDA receptors (Purves et al., 2018c). Without the blocking of Mg^{2+}, these receptors, which are activated by glutamate and cellular depolarization (caused by an influx of cations through AMPAR), allow the influx of Ca^{2+} (Purves et al., 2018c). This second-messenger induces LTP (Purves et al., 2018c). In the early phase LTP, AMPAR from recycling endosomes are inserted into the postsynaptic membrane by synaptotagmin, SNAP47 and syntaxin4 (Kádková et al., 2019; Mohanasundaram & Shanmugam, 2010; Purves et al., 2018c). This leads to an increased concentration of the aforementioned receptors on the postsynaptic site, which strengthens the response to glutamate of the postsynaptic neuron (Kádková et al., 2019; Mohanasundaram & Shanmugam, 2010; Purves et al., 2018c). Activation of postsynaptic signal transduction cascades by the Ca^{2+}-dependent activation of kinases (such as PKC, MAP kinase, and creb) is also an event of the early LTP (Brady et al., 2012c; Purves et al., 2018c). When activated, the CAMKII translocates to the postsynaptic density zones (PSD), which is thought to cause phosphorylation of AMPA receptors and other targets, aiding the transport of extrasynaptic AMPA receptors to the synapse (Brady et al., 2012c; Purves et al., 2018c). PKC is also thought to have a similar role to CAMKII (Purves et al., 2018c).

In the LTP late phase, upon NMDA receptors activation, the Ras GTPase stimulates the Raf-MEK-ERK pathway, the MEK-JNKK-JNK pathway, and the PI3 kinase pathway (that leads to the activation of Akt/PKB – protein kinase B) (Brady et al., 2012a). All pathways, as mentioned earlier, activate transcription factors, such as CREB, Elk, $NF_{\kappa}B$, c-Jun, c-Fos, and ATF2 (Brady et al., 2012a). Regarding CREB specifically, CAMKIV may be important for its direct but transient phosphorylation and for phosphorylation of CBP (CREB-binding protein) that consequently activates CREB (Wayman et al., 2008). These transcription factors stimulate the expression of genes that encode for transcription factors, kinases, AMPA receptors, between others, whose contribution remains unknown (Brady et al., 2012c; Purves et al., 2018c).

LTD is a mechanisms that allows the changes inducted by LTP to be reversed, which permits the encoding of new information (Purves et al., 2018c). For LTD early phase induction, the Ca^{2+} increases must be small and slow (as opposed to large and fast in LTP), leading to the Ca^{2+}-dependent activation of phosphatases (PP1 – protein phosphatase 1 - and PP2B - calcineurin) (Purves et al., 2018c). Also, in the early phase, the AMPA receptors decrease in number, which may be due to internalization into sorting endosomes (Purves et al., 2018c). Synthesis of new proteins is a process required for LTD late phase, as is for LTP (Purves et al., 2018c).

1.5. Experimental models

1.5.1. *Escherichia coli bacterium*

Many host organisms can be chosen to synthesize the desired protein (Rosano & Ceccarelli, 2014). *Escherichia coli* is one common species that serves this purpose; this happens due to its short doubling time (about 20 min), its capability to achieve high cell density, and its ability to be easily transformed with exogenous plasmids (Rosano & Ceccarelli, 2014).

Plasmids used for this purpose need to have five main components: Replicon (origin of replication and its cis-acting control elements), promotor, selection marker, affinity tags and multiple cloning site (MCS) (Meyers, 1995; Rosano & Ceccarelli, 2014). The replicon allows plasmid replication by the host and controls the number of copies that can be present in one cell (Meyers, 1995; Rosano & Ceccarelli, 2014). The promotor is responsible for driving the transcription of the interest gene and regulating the protein expression levels (Nora et al., 2019). An example of a selection marker is antibiotic resistance, being an essential characteristic to allow the preferential growth of the transformed cells (Meyers, 1995; Rosano & Ceccarelli, 2014). The affinity tags are useful for protein detection throughout the expression and purification process, for an easy purification process and added protein solubility (Rosano & Ceccarelli, 2014). These tags can be of two types: peptide tags or non-peptide fusion partners (e.g., GST) (Rosano & Ceccarelli, 2014). The MCS contains various restriction enzymes recognition sites, which enables the cloning of the target gene (Nora et al., 2019).

1.5.2. C57BL/6 mice and amisyn KO lines

C57BL/6 is a mouse strain widely used for pharmacological, genetic and behavioural research, and one of its applications is being a background for KO mice generation (Mayorga & Lucki, 2001). Mice are a useful model due to their genetic similarity to humans (99% of the same genes are shared), their short life spans, and their high fertility (Hall et al., 2009).

In case a knock-out of a specific gene leads to developmental lethality, the systems Cre/loxP and Flp/FRT can be implemented (conditional KOs) (Hall et al., 2009). In these systems, the mice have the alleles of the gene of interest floxed (DNA placed between two loxP or FRT sites), keeping a wild-type phenotype (Hall et al., 2009). Then, these mice are crossed with Cre or Flp (recombinases) expressing mice, that perform excision of the DNA of interest in the location determined by the Cre or Flp promotor (Hall et al., 2009). To have temporal control of expression, there is the possibility of expression inducible by drugs (e.g., tamoxifen) or viruses (Hall et al., 2009). There is also another strategy of conditional KOs ("KO-first") where the initial allele is null by splicing to a LacZ trapping element present in the gene of interest (tm1a allele) (Skarnes et al., 2011). If desired, the allele of these mice can be altered through crossing with Cre or Flp expressing mice, which results in KO (tm1b) and WT (tm1c) phenotypes, respectively (see **Figure 7**) (Skarnes et al., 2011). The tm1c allele containing mice can be further modified by crossing with Cre expressing mice resulting in KO phenotype (tm1d) (Skarnes et al., 2011).

1.6. Objectives

It was reported that defects in amisyn and tomosyn, two negative regulators of exocytosis, genes are associated with ASD (Autism spectrum disorders) (Castermans et al., 2010; Cazares et al., 2016), which is a group of neurodevelopment diseases characterized by abnormal social behavior (Won et al., 2013). Several mechanisms of this disease have been proposed and studied, one of them is associated with alterations in synaptic function and/or structure (synaptopathies) which are caused by defects in the proteins involved in synaptic transmission (Won et al., 2013). Since amisyn and tomosyn have a regulatory role in this process and that their role in ASD is poorly understood, is of most importance that further research is done on these proteins.

This project had three main objectives. First, the characterization of the amisyn protein through a comparison between wild-type amisyn and AADD (PH domain) mutant amisyn binding capacities to phospholipid PI(4,5)P_2, and to understand if the membrane association of amisyn depends on its PH domain. Second, the characterization of the amisyn mutant mice line through the comparison between wild-type and knock-out mice gene expression of different proteins, to assess if the lack of amisyn interfered with gene expression of any other synaptic proteins. Third, the characterization of the amisyn mutant mice line through the comparison between wild-type and knock-out mice levels of proteins involved in synaptic transmission. Additional goals of this dissertation were to obtain the current knowledge available regarding amisyn and the processes where it is required, and to get familiar with biochemical techniques and independently use them.

2. Materials and Methods

2.1. Protein expression and purification in *E. coli*

2.1.1. Plasmids

The plasmids used in this study are illustrated in **Figures 4** and **5**. Both plasmids have a pGEX-6p1 vector backbone that contains the gene of interest (amisyn WT or mutant), the GST gene, an ampicillin resistance gene, the promotor Ptac (trp/lac) that responds to IPTG and a coding region (lacIq) (GE Healthcare, n.d.). The lacIq is responsible for the prevention of expression, until the induction by IPTG takes place, by binding to the operator of the tac promotor (Merck, 2014). GEX5 for, GEX3 rev-25 and GEX3 rev represent the sequencing primers binding sites, and the remaining elements are restriction sites recognized by different enzymes(AddGene, n.d.). The four mutations present in the PH domain of the amisyn gene, that are discriminated in **Figure 5**, were all substitutions of a K (lysine; AAG or AAA) to an A (alanine; GCG) in the case of positions 30 and 32 or to a D (aspartate; GAT) in the positions 64 and 66.

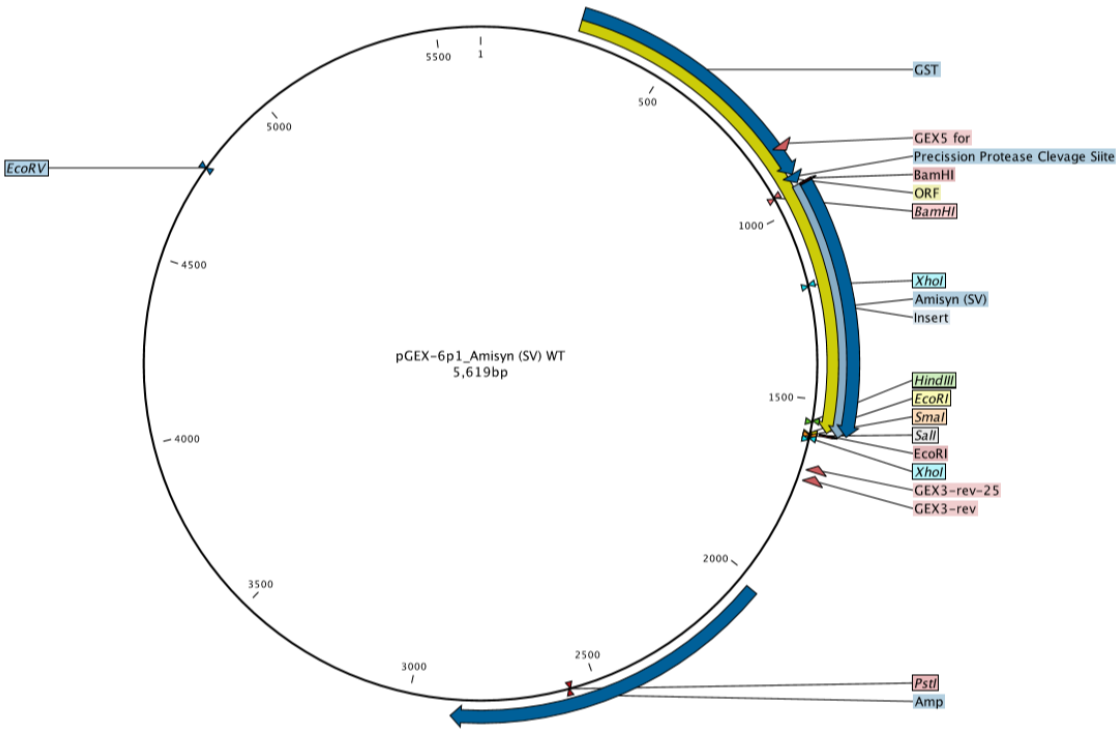

Figure 4- Illustrative figure of the short version (SV) amisyn wild-type plasmid used for the protein purification and lipid co-sedimentation assay. bp: base pairs.

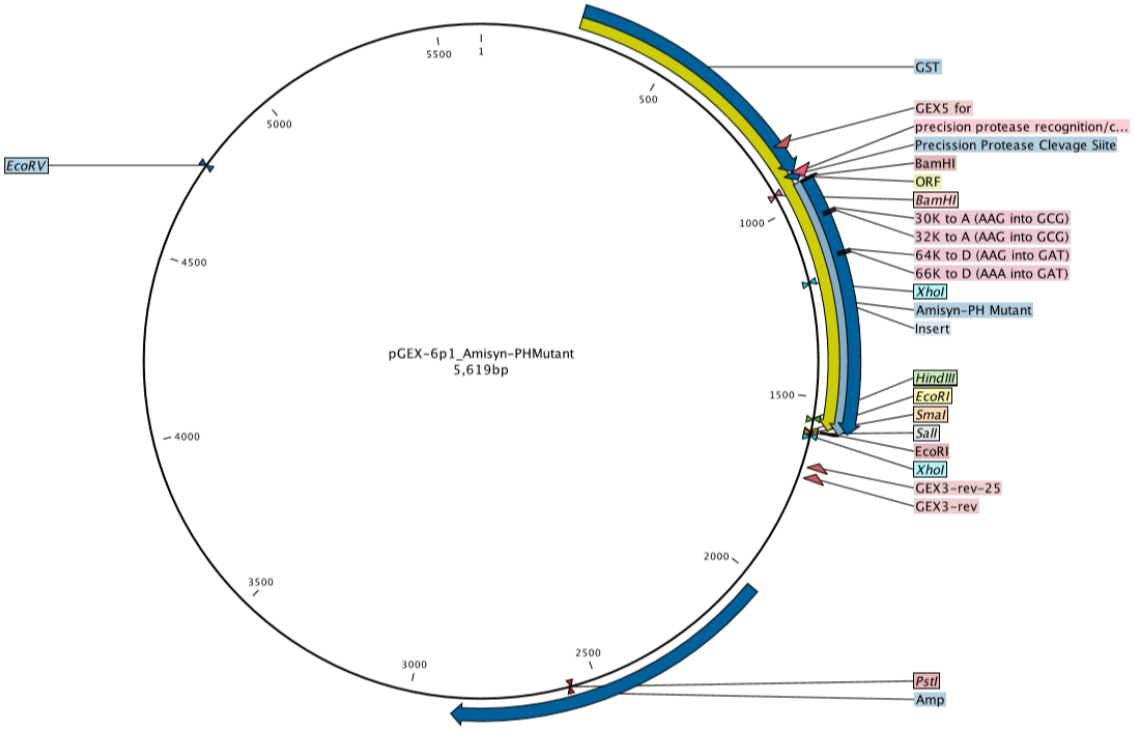

Figure 5- Illustrative figure of the amisyn AADD PH mutant plasmid used for the protein purification and lipid co-sedimentation assay. bp: base pairs.

2.1.2. Transformation and culture of *E. coli*

The *E. coli* BL21 rosetta competent cells (Merck 70954-4) were thawed on ice for 15-30 min to avoid damage derived to heat-shock, and the cells were mixed with the plasmid (mutant or wild-type, kindly given by MSc UdhayaBhaskar SathyaNarayanan). The mixture was incubated at 4°C for 15-30 min, heat-shocked (Eppendorf, Thermomixer comfort) for 45 sec and incubated at 4°C for 5 min. 400 µl of SOC medium (constituted by 0.5% yeast extract – Chemsolute, LP0021B -, 2% tryptone – Roth, 8952.2 -, 10 mM NaCl - Roth, P029.3 -, 2.5 mM KCl – Roth, HN02.3 -, 10 mM $MgCl_2$ – Roth, HN03.2 -, 10 mM $MgSO_4$ – Fluka Analytics, 00627 - and 20 mM glucose – Roth, HN06.4) were added to the bacteria. This mix was incubated at 400 rpm for 1 h at 37°C in the thermomixer. On pre-warmed plates containing LB agar (prepared accordingly with the manufacturer's specifications, 15 g/l of agar-agar – Roth, 5210.3) with 100 µg/ml ampicillin (Roth, K029) and 34 µg/ml chloramphenicol (Sigma Aldrich, C0378) was added 150 µl of the cultured bacteria and these plates were incubated at 37°C overnight (ON).

Some of the grown isolated colonies were picked and transferred into test tubes containing 4 ml of LB medium (with a constitution of 1% tryptone, 0.5% yeast extract and 171.12 mM NaCl) in which it was added ampicillin (100 µg/ml) and chloramphenicol (34 µg/ml). After incubation at 37°C and 250 rpm of 2-3h, the bacteria were transferred to Erlenmeyer containing 100 ml of LB medium with added ampicillin (100 µg/ml) and chloramphenicol (34 µg/ml) and incubated again in the previously described conditions. Then the content of each Erlenmeyer was mixed with 2 l of LB medium with ampicillin (100 µg/ml), and this mixture is incubated at 37°C at 180 rpm until it reaches an optic density at 600 nm (OD_{600}) of 0.6-0.8. Each mixture was inducted by 100 µM IPTG (Roth,

2316.3) and incubated at 24°C ON. Samples from each mixture before and after induction were collected, centrifuged at 11000g, and stored at -20°C.

2.1.3. Cell harvest, lysis and fast protein liquid chromatography (FPLC)

The cultured bacteria were centrifuged (Beckman Coulter, J6-MI High Capacity Centrifuge, JA-10 rotor) for 15 min at 6000g and 4°C, and the resulting supernatant was discarded. The pellet was resuspended at 4°C with 50 ml of lysis buffer, constituted by 150 mM NaCl, 50 mM HEPES (Roth, HN78.1), 2 mM EDTA (Roth, 8040.3), 2 mM β-mercaptoethanol (AppliChem, A1108) and 1 tablet of protease inhibitor (Roche, 5892953001). The cell suspension was run through the fluidizer (Microfluidics, Model 110S) 8-10 times at 80 psi. The resulting fluid was ultra-centrifuged (Thermo Scientific, Sorvall RC6, SS-34 rotor) for 30 min at 35000 g and 4°C, and the supernatant was filtered (0.2 μm).

The whole process of FPLC (P-920 ÄKTA FPLC system) was performed at 4°C and was started by loading the filtered supernatant into a glutathione sepharose column (Protino, GST/4B). The GST-amisyn was eluted by an elution buffer composed by 100 mM NaCl, 50 mM Tris (Roth, 5429.2) and 15 mM reduced glutathione (AppliChem, A2084). The resulting fractions went through dialysis in protease cleavage buffer (with a constitution of 150mM NaCl, 50mM Tris, 1mM EDTA and 1mM DTT – Roth, 6908.1) ON, sealed and with low agitation. The dialysate was loaded onto the glutathione sepharose column, that interacts with GST, and the purified amisyn protein was eluted, originating multiple fractions of 1 ml. Before and after dialysis, a sample was collected.

2.1.4. Protein quantification and storage

The Pierce BCA assay was used to assess the protein concentration of each chromatography fraction. The fractions were diluted 1:10 in lysis buffer, and the standard curve BSA solutions were prepared accordingly with the kit instructions (Thermo Scientific, 23225). The microplate procedure was the followed manufacturers protocol. In short, it was added, in each well of the plate, 200 µl of the reaction mix (A – Thermo Scientific, 23228 - and B – Thermo Scientific, 1859078 - solutions in a proportion of 50:1) and 25 µl of sample, standard or blank. The incubation of the plate was performed at 37°C for 30 min away from light, and after this period, the plate was read at 560 nm in the Infinite F200 (TECAN) using the iControl 2.0 software.

Once the protein concentration was known, the fractions were stored in -80°C with 15% glycerol (Roth, 3783.1), to stabilize the purified protein.

2.2. Validation of expressed protein

2.2.1. Sample preparation

The pellets obtained before and after induction with IPTG were prepared by adding SDS loading buffer 2x (dilution of SDS loading buffer 6x) and dH_2O in a 1:1 proportion. The preparation of the before and after dialysis samples, and the purified fractions was done by adding water, to equal the concentrations between samples, and SDS loading buffer 6x in a 1:6 proportion. The SDS loading

buffer 6x was constituted by 6.48 M glycerol, 0.97 M Tris-HCl (Roth, 9090.3), 0.42 M SDS (Roth, 2326.2) and 0.73 M Brilliant Blue R (Sigma Aldrich, 27816). After these preparations, both types of samples were boiled at 95°C (Eppendorf, thermomixer comfort) for 5 min.

2.2.2. Electrophoresis

To run the samples through electrophoresis, we prepared a polyacrylamide gel with a resolving gel of 10% and a stacking gel of 5%. Recipes are presented in **Table 1**.

Table 1 - Recipes used to prepare the resolving (12% or 10%) and stacking (5%) gels.

Constituents	**Supplier**	**12%**	**10%**	**5%**
Aqua bidest	-	6.6 ml	7.9 ml	2.7 ml
30% Polyacrylamide	Roth, 3029.1	8.0 ml	6.7 ml	670 µl
1.5 M Tris (pH 8.8)	Roth, 5429.2	5.0 ml	5.0 ml	-
1.0 M Tris (pH 6.8)	Roth, 5429.2	-	-	500 µl
10% SDS	Roth, 2326.2	200 µl	200 µl	40 µl
10% APS	Roth, 9592.2	200 µl	200 µl	40 µl
TEMED	Roth, 2367.1	8 µl	8 µl	4 µl

After the polymerization of the gels, the samples (35 µg/well, except the pelleted samples that are not quantified) and the PageRuler™ Plus Prestained Protein Ladder (Thermo Scientific, 26619) were loaded onto the gel wells.

The electrophoresis was performed using a BioRad power supply (PowerPack™ Basic) which was set for 80 V for the first 30 min and then increased to 150 V for the rest of the run. The electrophoretic tank (BioRad, MiniPROTEAN® Tetra Cell) had running buffer, constituted by 24.76 mM of tris, 191.82 mM of glycine (Roth, 3908.3) and 2.08 mM of SDS (pH 8.3), to allow the passage of current through the gel and samples equally.

2.2.3. Staining, destaining, and scanning of gels

To be stained, the gel was covered with Coomassie blue (0.1% in destaining solution), heated, and incubated in the shaker for 30-40 min. For three times, the gel was rinsed with dH_2O, covered with a destaining solution (composed by acetic acid - Roth, 7332.3 -, methanol - Roth, 8388.3 - and dH_2O in a proportion of 1:4:5) and incubated in the shaker for 30 min, in the last repetition the gel was left with agitation overnight. After the completion of the destaining step, the gel was scanned (Epson, Scanner perfection V700 photo).

2.3. Liposome co-sedimentation experiment

With the purified wild-type and mutant (AADD) amisyn, Ph.D. Ira Milosevic performed a co-sedimentation assay. The liposomes prepared had a constitution of 48 mol% of phosphatidylcholine (PC), 30 mol% of phosphatidylethanolamine (PE), 20 mol% phosphatidylserine (PS) and 2 mol% of $PI(4,5)P_2$. All the phospholipids were mixed and dried with a nitrogen stream for 2h, and their

concentration was adjusted to 1 mg/ml by the addition of a buffer (constituted by 150 mM NaCl and 20 mM HEPES pH 7.4). Using the previously mentioned buffer, the lipid mixture was hydrated for 1h, being this procedure followed by seven freeze-thaw cycles using liquid nitrogen. The liposomes were extruded through a 100 nm filter (Nucleopore Track-Etch, Whatman) around 20 times. The purified amisyn (10 µg; wild-type or mutant) was incubated with the liposomes at 37°C for 20 min, and then the mixture was centrifuged at 70000 rpm (Sorvall RC-M120, rotor S120-AT3) for 1h (see **Figure 6**). The pellet and supernatant were separated and analyzed through an SDS-page (12% resolving gel), followed by Coomassie blue-staining as described above.

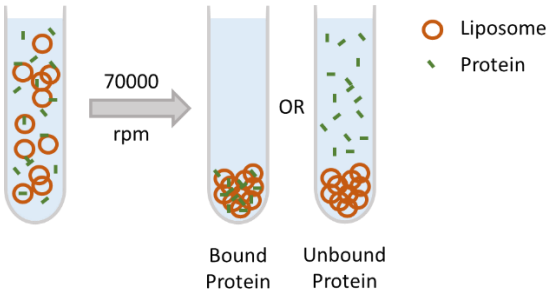

Figure 6- Diagram of the possible results of the liposome co-sedimentation experiment. rpm: rotations per minute. It is adapted from: (N. Takahashi et al., 2014).

2.4. Prediction of phosphorylation sites

The three online predictors, used together for more probable predictions, were the following: NetPhos 3.1 Server (Blom et al., 1999), NetPhospan 1.0 (Fenoy et al., 2019), and GPS Web Service (Xue et al., 2011). In each server, the amisyn fasta sequence (mouse) was required, being obtained in the UniProt platform (The UniProt Consortium, 2019). In the NetPhospan 1.0, the selected method was the "Generic method". In the GPS Web Server, PKA, PKC and CDK were the selected kinase families.

After obtaining the results from all platforms, the three best predictions of each server were selected. For each predicted site in one server, the corresponding predictions from the other two servers were searched to see which of the predicted sites were most predicted, and therefore more probable. In the case of NetPhos3.1 Sever and NetPhospan the predictions under 0.5 were not considered since the scale was between 0 and 1 (closer to 1 is more probable to be a phosphorylation site), but with the GPS Web service, this method wasn't possible being considered all the values.

Using PyMol (Schrödinger LLC, n.d.) and the amisyn PH domain model produced by Ph.D. Anita Krisko and Ph.D. Ira Milosevic for a PNAS paper (Kondratiuk et al., 2020), the predicted phosphorylation sites and the PI(4,5)P_2 interaction site were highlighted.

2.5. Amisyn mouse line and ethics permits

All animal-related procedures were performed according to the European guidelines for animal welfare (2010/63/EU), with the explicit permission from the Niedersächsisches Landesamt für Verbraucherschutz und Lebensmittelsicherheit (LAVES), registration 18/2994. Animals were

housed and bred in the Zentrale Tierexperimentelle Einrichtung (ZTE) Göttingen, with ad libitum access to water and food. Mice were kept in groups of 1–3 animals on a 12 h light/12 h dark cycle in individually ventilated cages. Both male and female animals were used for these studies at the age and genotype as indicated.

For the generation of our mouse line, the cultivated and genetically altered embryonic stem cells (ES cells; KOMP Repository, Project#38643) from the JM8A3.N1 line were used. JM8A3.N1 is a sub-line of the JM8 line, which has a corrected mutation in the agouti gene, that confers an agouti coat color to these mice (Pettitt et al., 2009). The STXBP6 gene was altered by the insertion, into an intron of the gene, of a LacZ trapping cassette and a floxed promotor-driven neo cassette, resulting in the interruption of gene activity. These alterations (tm1a) are represented in **Figure 7**, where 1, 2, and 3 represent exons of the amisyn gene, *FRT* illustrates the flippase (Flp) recognition target and *loxP* describes Cre substrate sites.

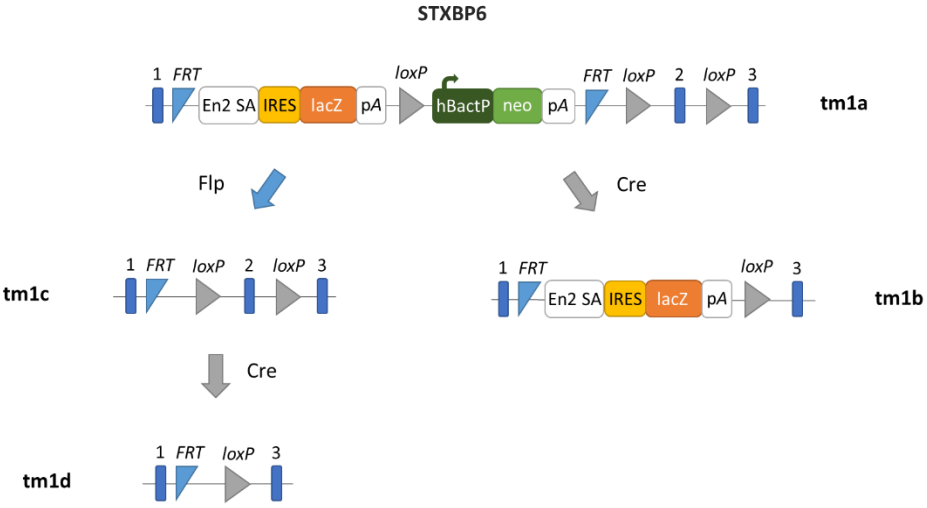

Figure 7- Illustration of the genetic alterations present in the STXBP6 gene (amisyn) in the amisyn KO mice (tm1a) and its possible resulting alleles upon genetic modification, adapted from KOMP allele types (*KOMP Allele Types*, n.d.). 1, 2 and 3: Exons; *FRT*: flippase (Flp) recognition target; *loxP*: Cre substrate sites; En2 SA: Splice acceptor of mouse Engrailed 2; IRES: Internal ribosomal entry site; LacZ: Gene that encodes β-galactosidase; p*A*: Polyadenylation site; hBactP: Human β-actin gene promotor; neo: neomycin resistance gene (Gobé et al., 2019).

After receiving the modified ES cells, Ph.D. Ilona Kondratiuk, Ph.D. Ira Milosevic, and collaborators multiplied these cells without differentiating them, and then injected these cells into blastocysts (from a C57BL/6N-Atm1Brd female mouse). Subsequently, blastocysts were inserted into another pseudo-pregnant mouse. The resulting male chimeras, which were identified by their agouti and black coats, were then tested to see if they had the mutation in their germline cells. The ones who could pass the mutation to the next generations were matted with wild-type C57BL/6N female mice and the resulting heterozygotes were mated for 5 generations, each time with new C57BL/6N female mice (**Figure 8**). Only after this process, the conditional potential knock-out (KO) mice of the generated line could be used.

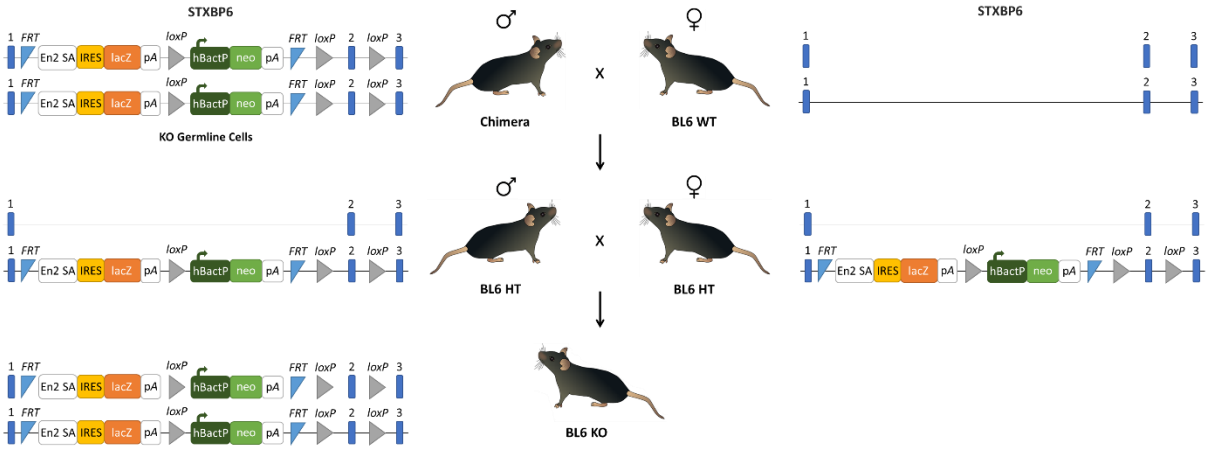

Figure 8- Representation of the amisyn mice generation process and the genetic information present in both alleles of each mouse regarding the STXBP6 gene (amisyn) (tm1a). 1, 2 and 3: Exons; *FRT*: flippase recognition target; *loxP*: Cre substrate sites; En2 SA: Splice acceptor of mouse Engrailed 2; IRES: Internal ribosomal entry site; LacZ: Gene that encodes β-galactosidase; p*A*: Polyadenylation site; hBactP: Human β-actin gene promotor; neo: neomycin resistance gene (Gobé et al., 2019); WT: wild-type; KO: knock-out; HT: heterozygous; ♂: male; ♀: female.

2.6. Mouse brain dissection

The mice used in this study were mainly females and had between 1 and 3 months old. Ph.D. student Jialin Jin euthanized the mice with diethyl ether (Roth, 8810.1) exposure until the animals presented no reaction to stimuli (about 1-2 min). After that, the head was cut off, and the skull was cut from the foramen magnum until the posterior tip of the frontal bone. The parietal, interparietal, and occipital bones were then open to give access to the brain and this organ was scooped out of the skull into fresh PBS (prepared accordingly with manufacturer's instructions - Sigma Aldrich, P4417-100TAB), where the brain was cut in half through the interhemispheric longitudinal fissure. The isolation of the hippocampus was done by peeling the cortical hemisphere laterally, beginning from the transverse sinus, and rolling the hippocampus gently in a lateral manner (Sultan, 2013). Each isolated part was quickly frozen by liquid nitrogen and was kept at -80°C until needed.

2.7. Mice genotyping

2.7.1. Sample preparation

Once the mice in the new litter born within the colony were three weeks old, the animal facility collected an ear sample from each mouse (resulting from the ear punches) and sent it to the lab. The samples were then fully digested at 55°C at 400 rpm in a thermomixer (PeqLab, Thriller) for 1-3 h by 300 µl per sample of a mixture of proteinase k (20 mg/ml; Roth, 7528.1) and SNET buffer (constituted by 20 mM Tris, 5 mM EDTA, 400 mM NaCl and 0.5% SDS) (in a 1:120 proportion). To precipitate the DNA, 750 µl of ethanol absolute (Chemsolute, 2246.1000) was added, and the tubes were centrifuged (Eppendorf, centrifuge 5417R) at 11000 g for 30 min at 4°C. The resulting supernatant was discarded, and the pellet was washed by the addition of 900 µl of 70% ethanol and the centrifugation at 11000 g for 20 min at 4°C. The supernatant was removed, 50 µl of TE

buffer (composed by 10 mM Tris-HCl and 0.2 mM EDTA pH 7.5) were added, and the tubes were left in a thermomixer (PeqLab, Thriller) at 55°C and at 400 rpm for 1h with an open lid to allow ethanol evaporation.

2.7.2. Polymerase chain reaction (PCR)

For the PCR reaction 2 master mixes were prepared on ice, one for the wild-type reaction and another for the floxed reaction which had the following forward and reverse primers TGCTCAAGGTGGAATGATTGTCC (CSD-F, Eurofins Genomics H319 47-4171-3/4), CAAGTGCACAATTACAGCTCTCAGG (CSD-ttR, Eurofins Genomics H319 47-4171-4/4) and GAGATGGCGCAACGCAATTAATG (CSD-loxF, Eurofins Genomics H319 47-4171-1/4), ATGTGTAAGCACAAAAGGAAATGGG (CSD-R, Eurofins Genomics H319 47-4171-2/4), respectively. In addition to the primers each master mix had also dH2O, 5x Green GoTaq® Flexi Reaction Buffer (Promega, M891A), 25 mM MgCl2 (Promega, A351H), 10 mM dNTP (BioLabs, N04475), DMSO (Sigma, 41639), 5 M betaine (Sigma, B0300) and Taq polymerase (5 U/µl, Promega, M780B) in the quantities specified in **Table 2**.

Table 2 – PCR master mix recipe for one sample.

Reagents	**V (µl)**
dH_2O	8.225
5x Reaction Buffer	5.0
$MgCl_2$ 25 mM	1.75
dNTP 10 mM	0.5
Primer F	0.25
Primer R	0.25
DMSO	0.325
Betaine 5 M	6.5
Taq Pol (5 U/µl)	0.2

To do the PCR reaction mixes, 23 µl of the master mix and 2 µl of the template (sample or control) were added to each well, being that both reaction mixes had three controls, one positive, one negative and one blank, to indicate if the PCR reaction was effective. The tubes were then put into the thermocycler (Eppendorf, Mastercycler epgradient S), where the selected program is presented in **Table 3**.

Table 3 – Program selected in the thermocycler for the amplification of the amisyn gene.

94°C	5 min	1 cycle
94°C	15 sec	10 cycles
63°C	30 sec	
72°C	40 sec	
94°C	15 sec	30 cycles
58°C	30 sec	
72°C	40 sec	
72°C	5 min	1 cycle
4°C	∞	∞

2.7.3. Electrophoresis

After the PCR reaction, electrophoresis was done, recurring to a mixture of 1.2% agarose gel (agarose powder – Biozym, 840004 – diluted in 1xTAE buffer) and ethidium bromide (VWR, E406) (in a proportion of 4000:1), where samples, controls and DNA ladder (100 bp, BioLabs, N3231S) were loaded. The electrophoresis machine (Power supply - CONSORT, EV231- and tank – DNA Sub-Cell) was set to 100 V for 50 min. In the chamber 1xTAE buffer (composed by 39.95 mM Tris, 19.78 mM acetic acid and 5.89 mM EDTA) was covering the gel, allowing the passage of current through the wells which permitted the migration of samples accordingly with their molecular size.

2.7.4. Scan and data analysis

The resulting bands were seen recurring to Intas® UV-SYSTEME, FastGene Blue/Green transilluminator XL, Intas® camera (lens - Rainbow TV ZOOM LENS S6X11 11.5-69 mm 1:1.4) and Intas® GelDoc System v.0.2.24 software. A knock-out mouse had only a band in the floxed reaction, and a wild-type mouse had only a band in the wild-type reaction. The heterozygous mouse had 1 band in both responses.

2.8. Western Blot

2.8.1. Preparation of brain homogenates

Sample preparation was done first by grinding (CryoGrinder Kit™ 230 V – OPS DIAGNOSTICS, CG 08-01-230) the tissue (cortex or hippocampus), maintaining its frozen state, followed by the addition of 3 metallic beads and 360 µl of a homogenization buffer, constituted by 80 mM NaCl, 1 mM EDTA, 20 mM HEPES pH 7.4 (Roth, HN78.1), 0.08 g of cOmplete Protease Inhibitor Cocktail (Roche, 05892953001), 1 tablet of phosSTOP phosphatase inhibitor (Roche, 04906837001) and 0.0016 g of dithiothreitol (Roth, 6908.1) in a final volume of 10 ml. After that, the tubes were subjected to oscillation in a bead mill (Retsch, MM400) for 1 min at 20-30 Hz (depending on if it was hippocampal or cortical tissue, respectively) and to spin down (Eppendorf, centrifuge 5424) at the maximum speed for 10 sec (to reduce the amount of foam). Next, 40 µl of 20% SDS at 60°C were added, the tubes were oscillated at 20-30 Hz for 1 min and were spin down for 10 sec at max speed. Finally, up and down 15-30x with a 27G needle (Braun, 4657705) in a 1 ml syringe (NORM-JECT®, 4010-200V0) was performed.

2.8.2. Quantification of brain homogenates

To quantify the prepared samples, BCA assay was done as described in 2.1.4., however, the brain homogenates were diluted 1:20 with homogenization buffer.

2.8.3. Samples preparation and electrophoresis

In an Excel, sheet the absorbances were converted to concentration using the equation given by the standard curve and calculated the necessary sample dilutions to obtain a final concentration

of protein per well of 35 µg. The samples dilution was done with homogenization buffer and sample loading buffer. Then the samples were boiled at 95°C for 5 min in the thermomixer comfort (Eppendorf).

The electrophoresis and its preparation steps were done as described in 2.2.2. section.

2.8.4. Transfer to a membrane and blocking

The cassettes were mounted, with 2 filter papers, 2 sponges, a nitrocellulose membrane (GE Healthcare, 10600001), and the gel, in transfer buffer, which was constituted by 24.76 mM of tris, 199.81 mM of glycine and 20% (v/v) of methanol. The machine (power supply and chamber) was set to 100 V for 90 min and maintained at 4°C. When the membrane was ready, it was cut in the desired way and blocked for 1 h at room temperature (RT) with milk 5% (Roth, t145.2) diluted in TBS-T (TBS is composed by 19.81 mM Tris and 149.90 mM NaCl pH 7.6, TBS-T is prepared by adding 0.1% of Tween20 – Roth, 9127.1 - to TBS).

2.8.5. Incubations with primary and secondary antibodies

After three washings of the membrane with TBS-T for 5 min at RT, the membrane was incubated with the primary antibody at 4°C overnight (ON) with soft agitation. The primary antibodies used are discriminated in **Table 4**.

Table 4 - Primary antibodies used for Western Blot with their corresponding dilutions.

Target protein	Manufacturer	Species	Concentration	Diluted in
Endophilin-A1 L-18	Santa Cruz sc-247945	Goat	1:2000	Milk 5% in TBS-T
Rab7A	NovusBio NBP1-05048	Rabbit	1:1000	Milk 5% in TBS-T
Synapsin1/2	SySy 106002	Rabbit	1:5000	Milk 5% in TBS-T
α-synuclein	Sysy 128002	Rabbit	1:1000	Milk 5% in TBS-T
Rab3A/B	Sysy 107011	Mouse	1:1000	Milk 5% in TBS-T
GluA2	Millipore MAB397	Mouse	1:1000	Milk 5% in TBS-T
CaVα2δ4	Alomone Labs ACC-104	Rabbit	1:200	BSA 1% in PBS
RPL7	Abcam ab72550	Rabbit	1:6000	BSA 3% in PBS
PSD95 PDZ domain	Sysy 124011	Mouse	1:1000	BSA 2.5% in TBS with 0.2% of Tween20
CDK5 C-8	Santa Cruz sc-173	Rabbit	1:200	Milk 5% in TBS-T
RIM1	Sysy 140003	Rabbit	1:1000	Milk 5% in TBS-T
Synaptotagmin1	Sysy 105011	Mouse	1:1000	Milk 5% in TBS-T
Synaptophysin1 7.2	Sysy 101011	Mouse	1:5000	Milk 5% in TBS-T
Amisyn	Amichen #172 (custom-made Ab)	Rabbit	1:500	TBS-T
Amisyn	Sigma-Aldrich HPA003552	Rabbit	1:500	Milk 5% in TBS-T
GST	EMD Millipore AB3282	Rabbit	1:10000	Milk 5% in TBS-T
VAMP2 69.1	Sysy 104211	Mouse	1:1000	Milk 5% in TBS-T

Rabphilin3 R44	Sysy 118002	Rabbit	1:1000	Milk 5% in TBS-T
Homer1	Sysy 160003	Rabbit	1:1000	Milk 5% in TBS-T
Syntaxin1A	Sysy 110302	Rabbit	1:1000	Milk 5% in TBS-T
Syntaxin16	Sysy 110162	Rabbit	1:1000	Milk 5% in TBS-T
EEA1	Sysy 237 002	Rabbit	1:1000	Milk 5% in TBS-T
SNAP47	Sysy 111403	Rabbit	1:1000	Milk 5% in TBS-T
ERK1/2	Cell Signalling #9102	Rabbit	1:1000	Milk 5% in TBS-T
P-ERK1/2	Cell Signalling #9101	Rabbit	1:1000	Milk 5% in TBS-T
CREB (48H2)	Cell Signalling #9197	Rabbit	1:1000	Milk 5% in TBS-T
P-CREB (87G3)	Cell Signalling #9198	Rabbit	1:1000	Milk 5% in TBS-T

On the next day, the membrane was washed with TBS-T three times for 10 min at RT and then was incubated with the corresponding secondary antibodies for 1 h at RT protected from light. The secondary antibodies used were all diluted 1:7000 in milk 5% (in TBS-T) and the following were used: 800CW donkey anti-goat (LI-COR IRDye®, 926-32214), 680LT goat (polyclonal) anti-mouse (LI-COR IRDye®, 926-68020), 680LT goat (polyclonal) anti-rabbit (LI-COR IRDye®, 926-68021) and 800CW goat anti-rabbit (LI-COR IRDye®, 926-32211).

2.8.6. Membrane scans and data analysis

After the incubation, the membrane was washed with TBS-T three times for 10 min at RT and scanned with Odyssey infrared imaging system (LI-COR) and Image Studio Ver. 5.2 software to see the protein bands identified by the fluorophores present in the secondary antibodies.

The bands visualized in the membrane were quantified recurring to the ImageJ Fiji Software. Next, the value corresponding to each protein band was normalized to the control protein (RPL7). The wild-type mice were then compared with the knock-out mice through statistical analysis with a paired T-test using Microsoft Excel 2016 (16.0.5017.1000). The graphs were done resorting to Graph Pad Prism 8.

2.9. Real-time polymerase chain reaction (qPCR)

2.9.1. RNA isolation

To isolate the RNA, the tissue was grinded until it became a thin powder, then it was added 1 ml of Trizol (Sigma, T9424), and the mixture was incubated for 5 min at RT. After the incubation, 0.2 ml of chloroform (Applichem, AO642.1000) was added, followed by incubation at RT for 3 min and centrifugation (Eppendorf, Centrifuge 5415 R) at 12000 g for 15 min at 4°C. The aqueous phase formed was retrieved, it was added to it 0.5 ml of 100% isopropanol (Roth, T910.1), it was incubated for 10 min at RT and centrifuged at 12000 g at 4°C for 10 min. Then the supernatant was discarded, it was added 1 ml of 75% ethanol (J. T. Baker, 8025), the tubes were centrifuged at 12000 g for 10 min at 4°C and let air dry for 10 min. Finally, 20-50 µl (depending on the size of the pellet) of RNAse-Free water (Biolab products, 31-00847) were added, the tubes were incubated for 15 min at 55°C in the heat block (bioSan, TDB-120) and the respective concentration was measured in Nanodrop® Spectrophotometer ND-1000 (PeqLab) recurring to ND-1000 V.3.8.1 software.

2.9.2. cDNA synthesis

A master mix composed of 5 µl of nuclease-free water, 4 µl of 5x iScript reaction mix, and 1 µl of iScript reverse transcriptase (cDNA synthesis kit – BioRad, 1708890) (volumes per reaction) was done. Next, the dilution of the isolated RNA with nuclease-free water (in a final volume of 10 µl) was performed, and the solution obtained had an RNA mass of 1000 ng. Next, to the wells were added 10 µl of master mix and 10 µl of diluted RNA. The tubes were put into the thermocycler (UNOII Biometra®), where the program presented in **Table 5** was selected. After about 20 min, the cDNA was diluted with miliQ water in a proportion of 1:50.

Table 5- Program selected in the thermocycler for the cDNA synthesis.

5 min	25°C
20 min	46°C
1 min	4°C
∞	4°C

2.9.3. qPCR

The qPCR was done in a 384 well plate where 4 µl of master mix (90% SYBR® Green - BioLabs, M3003E -, 5% of reverse primer and 5% of forward primer) and 4 µl of the sample were added in each well. All the primers used are listed in **Table 6**.

Table 6 – List of the qPCR primers used. F: forward, R: reverse.

Protein	Gene	Primer		Manufacturer
mAmisyn	STXBP6	F	AGCACGGCCTCAGAAAAGTG	IDT
		R	AGGATGCTGTTTCCTCCCATA	
mPSD95	DGL4	F	TGAGATCAGTCATAGCAGCTACT	IDT
		R	CTTCCTCCCCTAGCAGGTCC	
mRPL7	RPL7	F	CTGCTGGGCCAAAAACTCTCA	IDT
		R	CCTTCAACTCTGCGAAATTCCTT	
mCAMK4	CAMK4	F	CTCTCACACCCGAACATCATAAA	IDT
		R	CTCACTGTAGTATCCCTTCTCCA	
mCAMK2B	CAMK2B	F	CGTTTCACCGACGAGTACCAG	IDT
		R	GCGTACAATGTTGGAATGCTTC	
mCREB	CREB1	F	CAGTGGGCAGTACATTGCCAT	IDT
		R	CTGCTGTCCATCAGTGGTCTG	
mPKC	PRKCA	F	GTTTACCCGGCCAACGACT	IDT
		R	GGGCGATGAATTTGTGGTCTT	
mPKA	PRKACA	F	AGATCGTCCTGACCTTTGAGT	IDT
		R	GGCAAAACCGAAGTCTGTCAC	
mCDK5	CDK5	F	CCCTGAGATTGTGAAGTCATTCC	IDT
		R	CCAATTTCAACTCCCCATTCCT	
mRhoA	RHOA	F	AGCTTGTGGTAAGACATGCTTG	IDT
		R	GTGTCCCATAAAGCCAACTCTAC	
mSTX1A	STX1A	F	CCCACAAGGAGATACATTCCCA	IDT

		R	AACGAAATCCAAAACGGCAGT	
mTomosyn	STXBP5	F	CCAGAGCCATGCAAGCCTATC	IDT
		R	CAGAGTGTGAGAAAGTCAACGAT	
mComplexin2	CPLX2	F	AAGAGCGCAAGGCGAAACA	IDT
		R	TGGCAGATATTTGAGCACTGTG	
mSTX2	STX2	F	TGTGGAGAAGGATCATTTCATGG	IDT
		R	TGCTCAATAGACTTCAGCTTGC	
mSTX4	STX4	F	CCCGGACGACGAGTTCTTC	IDT
		R	TTTGATCTCCTCTCGCAGGTT	
mSNAP25	SNP25	F	CAACTGGAACGCATTGAGGAA	IDT
		R	GGCCACTACTCCATCCTGATTAT	
mMunc13-1	UNC13A	F	CATCCTCCTGGACGCTCATTT	IDT
		R	TTCTCCCCAGCCAAAGTAATTC	
mMunc18	STXBP1	F	GTGGACCAGTTAAGCATGAGG	IDT
		R	GCTCTCGGCGCTTGTTGAT	
mSV2A	SV2A	F	GGCTTTCGAGACCGAGCAG	IDT
		R	GACCTTCGGGAATACTCATCCT	
mα-synuclein	SNCA	F	GCAAGGGTGAGGAGGGGTA	IDT
		R	CCTCTGAAGGCATTTCATAAGCC	
mRab3A	RAB3A	F	TCTTCCGCTACGCAGATGACT	IDT
		R	TGTCGTTGCGGTAGATGGTTT	
mSyn1	SYN1	F	CCAATCTGCCGAATGGGTACA	IDT
		R	GCGTTAGACAGCGACGAGAA	
mITSN1	ITSN1	F	CACCAGCATTTGGTATAGGAGG	IDT
		R	GGACAGAAGATACTAAGGGTGGA	
mDynamin1	DNM1	F	AATATGCCGAGTTCCTGCACT	IDT
		R	GTCTCAGCCTCGATCTCCAG	
mBassoon	BSN	F	GGGCAGCCAGAGAACAACTT	IDT
		R	GGGACAGAGTAGGGTGACG	
mDBH	DBH	F	GAGGCGGCTTCCATGTACG	IDT
		R	TCCAGGGGGATGTGGTAGG	
mVAMP2	VAMP2	F	GCTGGATGACCGTGCAGAT	IDT
		R	GATGGCGCAGATCACTCCC	
mSyt1	SYT1	F	CTGTCACCACTGTTGCGAC	IDT
		R	GGCAATGGGATTTTATGCAGTTC	
mSTX6	STX6	F	ACAGGCCGTCATGCTAGATG	IDT
		R	GGATGGCTATGGCACACCAC	
mHomer1	HOMER1	F	CCCTCTCTCATGCTAGTTCAGC	IDT
		R	GCACAGCGTTTGCTTGACT	
mRab7A	RAB7A	F	CCTGGGGGACTCTGGTGTTG	IDT
		R	TGTCGTCCACCATCACCTCC	
mRab5A	RAB5A	F	AGTCTGCTGTTGGCAAATCAAG	IDT
		R	CCGTTCTTGACCAGCTGTATCC	
mNPY	NPY1R	F	TGGACTGACCCTCGCTCTAT	IDT
		R	TGTCTCAGGGCTGGATCTCT	
mEndoA1	SH3GL2	F	TCATTGGACATGGAAGTGAAGC	IDT
		R	ACTCGGCGATTTCTTTAGACTCA	

The plate was centrifuged (brand) at 3000-5000 g for 1-2 min, to remove the air bubbles, and was put in the thermocycler (QuadStudio 6 Flex, Applied Biosystems by Life Technologies) where the program in **Table 7** was used.

Table 7 – Program used in the thermocycler for sequence amplification.

Stage 1 (x1)	95°C	10 min
Stage 2 (x40)	95°C	21 sec
	56°C	30 sec
	72°C	30 sec
Melt Curve (x1)	85°C	15 sec
	52°C	30 sec
	95°C	15 sec

2.9.4. Data analysis

The data generated from the machine was exported to an excel file using the QuantStudio Real-Time PCR Software. The CT values were converted in delta delta CT by normalizing the data to RPL7 gene and then, these values were converted into expression levels. The mean of the wild-type (WT) mice was compared with the mean of the knock-out (KO) mice by performing a one-tailed t-test for two samples with unequal variance. Graph Pad Prism 8 was the chosen program to do the diagrams.

3. Results

3.1. Expression of amisyn by bacterial *E. coli* expression system and purification by liquid chromatography (LC)

Kondratiuk et al. (2020) discovered that amisyn's association with the plasma membrane is mediated through signaling phospholipid PI(4,5)P_2. My first task was to explore if the amisyn's association with PI(4,5)P_2 was dependent on the PH domain. To this end, I purified WT amisyn protein, as well as amisyn mutant AADD. Amisyn AADD is a particular mutation of amisyn in which its PH domain is mutated (K30A, K32A, K64D, K66D). It was proven by in vitro experiments that this AADD amisyn could not bind with the plasma membrane (Kondratiuk et al., 2020). I have first expressed WT amisyn protein in the bacterial *E. coli* heterologous expression system, as detailed in Methods. To verify the efficacy of the IPTG induction of the amisyn expression, a Coomassie staining was made on the samples collected before and after the aforementioned induction. In **Figure 9**, it is visible that after induction the amount of GST-amisyn is much higher than before IPTG was introduced, which shows that the expression process is effective.

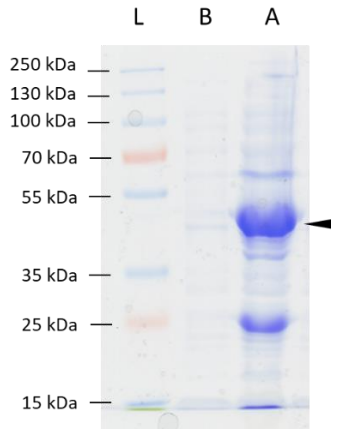

Figure 9– Coomassie blue-stained gel with samples WT before (B) and after (A) IPTG induction. kDa: kilodaltons; L: Molecular weight marker; Black arrowhead: GST-amisyn band.

We next isolated expressed protein from the broken bacterial cells and subjected it to fast protein liquid chromatography (FPLC), followed by cleavage of the GST tag. To assess the effectiveness of the glutathione sepharose column in separating the GST tag from amisyn, a Western Blot was made comparing a purified sample and a sample after dialysis. As can be observed in **Figure 10**, the purified sample has a major decrease in the amount of GST when compared to the sample after dialysis; however, some GST remains in the purified sample, as well as some amisyn-GST.

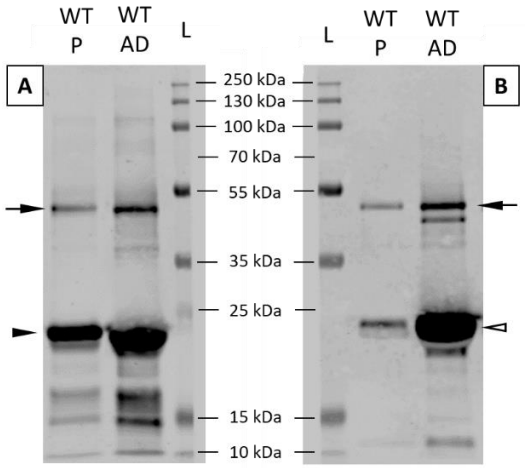

Figure 10- Western Blot with samples of the WT amisyn purification after dialysis (WT AD) and after the conclusion of the WT amisyn purification (WT P). A) Incubation with anti-amisyn (Sigma-Aldrich) antibody and B) with anti-GST antibody (EMD Millipore). kDa: kilodaltons; L: Molecular weight marker; Arrow: Amisyn-GST band; Black arrowhead: Amisyn band; White arrowhead: GST band.

3.2. Liposome co-sedimentation assay reveals that amisyn interacts with PI(4,5)P_2 through its PH domain

To assess if the amisyn association with PI(4,5)P_2 in the membrane was dependent on the existence of the PH domain in the molecule, the co-sedimentation lipid assay was performed as described in Methods. **Figure 11** shows the results of this experiment (performed three times with consistent results). First, it is possible to observe a control band in the WT and AADD amisyn supernatant without liposomes. Curiously, WT amisyn co-sedimented with PI(4,5)P2 containing liposomes, but amisyn AADD mutant did not. These results indicate that amisyn (WT) binds to PI(4,5)P_2 through its PH domain: when the PH domain is mutated in such a way that it cannot bind PI(4,5)P2, the mutant protein remains in the supernatant.

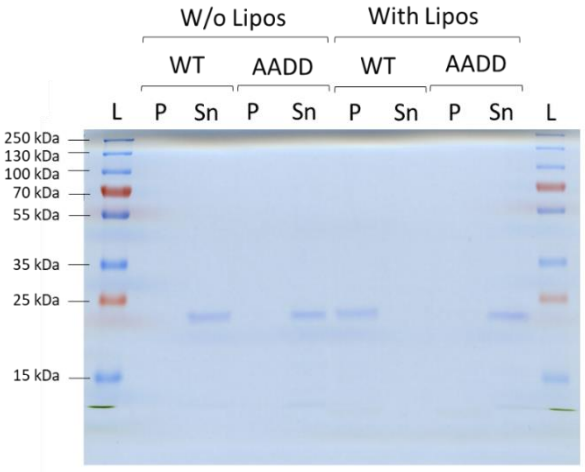

Figure 11- Liposome co-sedimentation assay result between liposomes ("Lipos") containing 2% PI(4,5)P_2 and amisyn (WT and AADD). n (number of technical repetitions) =3; kDa: kilodaltons; L: Molecular weight marker; P: pellet; Sn: supernatant; W/o: without.

3.3. Phosphorylation sites predictions

For many proteins, their interaction with phospholipids in the biological membranes has been tightly regulated by phosphorylation by various kinases: a good example of this is the phosphorylation of endophilin-A by LRRK2, which modulates synaptic vesicle endocytosis (Matta et al., 2012). We, therefore, wanted to explore if amisyn may undergo phosphorylation that would regulate its interaction with the PI(4,5)P_2-rich plasma membrane. The predictions of possible phosphorylation sites in amisyn were done with the intent of understanding if phosphorylation could be one of the regulation mechanisms of this protein's recruitment to the membranes. In **Table 8**, one can observe that amino acids T29, T135, and T58 are the only sites predicted by all three software used (GPS Web Service, NetPhos3.1 server, and NetPhospan), being more likely the key phosphorylated sites on amisyn protein.

Table 8- Predicted phosphorylation sites and their corresponding prediction values which were given by each software. In blue, the three phosphorylation sites predicted by three software are highlighted.

Position (Aminoacid)		**DTU Health Tech**	
GPS Web Service		**NetPhos3.1 Server**	**NetPhospan**
29 (T)	42.021 - PKC	0.923 - PKC	0.6582 - PKCA
51 (S)	Not Predicted	0.893 - PKC	Predictions under 0.5
53 (T)	35.614 - CDK	0.893 -PKC	Predictions under 0.5
58 (T)	32.637 - CDK	0.595 - PKC	0.5283 - PKCA
61 (S)	135.88 - PKC	0.660 - PKC	Predictions under 0.5
135 (T)	19.021 - PKC	0.803 - PKC	0.5148 - PKCA
153 (S)	109.454 - PKC	Predictions under 0.5	Predictions under 0.5

With the objective of understanding if the sites predicted could play a role in the regulation of membrane binding, their locations were highlighted in a PH domain model. **Figure 12** shows the models of the amisyn PH domain, where the identified Threonine 58 (T58; shown in blue) and Threonine 135 (T135; shown in purple) are close to each other in the structure and are positioned opposite of the active site of the PH domain, capable of binding PI(4,5)P_2. In **Figure 13**, it is observable that the T29 is in close proximity to the four mutation sites present in amisyn AADD, which might be an indicator of regulation of the interaction between amisyn's PH domain and PI(4,5)P_2. These data need to be confirmed experimentally.

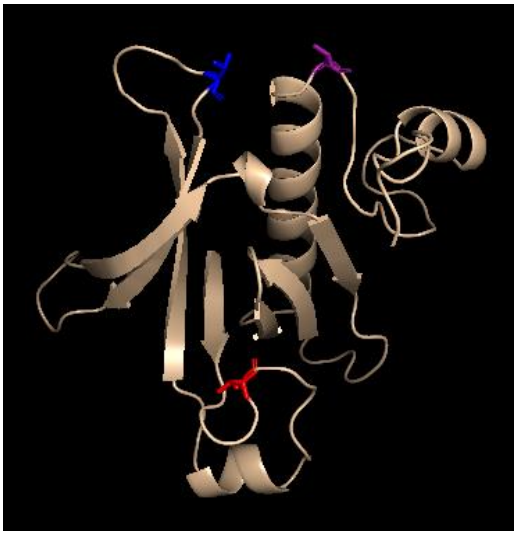

Figure 12- Model of the amisyn PH domain, where it is identified in blue the Threonine 58 (T58), in purple the Threonine 135 (T135) and in red the Threonine 29 (T29). Model produced by Ph.D. A. Krisko and Ph.D. I. Milosevic.

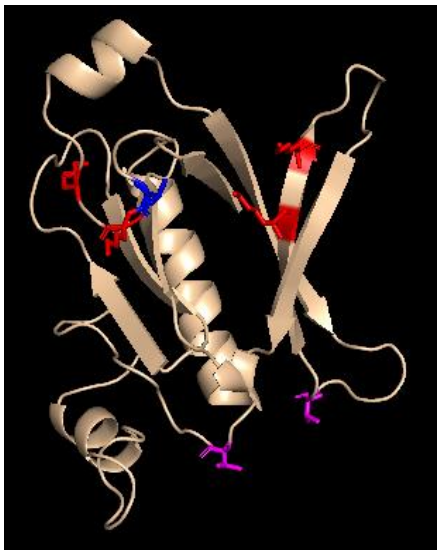

Figure 13- Model of the amisyn PH domain, where the T29 is identified in blue, the T58 and T135 are highlighted in pink and in red are illustrated the mutation sites present in the AADD amisyn. Model produced by Ph.D. A. Krisko and Ph.D. I. Milosevic.

3.4. Genotyping of amisyn KO mice and gross phenotype of amisyn mutants

The genotyping of the mice was a procedure done routinely for the many experiments detailed below and to know the genotype of each mice tested, which could be WT, KO, or heterozygous (HT). In the example presented in **Figure 14**, it is possible to observe one band in both reactions for the numbers 684, 688 and 692 indicating that they are HT. In the numbers 685, 690 and 691 there is only a band in the LoxF reaction meaning that they are KO, and the remaining numbers (686, 687, and 689) are WT since they only have a band in the WT reaction.

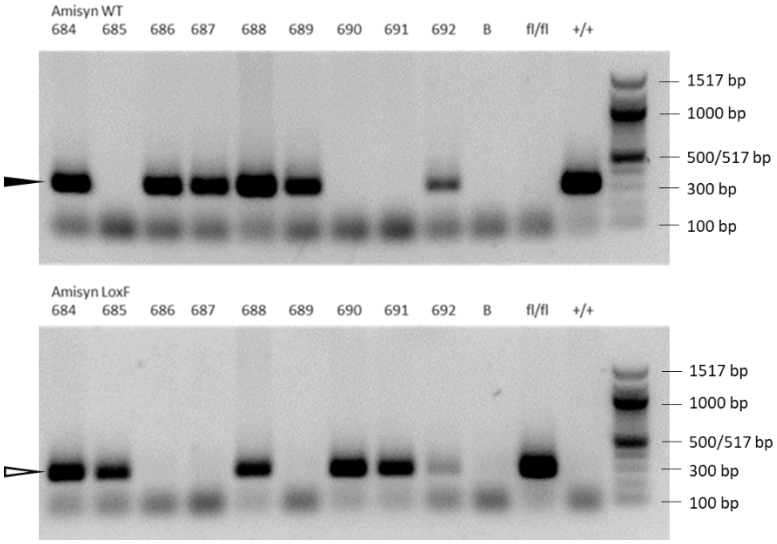

Figure 14- Genotyping of the mice identified by the numbers 684-692. B: blank; fl/fl: negative control (KO); +/+: positive control (WT); bp: base pairs; Black arrowhead: band that corresponds to WT allele; White arrowhead: band corresponding to KO allele.

When observing amisyn HT and amisyn KO mice in comparison to littermate controls (WT mice), no obvious differences in animal size, weight, or shape can be seen. Amisyn KO mice are born according to the Mendelian ratio and are viable. All inspected organs look normal when examined by the naked eye, including the brain.

3.5. Characterization of protein expression in amisyn mutant mice

To assess if the lack of amisyn would affect the protein levels in the brain, various Western Blots were done using hippocampal and cortex homogenates to test for the levels of proteins involved in various phases of synaptic transmission. To do this, the hippocampus and cortex were isolated, and protein homogenates were prepared as detailed in Methods. After the sample preparation, the Western Blot technique was executed, where the proteins in a gel were transferred to membranes, which were stained with the desired primary and secondary antibodies. Finally, the membranes were scanned and analyzed statistically with a paired T-test.

3.5.1. Amisyn is expressed in mouse hippocampus and cortex tissue

Based on the data shown in Scales at al. (2002), amisyn is mainly a brain-enriched protein. We wanted to inspect its presence in the homogenates prepared from the hippocampus and cortex. The hippocampal area is an important tissue to test since it is the site where amisyn is most expressed based on unpublished data present in Milosevic's laboratory (Jin, and Milosevic, private communications) and due to its putative function in memory formation (Cohen, Jin, and Milosevic, private communications). Cortex is also a tissue whose testing is essential because of its importance in behavior assays that relate to ASD, such as the novel vs. familiar object recognition test. In this assay, the amisyn KO mice were found to have no difference in the preference between the novel and the familiar object, opposed to the increased preference of the WT animals for the novel object

(Cohen and Milosevic, unpublished lab data). In **Figure 15**, it is possible to observe that amisyn is expressed in the cortex and hippocampus of the WT mice. Since the same amount of protein homogenate is loaded on the gel (35 µg/lane), one can observe that amisyn is expressed in hippocampus 1.25 times more than in the cortex (mean of 8 samples from 2 gels – cortex -, mean of 7 samples from 2 gels - hippocampus).

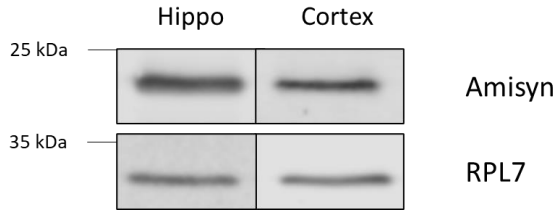

Figure 15- Expression of amisyn in cortex and hippocampus of WT animals. A custom-produced anti-amisyn (Amichen) antibody was used. kDa: kilodaltons. RPL7 was used as a loading control.

3.5.2. Levels of amisyn in the brain of amisyn mutant mice

Using Western Blot-based experiments, we next inspected for the remaining amount of amisyn in the amisyn KO brain tissue, if any. The knock-out first approach used to generate these mice is known to be somewhat 'leaky', meaning that there could be cells in the brain of amisyn KO mice where some amisyn is still expressed. Data obtained on a large number of animals show a large variability (about 3-fold) in amisyn levels, both in WT and amisyn KO mice (**Figure 16**). While a major decrease (about 71%) of expressed amisyn protein is observed in the hippocampus of amisyn KO mice, some small amount of protein remains (on average 29%). This result suggests the validity of the amisyn KO mouse line.

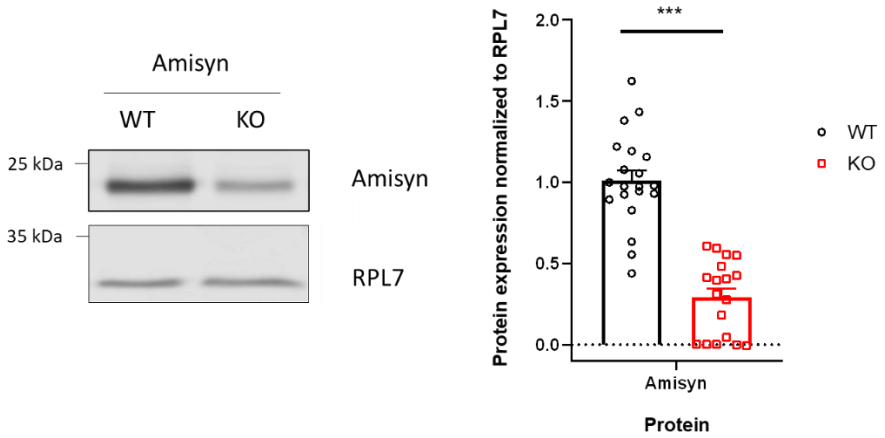

Figure 16- Levels of amisyn present in WT and KO hippocampal tissue. Custom-produced anti-amisyn (Amichen) antibody was used. n (number of biological replicates) =20 (WT) and n=18 (KO) mice; ***: p-value<0.001; kDa: kilodaltons. RPL7 was used as a loading control. Data are shown as mean±SEM.

3.5.3. Levels of endosomal proteins in the brain of amisyn mutant mice

To explore the effect of amisyn absence in the endocytic process in cortex and hippocampus, Western Blot was performed with both tissues of WT and KO mice to analyze the expression of endosomal proteins. EEA1 (early endosome antigen 1) is a Rab5 effector membrane-bound protein present specifically in early endosomes (Sun et al., 2020). We did not detect significant alterations in the levels of EEA1 protein in the amisyn KO mice (**Figures 17** and **18**). The late endosome protein Rab7A is a small GTPase related to Ras that has a key role in the endocytic process (Sun et al., 2020). We did not find a significant change regarding this protein in the amisyn KO mice (**Figures 17** and **18**). CDK5, a protein kinase responsible for the phosphorylation of dynamin1 (Tan et al., 2003), was also not significantly changed in the mice that lack amisyn (**Figures 17** and **18**). These results might indicate that amisyn does not interfere with the formation of early endosomes and CDK5 activity.

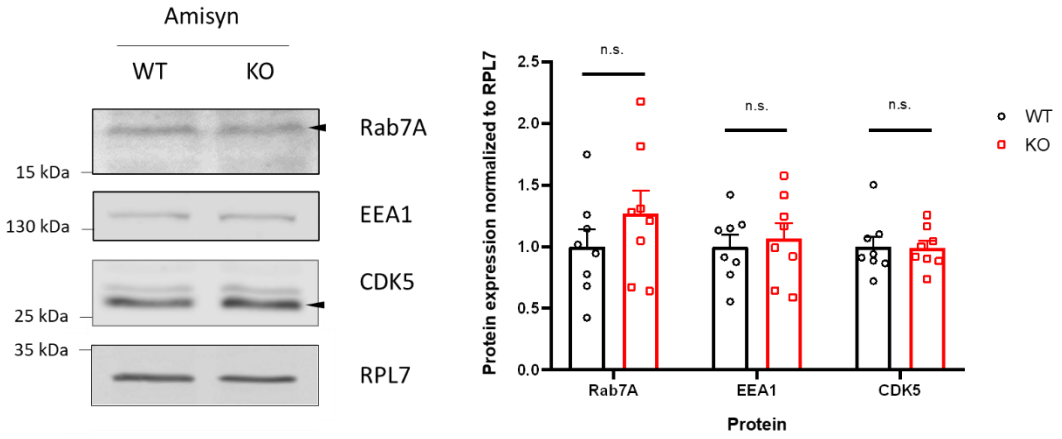

Figure 17- Levels of endosomal proteins present in WT and KO cortical tissue. n=8; n.s.: not significant; kDa: kilodaltons. RPL7 was used as a loading control. Data are shown as mean±SEM.

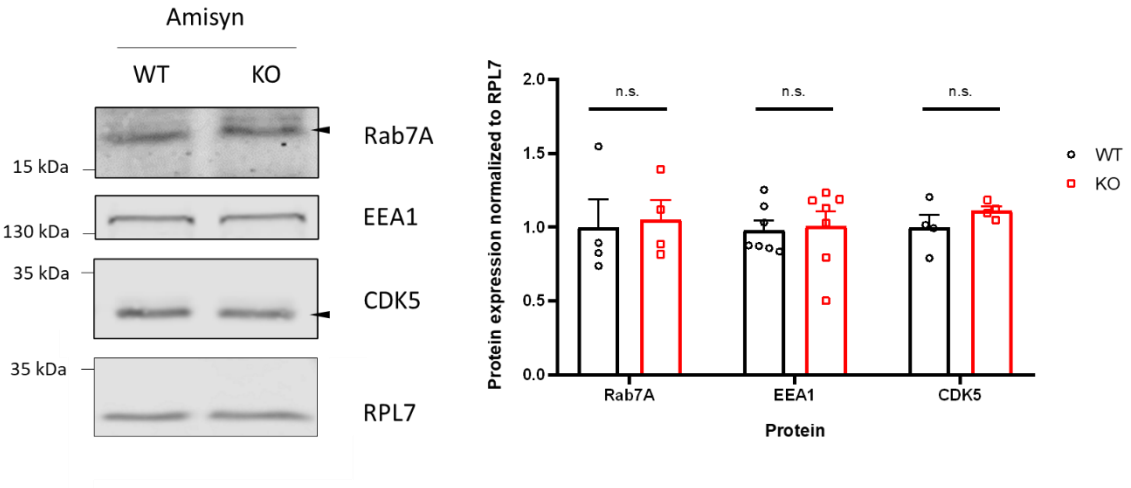

Figure 18- Levels of endosomal proteins present in WT and KO hippocampal tissue. n=4 (Rab7A and CDK5) and n=7 (EEA1); n.s.: not significant; kDa: kilodaltons. RPL7 was used as a loading control. Data are shown as mean±SEM.

3.5.4. Levels of peripheral vesicle proteins in the brain of amisyn mutant mice

Since tomosyn was reported to interact with synapsin and Rab3 (Cazares et al., 2016), we inspected if amisyn could influence the protein levels of the same or other peripheral proteins. To test this hypothesis, cortical and hippocampal tissue from WT and KO amisyn mice were used for Western Blot experiments to analyze the protein expression of such proteins. Endophilin-A1 is a protein that recruits dynamin to the neck of endocytic vesicles, allowing the termination of the budding process (Milosevic et al., 2011). We did not detect significant alterations in the levels of endophilin-A protein in the amisyn KO mice (**Figure 19** and **20**). In the case of Rab3A, a GTPase Ras-associated protein responsible for the recruitment of synaptic vesicles to the plasma membrane (Geppert et al., 1994), we observed a significant increase of Rab3A in the hippocampus of the KO amisyn mice (**Figure 20**). However, when cortex tissue was inspected, the similar increase in the Rab3 protein level was not detected (**Figure 19**). A similar observation was made for α-synuclein, a protein that negatively regulates neurotransmitter release (Emanuele & Chieregatti, 2015): α-synuclein protein levels were elevated in the hippocampus (**Figure 20**), but not the cortex of amisyn KO mice (**Figure 19**). An increase in the number of synaptic vesicles in the amisyn KO mice can be a potential explanation of our result. And this hypothesis might further explain the higher release probability seen in the amisyn KO mice (Jin and Milosevic, unpublished lab data). Protein levels differences between the two tested tissues might suggest its distinct functions in the hippocampus and cortex.

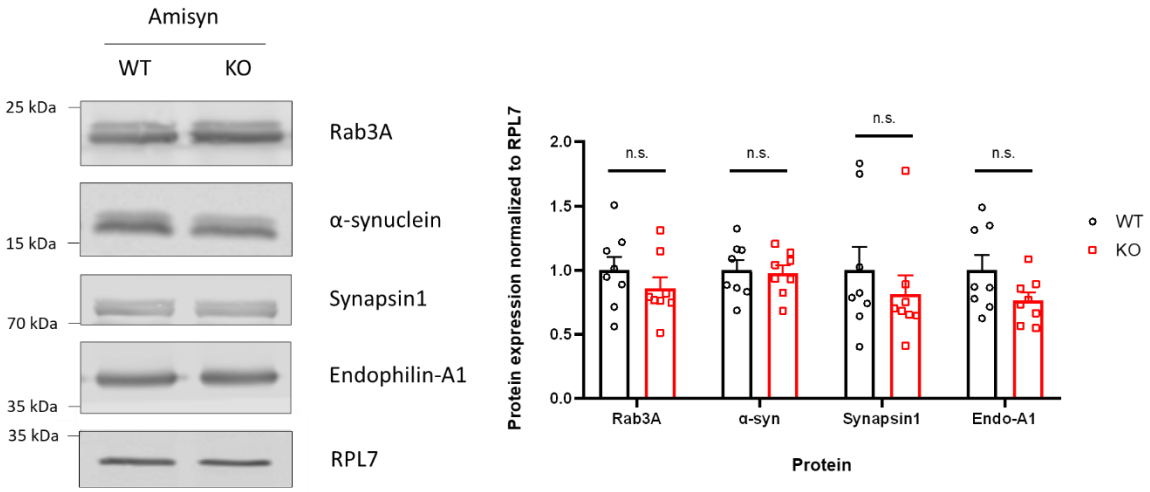

Figure 19- Levels of peripheral vesicle proteins present in WT and KO cortical tissue. n=8; n.s.: not significant; kDa: kilodaltons. RPL7 was used as a loading control. Data are shown as mean±SEM.

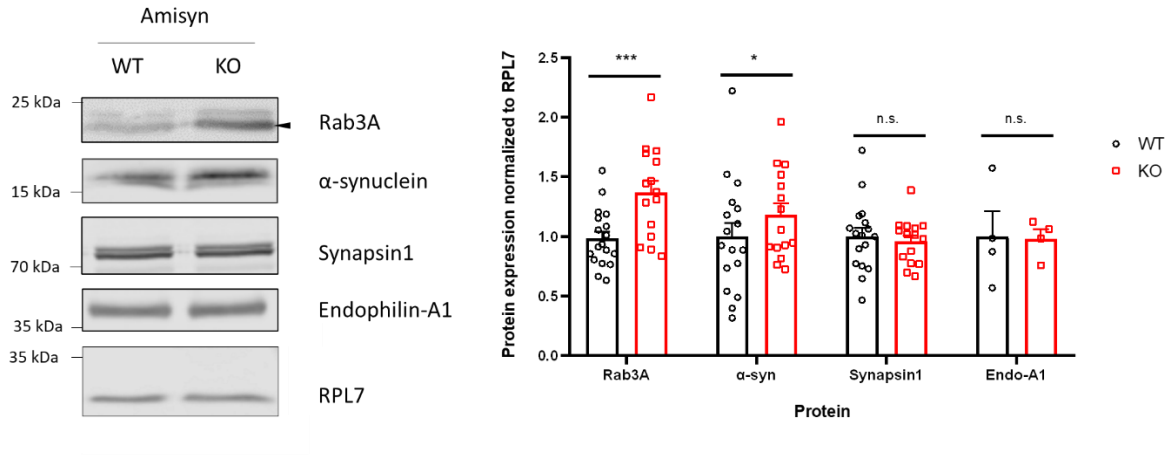

Figure 20- Levels of peripheral vesicle proteins present in WT and KO hippocampal tissue. n=18 (Rab3A WT), n=17 (α-syn and synapsin1 WT), n=15 (Rab3A, α-syn and synapsin1 KO) and n=4 (Endo-A1); n.s.: not significant; *: p-value<0.05; ***: p-value<0.001; kDa: kilodaltons. RPL7 was used as a loading control. Data are shown as mean±SEM.

3.5.5. Levels of integral synaptic vesicle proteins in the brain of amisyn mutant mice

Integral synaptic vesicle proteins were inspected via Western Blot next in hippocampal tissue from WT and KO mice, because VAMP2 was reported as one of the amisyn's competitors (Kondratiuk et al., 2020) and tomosyn is known to interact with synaptotagmin1 (Geerts et al., 2017). VAMP2 is a synaptic vesicle R-SNARE protein responsible for mediating the fusion of synaptic vesicles through SNARE complex formation (Salpietro et al., 2019). This protein was found to be significantly lower (about 8%, p-value=0.0164) in the amisyn KO hippocampus in relation to the WT animals (**Figure 21**). This might be because amisyn is a competitor of VAMP2 (Kondratiuk et al., 2020), and when there is a decrease of amisyn levels there is less need of VAMP2.

Synaptotagmin1 (SYT1) is a synaptic vesicle protein that triggers neurotransmitter release upon Ca^{2+} influx (Courtney et al., 2019), while synaptophysin1 is a synaptic vesicle protein responsible for ensuring the retrieval of VAMP2 to the synaptic vesicle during the endocytic process (Gordon et al., 2016). The two aforementioned synaptic vesicle proteins, as opposed to VAMP2, were found to be not changed in the amisyn KO hippocampal tissue (**Figure 21**).

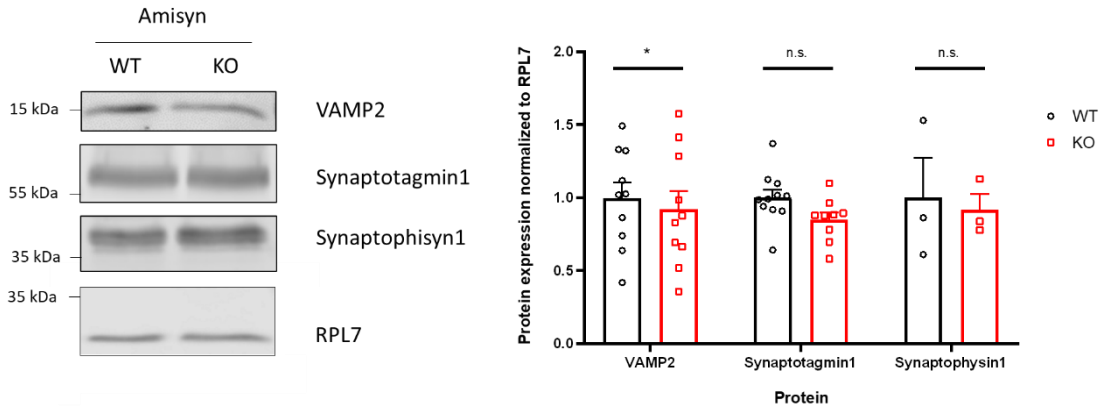

Figure 21- Levels of integral vesicle proteins present in WT and KO hippocampal tissue. n=10 (VAMP2), n=11 (SYT1 WT), n=9 (SYT1 KO) and n=3 (synaptophysin1); n.s.: not significant; *: p-value<0.05; kDa: kilodaltons. RPL7 was used as a loading control. Data are shown as mean±SEM.

3.5.6. Levels of Q-SNARE proteins in the brain of amisyn mutant mice

The protein levels of Q-SNARE proteins were inspected in WT and amisyn KO hippocampus via Western Blot because amisyn is known to interact with syntaxin1 and syntaxin4 (Scales et al., 2002). SNAP47 is a protein that mediates the insertion of AMPAR in the postsynaptic membrane (Kádková et al., 2019), while syntaxin16 (STX16) is responsible for the transport between the TGN and the endosome of lipids and proteins to aid the maturation process (Chen et al., 2010). Both of the previously mentioned proteins do not show any significant changes in the amisyn KO mice (**Figure 22**). Syntaxin1A (STX1A), a plasma membrane protein that is involved in the formation of the SNAREpin which mediates the synaptic vesicle fusion (Mason, 2017a), was also found not significantly changed even though it is one of the amisyn known interactors (Scales et al., 2002) (**Figure 22**).

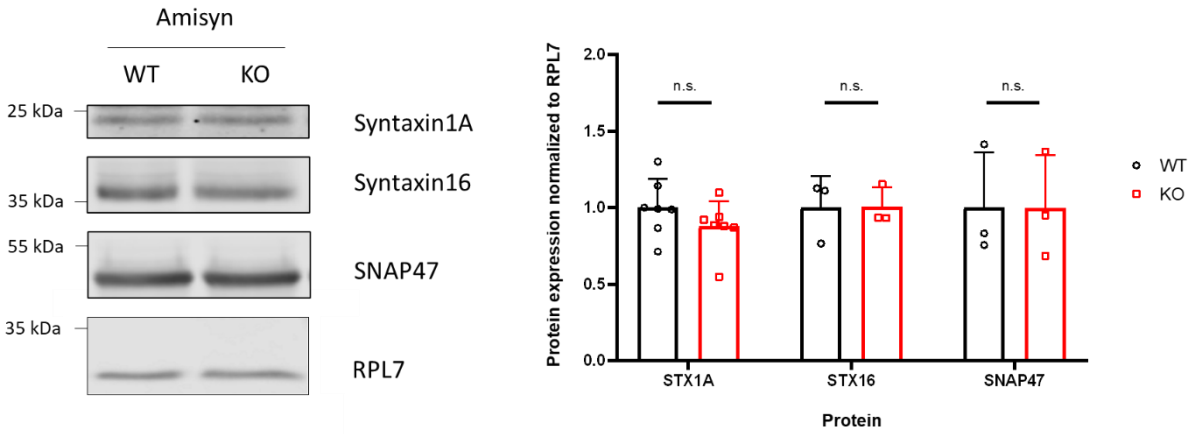

Figure 22- Levels of Q-SNARE proteins present in WT and KO hippocampal tissue. n=7 (STX1A) and n=3 (STX16 and SNAP47); n.s.: not significant; kDa: kilodaltons. RPL7 was used as a loading control. Data are shown as mean±SEM.

3.5.7. Levels of calcium channels in the brain of amisyn mutant mice

Through the Western Blot technique, the levels of CaVα2δ4, a calcium channel subunit, were tested in cortical and hippocampal tissue present in WT and KO amisyn mice, since the release probability in these KO mice was increased (Jin and Milosevic, unpublished lab data). CaVα2δ4 is a type of the Ca^{2+} channel subunit α2δ, which is responsible for regulating the biophysical properties of the channel and for the intracellular trafficking (Bean & McDonough, 2010). In **Figures 23** and **24**, one can see that the levels of calcium channels are not significantly altered in the KO tissues. This result may suggest that amysin does not affect the number of calcium channels, which might indicate that changes in the calcium channels are not the reason for the higher release probability verified (Jin and Milosevic, unpublished lab data).

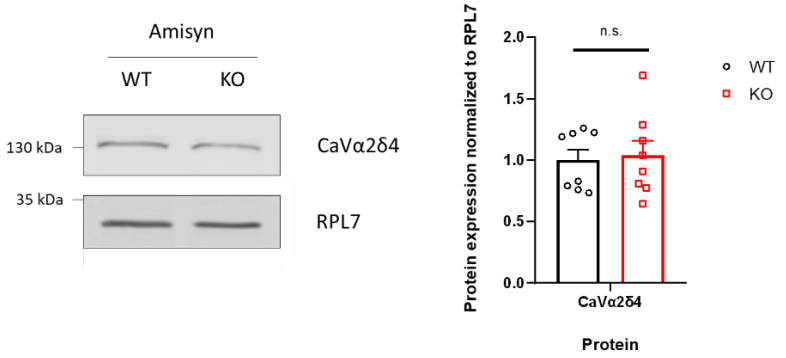

Figure 23- Levels of calcium channels present in WT and KO cortical tissue. n=8; n.s.: not significant; *: p-value<0.05; kDa: kilodaltons. RPL7 was used as a loading control. Data are shown as mean±SEM.

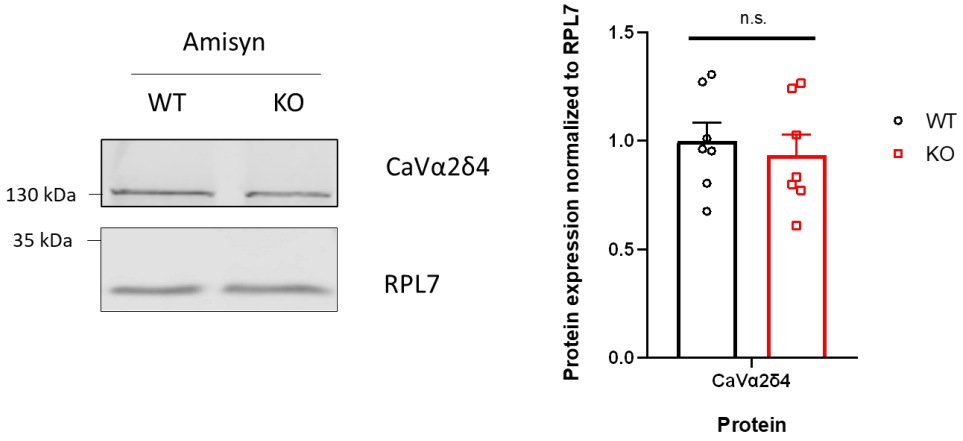

Figure 24- Levels of calcium channels present in WT and KO hippocampal tissue. n=7; n.s.: not significant; kDa: kilodaltons. RPL7 was used as a loading control. Data are shown as mean±SEM.

3.5.8. Levels of active zone proteins in the brain of amisyn mutant mice

The levels of active zone proteins were tested in WT and KO amisyn mice hippocampus via Western Blot, due to the fact that tomosyn co-localizes with bassoon (Geerts et al., 2017), a protein

that acts in the active zone (Südhof, 2012). RIM1 (Rab3-interactive protein) is a protein essential for the priming of synaptic vesicles (Lonart, 2002), which does not show any protein level changes in the amisyn KO mice (**Figure 25**). Rabphilin3, a protein that regulates vesicle docking (Ferrer-Orta et al., 2017), was also found to be not changed in a significant way in the amisyn KO mice when compared with the WT animals (**Figure 25**). These results may indicate that amisyn does not interfere with the priming/docking events mediated by the tested proteins.

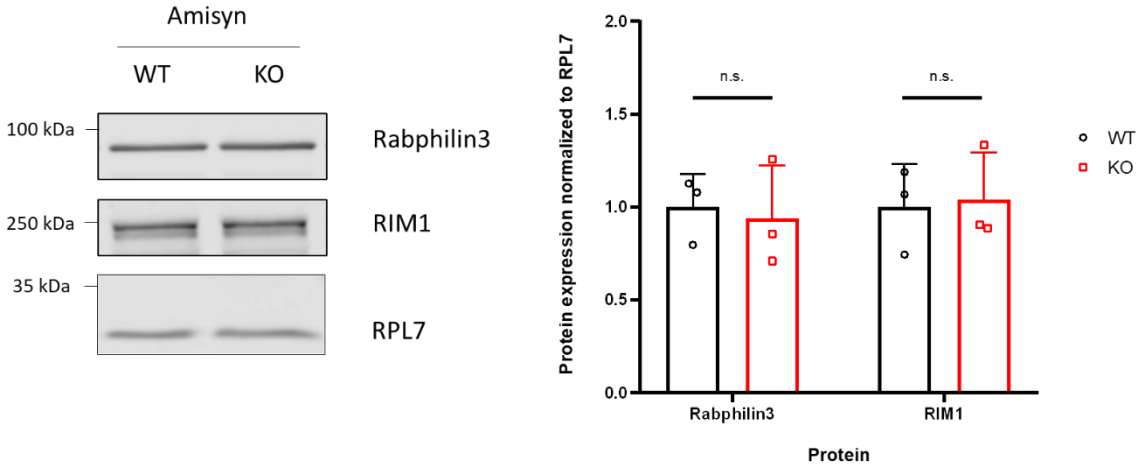

Figure 25- Levels of active zone proteins present in WT and KO hippocampal tissue. n=3; n.s.: not significant; kDa: kilodaltons. RPL7 was used as a loading control. Data are shown as mean±SEM.

3.5.9. Levels of postsynaptic proteins in the brain of amisyn mutant mice

Since tomosyn regulates RhoA (Shen et al., 2020), a postsynaptic protein, and ASD has been related to a mutation in the genes of postsynaptic proteins, such as PSD95 (Guang et al., 2018), we hypothesized that, in the absence of amisyn, some postsynaptic proteins could have alterations in their protein levels. These proteins were analyzed in the cortex and hippocampus of amisyn WT and KO mice using the Western Blot technique. GluA2 is a subunit of the AMPAR that regulates this receptors Ca^{2+} permeation (Salpietro et al., 2019), while Homer1 is a postsynaptic protein that regulates the function of the metabotropic glutamate receptors (mGluR) (Clifton et al., 2017). Neither GluA2 nor Homer1 were found to be significantly changed in the amisyn KO mice (**Figure 27**).

PSD95 is a protein required for the recruitment of NMDA and AMPA receptors to the postsynaptic membrane (Coley & Gao, 2018). As it can be seen bellow, PSD95 levels were significantly decreased (about 22%, p-value=0.0401) in the cortex (**Figure 26**). However, when analyzing the levels of the same protein, in the hippocampal tissue, there was no significant change (**Figure 27**). This results might be an indicator of a putative role of amisyn in the postsynaptic site, similarly to tomosyn (Shen et al., 2020).

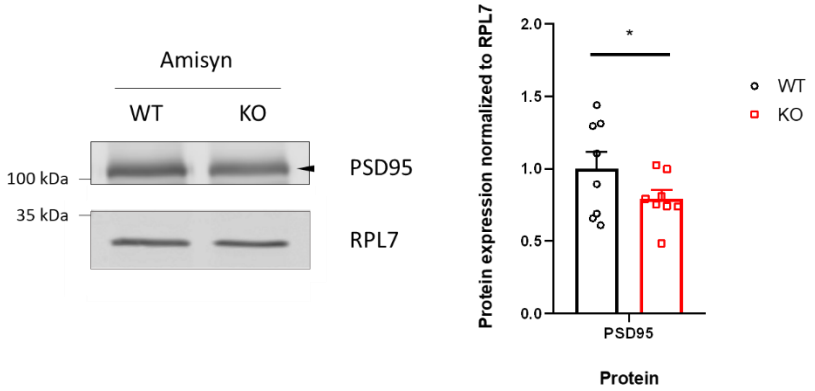

Figure 26- Levels of postsynaptic proteins present in WT and KO cortical tissue. n=8; *: p-value<0.05; kDa: kilodaltons. RPL7 was used as a loading control. Data are shown as mean±SEM.

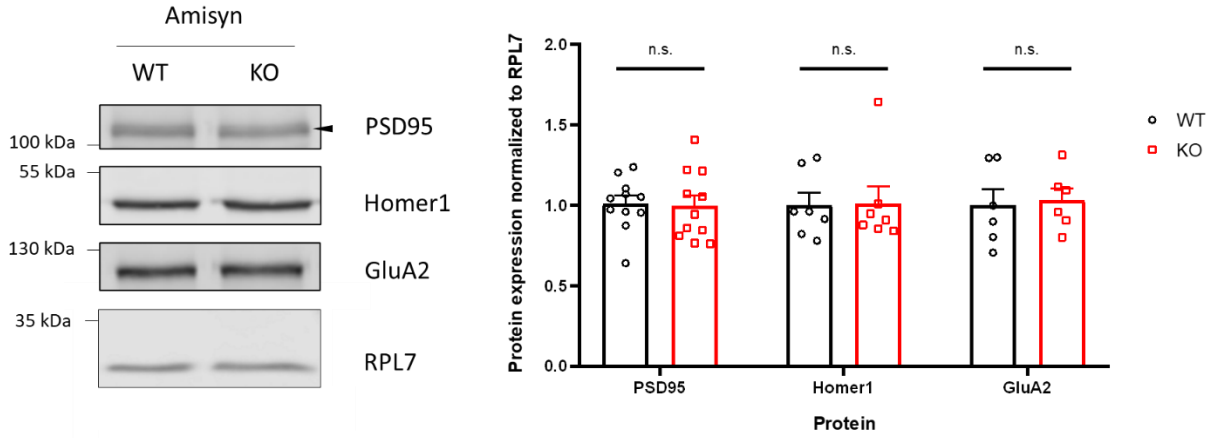

Figure 27- Levels of postsynaptic proteins present in WT and KO hippocampal tissue. n=11 (PSD95) and n=7 (Homer1 and GluA2); n.s.: not significant; kDa: kilodaltons. RPL7 was used as a loading control. Data are shown as mean±SEM.

3.5.10. Levels of LTP-associated proteins in the brain of amisyn mutant mice

Since we saw a difference in the protein levels of PSD95 in the amisyn KO mice (**Figure 26**), we tested some proteins associated with the LTP pathway via Western Blot. The levels of the proteins CREB, P-CREB, ERK, or P-ERK were analyzed in the hippocampal area of WT and KO amisyn mice. CREB (cAMP Response Element-Binding protein) is a mainly nuclear protein whose function is to act as a transcription factor, being activated when phosphorylated (H. Wang et al., 2018). ERK is a protein kinase that upon phosphorylation is translocated to the nucleus and activates transcription factors (McCain, 2013). We observed that the tested LTP-associated proteins do not show any level of alterations in the amisyn KO mice (**Figure 28**). These results might indicate that amisyn does not alter the levels of proteins linked to the LTP.

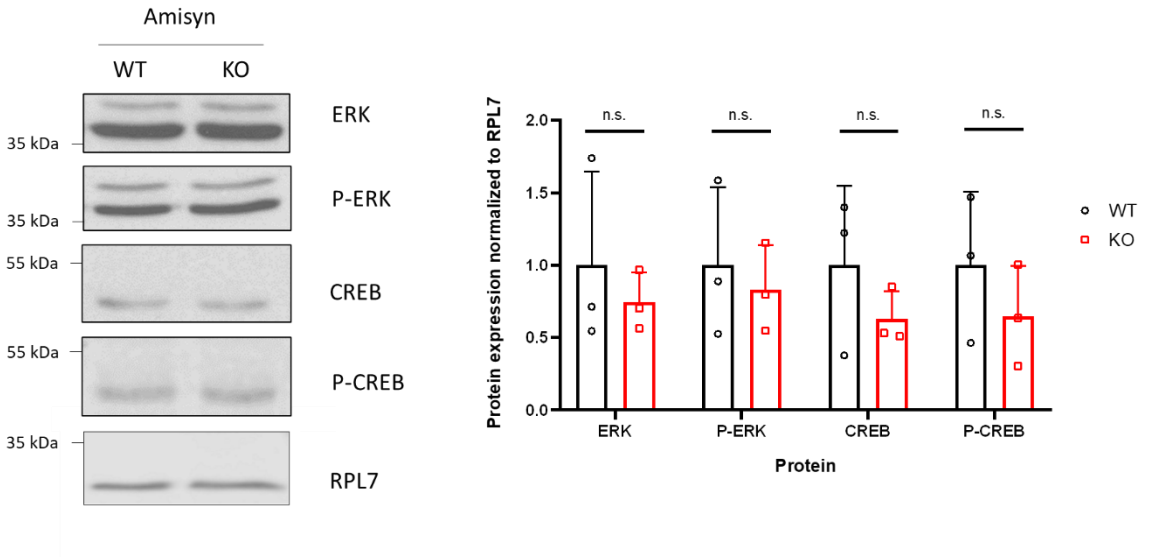

Figure 28- Levels of LTP associated proteins present in WT and KO hippocampal tissue. n=3; n.s.: not significant; kDa: kilodaltons. RPL7 was used as a loading control. Data are shown as mean±SEM.

3.6. Characterization of RNA expression in amisyn mutant mice by qPCR

Since it is known that amisyn competes with VAMP2 and inhibits exocytosis (Kondratiuk et al., 2020), we explored if the lack of amisyn could influence the RNA levels of the proteins involved in the exocytic process. To test the levels of expressed RNA as well as confirm the selective Western Blot results, the RNA levels between the WT and KO mouse brain tissue were assessed. To this extent, we isolated in hippocampal and cortical tissue of amisyn KO and WT mice, extract its RNA, synthesized its cDNA, and ran qPCR plates. The last step was analyzing the data and assess if there were statistical differences between WT and KO mice.

3.6.1. Transcript levels of amisyn in the brain of amisyn mutant mice

We detected that small transcript levels of the amisyn gene (on average 29%) remain expressed in amisyn KO mice, presumably due to the 'leaky' constructs. Thus, we first wanted to check if these remaining protein levels are matched by remaining amisyn transcripts as well. **Figure 29** shows a pool of data from several experiments: we detected a significant decrease of amisyn transcript levels of about 69% in the hippocampus, yet, the small amount of amisyn transcripts is still present. These data match the results obtained by Western Blot and, show that the expression of a small amount of protein persists.

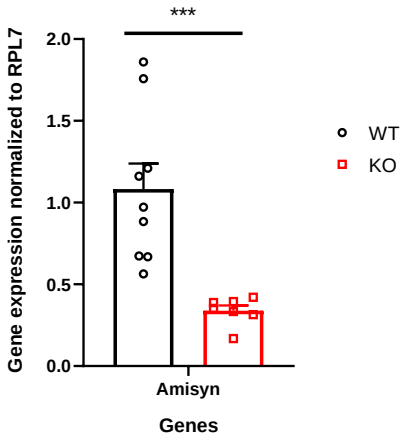

Figure 29- Transcript levels of amisyn present in WT and KO hippocampal tissue. n (number of biological replicates) =9 (WT) and n=7 (KO); ***: p-value<0.001. RPL7 was used as the reference gene. Data are shown as mean±SEM. Data obtained together with MSc student Joana Pires.

3.6.2. Transcript levels of dynamin1 and intersectin1 in the brain of amisyn mutant mice

Via qPCR, the transcript levels of the proteins dynamin1 and intersectin1 were analyzed in the cortical and hippocampal areas of WT and KO amisyn mice, to explore if vesicle endocytosis was affected since it was proven that amisyn inhibits exocytosis (Kondratiuk et al., 2020). Dynamin is a GTPase responsible for the budding of the endocytic vesicles (Ferguson & De Camilli, 2012), while intersectin1 is a cofactor responsible for recruiting dynamin (Haucke & Kozlov, 2018). Neither dynamin1 nor intersectin1 transcript levels were found to be changed in the amisyn KO mouse cortex (**Figure 30**) or hippocampus (**Figure 31**).

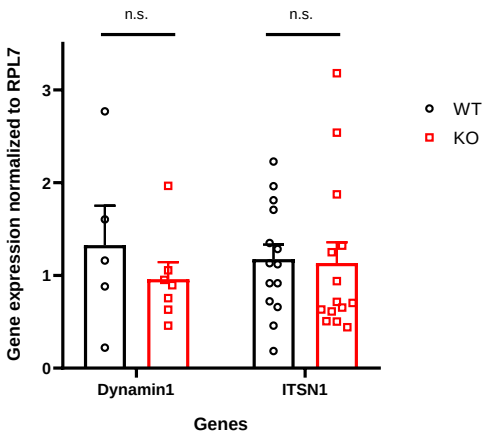

Figure 30- Transcript levels of dynamin1 and intersectin1 (ITSN1) present in WT and KO cortical tissue. n=9 (WT) and n=7 (KO); n.s.: not significant. RPL7 was used as the reference gene. Data are shown as mean±SEM. Data obtained together with MSc student Joana Pires.

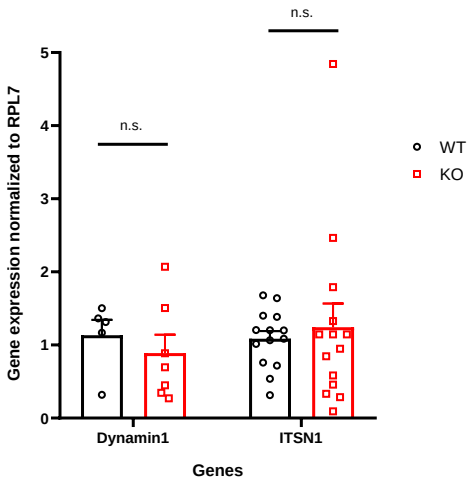

Figure 31- Transcript levels of dynamin1 and intersectin1 (ITSN1) present in WT and KO hippocampal tissue. n=5 (dynamin1 WT), n=7 (dynamin1 KO) and n=14 (ITSN1); n.s.: not significant. RPL7 was used as the reference gene. Data are shown as mean±SEM. Data obtained together with MSc student Joana Pires.

3.6.3. Transcript levels of endosome-associated proteins in the brain of amisyn mutant mice

The transcript levels of endosome-associated proteins were analyzed in the cortical and hippocampal areas of WT and KO amisyn mice via qPCR because amisyn was recently reported to inhibit exocytosis (Kondratiuk et al., 2020). Rab5 is an endosomal protein that is capable of recruiting various endocytic effectors (such as EEA1) to regulate events related to endocytosis (Yuan & Song, 2020). Rab7 is a very important protein for endocytosis and late endosome formation (Sun et al., 2020). As shown in **Figure 32**, there is a significant increase in the transcript levels of Rab7 of about 338% (p-value=0.0055) in the amisyn KO cortex, while no changes are observed in the hippocampus (**Figure 33**). Rab5 is unchanged in both tissues (**Figures 32** and **33**). The increase of Rab7 might indicate an attempt to form late endosomes because Rab7 is involved in endosome maturation (Vanlandingham & Ceresa, 2009). However, Rab7 protein levels are not altered in amisyn KO mice (**Figures 18** and **17**), which might indicate that there is post-transcriptional negative regulation of these transcripts (Guimaraes et al., 2014).

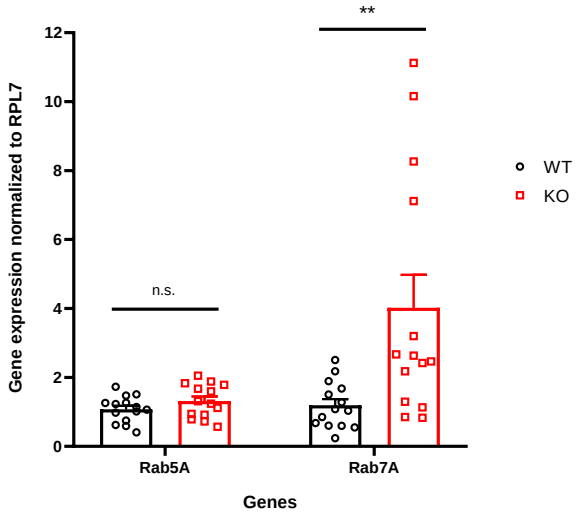

Figure 32- Transcript levels of endosome-associated proteins present in WT and KO cortical tissue. n=14; **: p-value<0.01. RPL7 was used as the reference gene. Data are shown as mean±SEM. Data obtained together with MSc student Joana Pires.

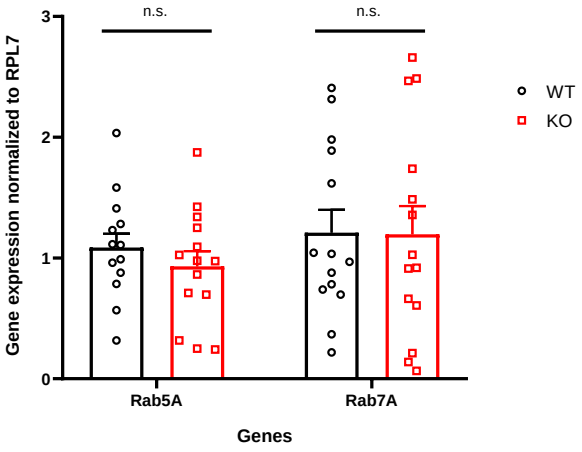

Figure 33- Transcript levels of endosome-associated proteins present in WT and KO hippocampal tissue. n=14; n.s.: not significant. RPL7 was used as the reference gene. Data are shown as mean±SEM. Data obtained together with MSc student Joana Pires.

3.6.4. Transcript levels of peripheral synaptic vesicle proteins in the brain of amisyn mutant mice

We investigated if the transcript levels of peripheral proteins changed upon lack of amisyn through qPCR using hippocampal and cortical tissues since tomosyn was reported to interact with synapsin and Rab3 (Cazares et al., 2016). α-synuclein is a negative regulator of neurotransmitter release (Emanuele & Chieregatti, 2015), which was found to be not changed in the amisyn KO mice cortex or hippocampus (**Figures 34** and **35**). Synapsin1 is a protein that maintains the synaptic vesicles tethered to the ResP (resting pool) (Purves et al., 2018d), which was also found to have no significant changes in the KO amisyn cortex or hippocampus (**Figures 34** and **35**) when compared with the WT animals. Rab3A is a protein responsible for the recruitment of synaptic vesicles to the

membrane (Geppert et al., 1994), while endophilin-A1 is protein that regulates the synaptic vesicle endocytosis. Rab3A was not found to be changed in the amisyn KO brain tissues tested (**Figures 34** and **35**), while endophilin-A1 levels were not altered in the cortex but were significantly decreased by about 40% (p-value=0.0145) in the hippocampal tissue (**Figures 34** and **35**). This might indicate an attempt to slow down clathrin uncoating since KO of endophilins leads to an accumulation of clathrin-coated vesicles in the presynaptic site (Milosevic et al., 2011). However, since the protein levels of endophilin are maintained (**Figures 19** and **20**), this might suggest that the transcripts of this protein are being post-transcriptionally positive regulated. In the cases of Rab3 and α-synuclein the protein levels were increased in the KO in relation to the WT animals. However, the transcript levels do not seem to be the reason for this, being possible that this might be due to an accumulation of these proteins.

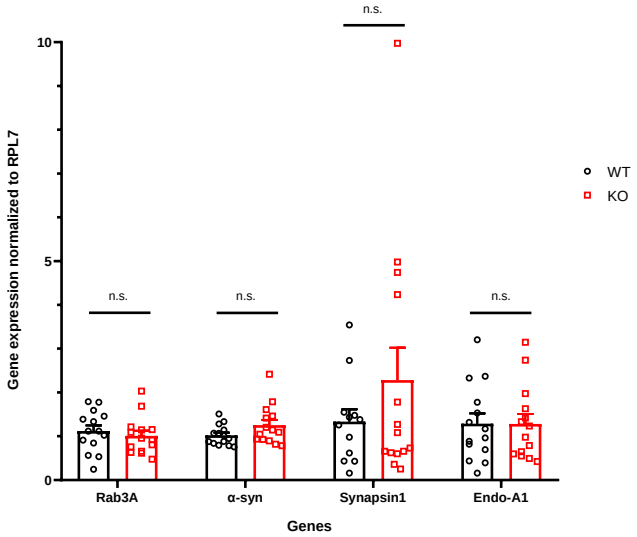

Figure 34- Transcript levels of peripheral synaptic vesicle proteins present in WT and KO cortical tissue. n=14; n.s.: not significant. RPL7 was used as the reference gene. Data are shown as mean±SEM. Data obtained together with MSc student Joana Pires.

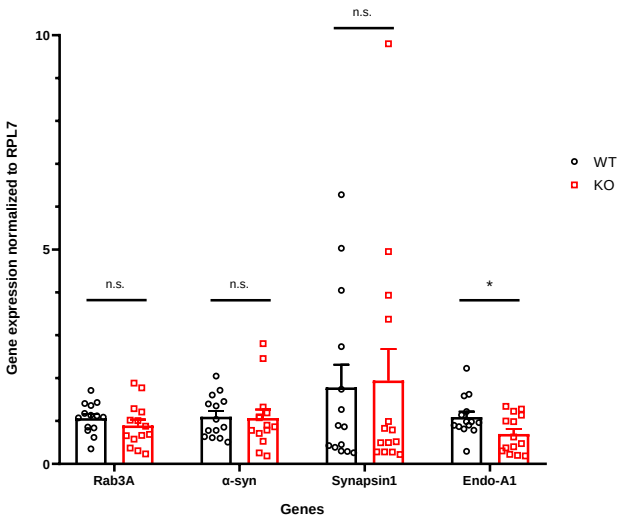

Figure 35- Transcript levels of peripheral synaptic vesicle proteins present in WT and KO hippocampal tissue. n=14; n.s.: not significant; *: p-value<0.05. RPL7 was used as the reference gene. Data are shown as mean±SEM. Data obtained together with MSc student Joana Pires.

3.6.5. Transcript levels of integral synaptic vesicle proteins in the brain of amisyn mutant mice

We analyzed the transcript levels of integral synaptic vesicle proteins in the amisyn KO hippocampus and cortex because amisyn is known to compete with VAMP2 (Kondratiuk et al., 2020). VAMP2 is a protein that takes part in the formation of a fusogenic SNARE complex, which allows synaptic vesicle exocytosis (Salpietro, Malintan, et al., 2019). SV2A is a protein that regulates synaptotagmin1 (SYT1) trafficking (Madeo et al., 2014), while SYT1 is a Ca^{2+} sensor that regulates neurotransmitter exocytosis (Courtney et al., 2019). None of these proteins showed any significant changes in their transcript levels in the KO amisyn cortex or hippocampus (**Figures 36** and **37**). Which might suggest that the decreased protein levels verified for VAMP2 via Western Blot are not justified by a decrease in the transcript levels, being possible that VAMP2 is being degraded in higher rates (Guimaraes et al., 2014).

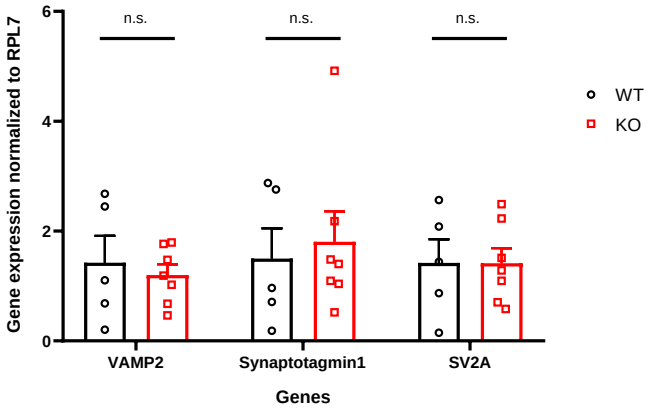

Figure 36- Transcript levels of integral synaptic vesicle proteins present in WT and KO cortical tissue. n=5 (WT) and n=7 (KO); n.s.: not significant. RPL7 was used as the reference gene. Data are shown as mean±SEM. Data obtained together with MSc student Joana Pires.

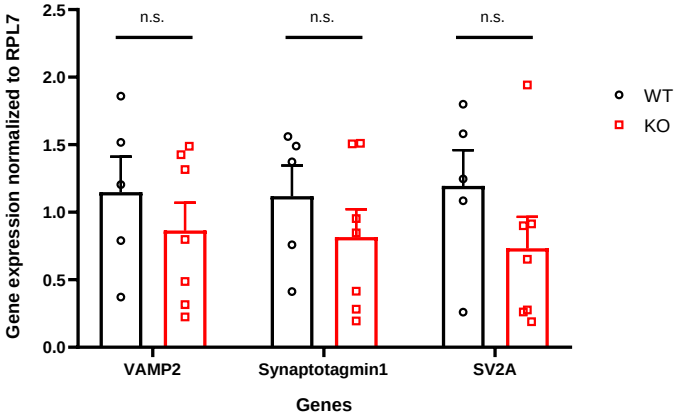

Figure 37- Transcript levels of integral synaptic vesicle proteins present in WT and KO hippocampal tissue. n=5 (WT) and n=7 (KO); n.s.: not significant. RPL7 was used as the reference gene. Data are shown as mean±SEM. Data obtained together with MSc student Joana Pires.

3.6.6. Transcript levels of Q-SNARE proteins in the brain of amisyn mutant mice

Q-SNARE protein transcript levels were tested by qPCR in amisyn KO mice hippocampus and cortex because amisyn was reported to interact with syntaxin1, syntaxin4, and SNAP25 (Scales et al., 2002), all Q-SNARE protein. Syntaxin1 (STX1) and SNAP25 are two proteins that participate in the formation of the fusogenic SNARE complex in conjunction with VAMP2 (Mason, 2017a). None of the aforementioned proteins had different transcript levels in the amisyn KO mice cortex and hippocampus (**Figures 38** and **39**). Syntaxin2 (STX2) is a SNARE protein that takes part in the constitutive exocytosis pathway (van den Bogaart et al., 2013), that was not found to have a significant difference in the amisyn KO mice cortex and hippocampus (**Figures 38** and **39**). Syntaxin4 (STX4) is a protein that mediates AMPAR insertion in the postsynaptic plasma membrane (Mohanasundaram & Shanmugam, 2010) while syntaxin6 (STX6) mediates the transport of proteins and lipids between the endosome and TGN (Jung et al., 2012). Neither syntaxin4 nor syntaxin6 show any differences between the transcript levels verified in the amisyn KO mice and the WT cortex and hippocampus (**Figure 38** and **39**). These results regarding syntaxin1 corroborate the findings obtained via Western Blot (**Figures 22**).

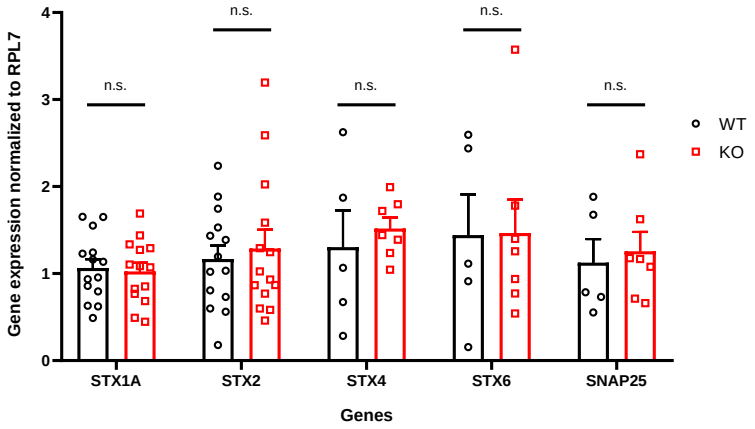

Figure 38- Transcript levels of Q-SNARE proteins present in WT and KO cortical tissue. n=14 (STX1 and STX2), n=5 (STX4, STX6 and SNAP25 WT) and n=7 (STX4, STX6 and SNAP25 KO); n.s.: not significant. RPL7 was used as the reference gene. Data are shown as mean±SEM. Data obtained together with MSc student Joana Pires.

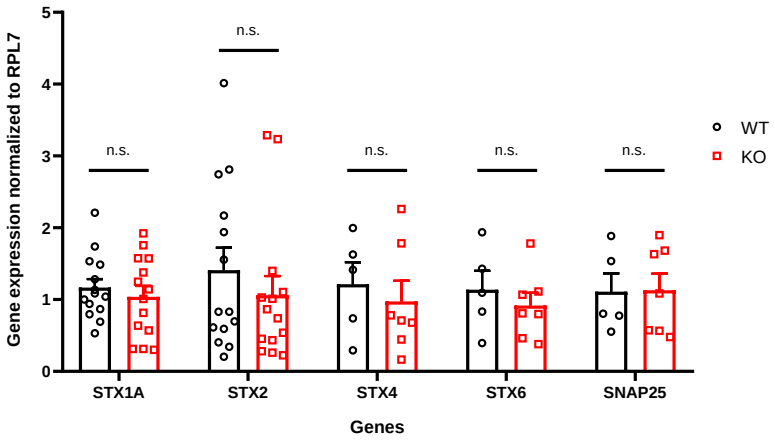

Figure 39- Transcript levels of Q-SNARE proteins present in WT and KO hippocampal tissue. n=14 (STX1 and STX2), n=5 (STX4, STX6 and SNAP25 WT) and n=7 (STX4, STX6 and SNAP25 KO); n.s.: not

significant. RPL7 was used as the reference gene. Data are shown as mean±SEM. Data obtained together with MSc student Joana Pires.

3.6.7. Transcript levels of SNARE regulator proteins in the brain of amisyn mutant mice

Based on the fact that tomosyn and amisyn are inhibitors of exocytosis (Geerts et al., 2017; Kondratiuk et al., 2020) and that tomosyn might compete with the Mun18-Munc13 pathway (Park et al., 2017), we tested by qPCR if any SNARE regulator proteins could have their transcript levels changed in the absence of amisyn. Munc13-1 is a protein involved in the priming of the synaptic vesicles (Jahn & Fasshauer, 2012), and Munc18-1 is a protein that mediates a conformational change of the SNAREpin, which allows the fusion of the vesicle membrane with the plasma membrane (Mason, 2017a). Tomosyn is a negative regulator of the SNAREpin formation (Geerts et al., 2017), while complexin2 prevents the fusion event until an action potential arrives at the presynaptic terminal (Mason, 2017a). As it is possible to observe in **Figures 40** and **41**, none of these SNARE regulator proteins show changes in transcript levels in the KO amisyn brain tissues analyzed, which might indicate that amisyn does not interfere with the regulation processes mediated by the tested proteins.

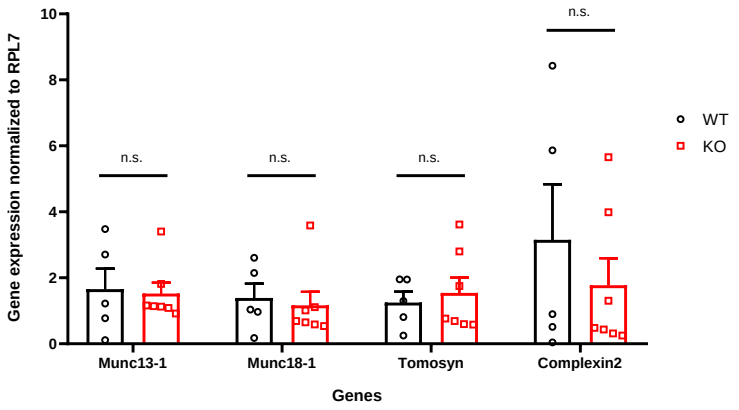

Figure 40- Transcript levels of SNARE regulator proteins present in WT and KO cortical tissue. n=5 (WT) and n=7 (KO); n.s.: not significant. RPL7 was used as the reference gene. Data are shown as mean±SEM. Data obtained together with MSc student Joana Pires.

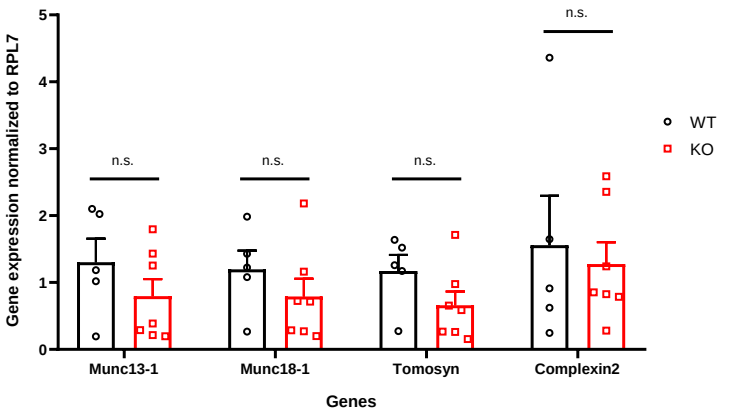

Figure 41- Transcript levels of SNARE regulator proteins present in WT and KO hippocampal tissue. n=5 (WT) and n=7 (KO); n.s.: not significant. RPL7 was used as the reference gene. Data are shown as mean±SEM. Data obtained together with MSc student Joana Pires.

3.6.8. Transcript levels of secretory proteins in the brain of amisyn mutant mice

Since tomosyn was found to co-migrate with neuropeptide Y (NPY) (Geerts et al., 2017), we explored the possibility of changes in secretory proteins when amisyn is decreased. Neuropeptide Y is a neurotransmitter present in dense-core vesicles that regulates synaptic transmission (Ramamoorthy & Whim, 2008), which was not found to be changed in the amisyn KO mice cortex and hippocampus (**Figures 42** and **43**). Dopamine beta-hydroxylase (DBH1), an enzyme that converts dopamine in noradrenaline (Lamouroux et al., 1987), was also unchanged in the amisyn KO cortex and hippocampus in comparison with the WT animals (**Figures 42** and **43**).

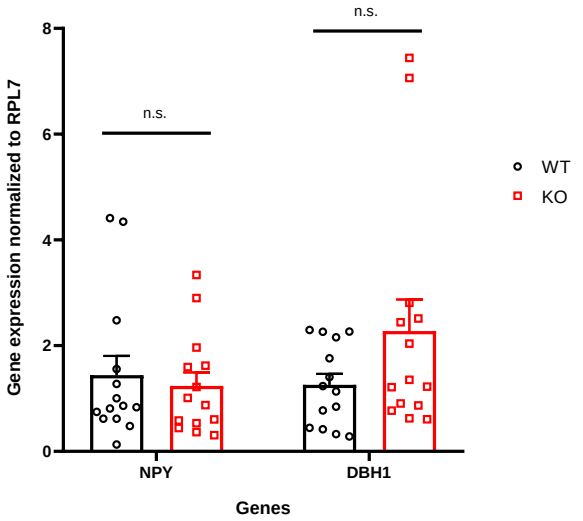

Figure 42- Transcript levels of secretory proteins present in WT and KO cortical tissue. n=14; n.s.: not significant. RPL7 was used as the reference gene. Data are shown as mean±SEM. Data obtained together with MSc student Joana Pires.

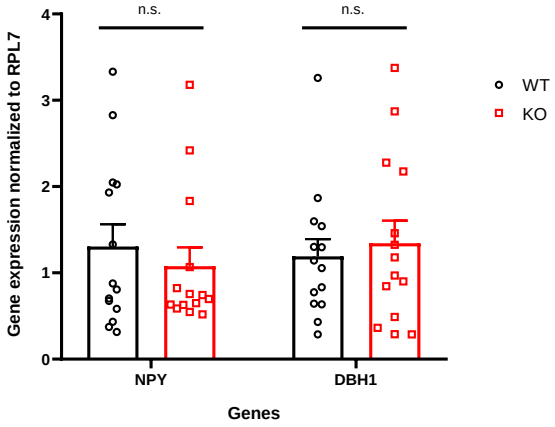

Figure 43- Transcript levels of secretory proteins present in WT and KO hippocampal tissue. n=14; n.s.: not significant. RPL7 was used as the reference gene. Data are shown as mean±SEM. Data obtained together with MSc student Joana Pires.

3.6.9. Transcript levels of active zone and postsynaptic proteins in the brain of amisyn mutant mice

The transcript levels of active zone and postsynaptic proteins were inspected in hippocampus and cortex of amisyn KO mice since tomosyn was reported to co-localize with bassoon (an active zone protein) (Geerts et al., 2017) and is known to regulate RhoA (a postsynaptic protein) (Shen et al., 2020). Bassoon is responsible for guiding the synaptic vesicles to the active zone (Südhof, 2012), while homer1 is responsible for the regulation of mGluR function (Clifton et al., 2017). Similarly to the Western Blot results, the active zone proteins and homer1 also maintained their transcript levels in cortex and hippocampus (**Figures 44** and **45**). However, PSD95, a protein that recruits NMDAR and AMPAR to the postsynaptic plasma membrane (Coley & Gao, 2018), has a significant decrease of about 35% (p-value=0.0254) in the amisyn KO hippocampus (**Figure 45**), while remaining unchanged in the cortex (**Figure 44**). Thus, the pattern observed for the PSD95 transcript is opposite to the observed for its protein levels (**Figures 26** and **27** above). RhoA, which induces retraction and loss of spine (Tolias et al., 2011), also shows a significant decrease of about 40% (p-value=0.0312) in the hippocampus, which when combined to the already presented results might indicate that amisyn plays a role in the postsynaptic site of hippocampus. Differences observed between Western Blot and qPCR are expected, because the transcript levels only correlate with the protein levels in about half of the cases (Guimaraes et al., 2014), as are the differences between tissues since they have different functions.

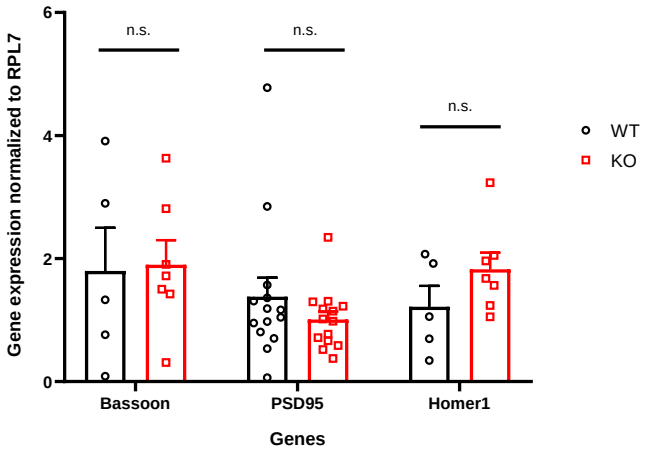

Figure 44- Transcript levels of active zone and postsynaptic proteins present in WT and KO cortical tissue. n=14 (PSD95), n=5 (WT, bassoon and Homer1) and n=7 (KO, bassoon and Homer1); n.s.: not significant. RPL7 was used as the reference gene. Data are shown as mean±SEM. Data obtained together with MSc student Joana Pires.

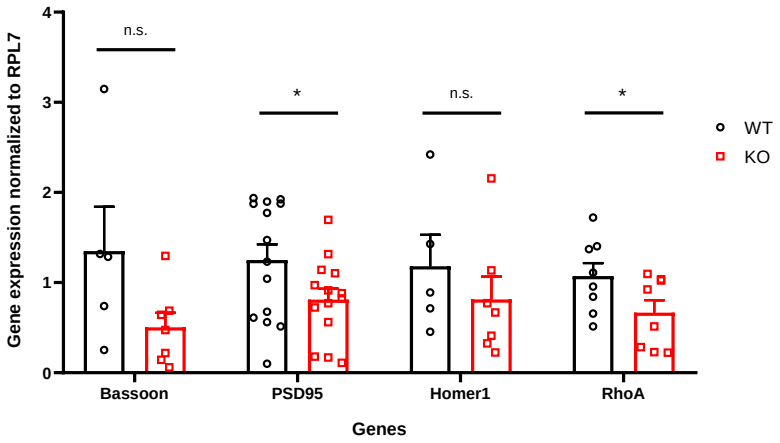

Figure 45- Transcript levels of active zone and postsynaptic proteins present in WT and KO hippocampal tissue. n=14 (PSD95), n=8 (RhoA), n=5 (WT, bassoon and Homer1) and n=7 (KO, bassoon and Homer1); n.s.: not significant; *: p-value<0.05. RPL7 was used as the reference gene. Data are shown as mean±SEM. Data relative to PSD95, Homer1 and bassoon obtained together with MSc student Joana Pires.

3.6.10. Transcript levels of protein kinases in the brain of amisyn mutant mice

Kinases are enzymes that are very important for the regulation of exocytosis by phosphorylating key proteins involved in that process (Brady et al., 2012e). We analyzed by qPCR is any changes were observed in the transcript levels of kinases because tomosyn was reported to be regulated by phosphorylation by various kinases (Cazares et al., 2016; Madera-Salcedo et al., 2018). PKC becomes active upon recruitment by diacylglycerol and, PKA is activated by cAMP (Kandel et al., 2013a). CDK5 is also a kinase, and it is capable of regulating endocytosis and tomosyn (Cazares et al., 2016; Rizzoli, 2014). The transcript levels of these kinases were not altered in the KO amisyn cortex and hippocampus (**Figure 46**), which corroborates the Western Blot results obtained for CDK5. This result suggests that the effects of amisyn absence do not involve significant regulation of the expression of these kinases, albeit their activity may be affected.

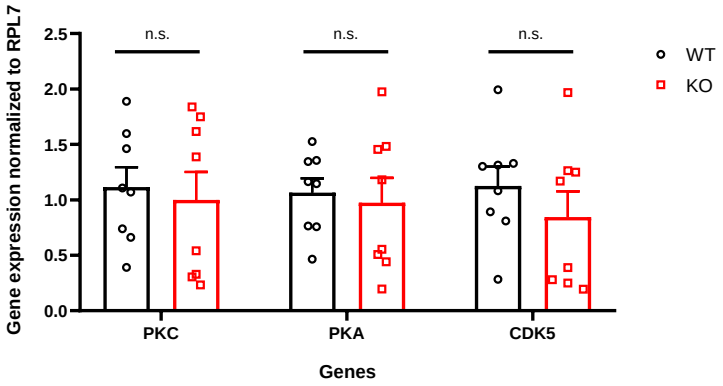

Figure 46- Transcript levels of protein kinases present in WT and KO hippocampal tissue. n=8; n.s.: not significant. RPL7 was used as the reference gene. Data are shown as mean±SEM.

3.6.11. Transcript levels of LTP associated proteins in the brain of amisyn mutant mice

Since we saw differences between the WT and amisyn KO mice regarding postsynaptic proteins, via Western Blot (**Figure 26**) and qPCR (**Figure 45**), we decided to explore if proteins associated with the LTP pathway could be affected. CAMK4 is a kinase present mainly in the nucleus that activates transcription factors, such as CREB (Wayman et al., 2008; Zech et al., 2018), and CAMK2B is a kinase that regulates the dissociation of synapsin from the synaptic vesicles (Purves et al., 2018d). CREB is a transcription factor that to be active needs to be in its phosphorylated form (H. Wang et al., 2018). Of the LTP associated proteins tested, only CAMK4 turned out to have significantly lower transcript levels (decrease of about 36% with p-value=0.0413) in the amisyn KO hippocampus (**Figure 47**), which is in agreement with the CREB results obtained via Western Blot. This result suggests that the expression of CAMKIV is regulated at the transcript level in the amisyn KO hippocampus.

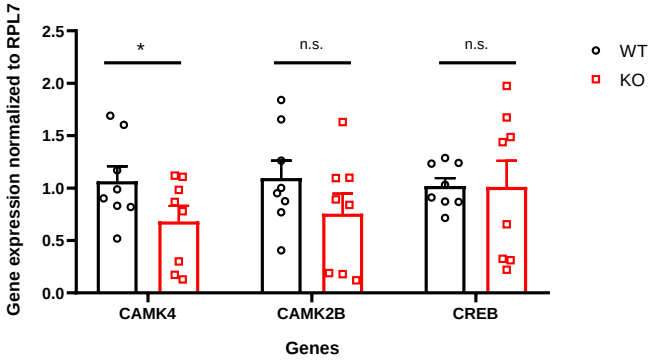

Figure 47- Transcript levels of LTP associated proteins present in WT and KO hippocampal tissue. n=8; *: p-value<0.05; n.s.: not significant. RPL7 was used as the reference gene. Data are shown as mean±SEM.

4. Discussion

This thesis shows the mechanism by which the protein amisyn interacts with membranes and provides insights on the functional consequences of loss of amisyn in vivo in a mouse model. Amisyn is a 24 kDa protein thought to regulate negatively the exocytic process.

It was reported recently that amisyn interacts with $PI(4,5)P_2$ (Kondratiuk et al., 2020). Because PH domains were found to interact specifically with phosphoinositide molecules, such as $PI(4,5)P_2$ (Lemmon, 2007), we tested the hypothesis that the amisyn PH domain mediates this interaction. In this work, we show that only WT amisyn co-sedimented with liposomes containing $PI(4,5)P_2$, while amisyn with a mutated PH domain remained in the supernatant phase. This indicates that amisyn interaction with $PI(4,5)P_2$ is dependent on its PH domain, which may suggest that amisyn function is regulated through its PH domain.

Syntaxin1 interaction with $PI(4,5)P_2$ mediates its phosphorylation by CK2 since $PI(4,5)P_2$ binding is critical for the accessibility of S14 (Khelashvili et al., 2012). The phosphorylation of S14 by CK2 results in an enhancement of syntaxin interaction with synaptotagmin, which leads to the maturation of the synapse (Snyder et al., 2006). A similar process occurs with AKT1 PH domain interaction with $PI(4,5)P_2$, where conformational changes mediated by binding to the phospholipid allow the phosphorylation of T308 AKT1 by PDK1 (Dannemann et al., 2010). However, it was also reported that the interaction of many proteins with membrane phospholipids is tightly regulated by phosphorylation, as in the case of Endophilin-A, where this interaction is regulated by LRRK2 (Matta et al., 2012). SNAP25 is also regulated by phosphorylation, by PKA (at T138) and PKC (at S187), which promotes exocytosis regardless of the inhibition or enhancement (respectively) of the formation of the SNARE complex (Gao et al., 2016). Since we report a PH domain interaction with the plasma membrane, the possible phosphorylation sites present in the amisyn molecule were predicted with the objective of understanding if this interaction regulated or was mediated by phosphorylation. The predicted T29 phosphorylation site, due to its structural proximity to the mutated sites present in the AADD mutant amisyn, might be a regulator of the amisyn PH domain interaction with $PI(4,5)P_2$, but it is also possible that it could be regulated by the binding to $PI(4,5)P_2$. The other two predicted (T58 and T135), could also mediate or be regulated by the binding to the phospholipid $PI(4,5)P_2$, however since they are present in the opposite site of the PH domain binding site it is also possible that they are involved in the regulation of other processes. This data might signify that amisyn interactions and function, i.e., exocytosis negative regulation, might be regulated by phosphorylation of amisyn PH domain.

Further studies regarding the amisyn PH domain are needed to fully understand its function and regulation. It would be interesting to alter the Threonine present in position 29 to another amino acid with different properties (disabling the phosphorylation of that site) and expressing it in mammal cells, with the objective of understanding if this site is relevant for exocytosis inhibition and amisyn PH domain binding to $PI(4,5)P_2$.

Since it was found that $PI(4,5)P_2$ interacts with amisyn, that it competes with VAMP2 (Kondratiuk et al., 2020) and that this protein interacts with SNARE proteins (Scales et al., 2002) it was hypothesized that amisyn could have a role in the regulation of synaptic vesicle exocytosis. To test this hypothesis, amisyn KO mice were generated. It was observed that in the amisyn KO mice, there is a higher release probability (Jin and Milosevic, unpublished lab data), so we formulated three possible hypotheses for what is happening. There could be more synaptic vesicles, more

vesicles present in the RRP, or more neurotransmitters in each vesicle. To test these hypotheses, the protein and RNA levels of proteins involved in various steps of synaptic vesicle exocytosis where tested.

It is reported in this thesis, that the Rab3A and α-synuclein protein levels are increased in the hippocampus of the amisyn KO mice. However, this was not due to increased transcription of the respective genes, as the transcript levels were unaltered. This suggests that in the absence of amisyn, there is decreased degradation of Rab3A and α-synuclein in the hippocampus. α-synuclein is a protein involved in the regulation of the vesicle membrane interaction with Rab3A-GTP (Burré, 2015; Daubner et al., 2011). Rab3A is a protein involved in vesicle priming (Schonn et al., 2010), that is reported to interact with tomosyn, possibly aiding in the regulation of the transition of vesicles between the TRP and the ResP (Cazares et al., 2016). This data might point to a direction where the amisyn KO mice have more readily releasable vesicles, which could signify that amisyn, like tomosyn, regulates the number of vesicles that are docked/primed and ready to be released. This control of the readily releasable vesicles number might be a way of neuroprotection, through a depression mechanism (M. Takahashi & Ohnishi, 2002). This hypothesis could be tested in the future by recurring to electron microscopy experiments.

In the cortex, the transcript levels of Rab7 were significantly increased when amisyn was decreased, which might indicate that in this part of the brain, more early endosomes are being matured to late endosomes, which might result in higher degradation levels. Also, it was seen a decrease in the endophilin-A1 transcript levels in the hippocampus of amisyn KO mice. This observation might indicate that the lack of amisyn augments the number of endocytic vesicles with a clathrin coat since, in endophilins KO mice, the lack of endophilins lead to an accumulation of clathrin-coated vesicles in the presynaptic site (Milosevic et al., 2011). This data might signify that the lack of amisyn impairs in some way the endocytic process, being possible that the recycling of synaptic vesicle proteins might be affected.

There is a decrease in the protein levels (but not in the transcript levels) of VAMP2, a known competitor of amisyn for the syntaxin1-SNAP25 SNARE complex (Kondratiuk et al., 2020), in the hippocampus of the amisyn KO mice which might indicate that since amisyn is decreased, there are fewer competitors available and thus there is a decrease in the demand for VAMP2 molecules for the formation of the SNARE complex.

PSD95 protein levels (but not RNA levels) were found to be changed in the cortical tissue and the transcript levels (but not protein levels) of the same protein were found changed significantly in the hippocampus. PSD95 is a postsynaptic density protein involved in the recruitment of NMDAR and AMPAR to the membrane, that is thought to be associated with ASD (Coley & Gao, 2018). These observed changes might explain the results obtained in the repetitive self-grooming test, where the amisyn KO mice spent around consecutive 23 seconds grooming while the WT only spent about 13 seconds (Cohen and Milosevic, unpublished lab data) since in PSD95 KO mice it was also verified this behavior (Feyder et al., 2010). These observations might indicate that amisyn reduces the sensitivity to neurotransmitters in the postsynaptic site, with a neuroprotection purpose, being possibly associated with the regulation of the formation of silent synapses (Coley & Gao, 2019).

A decrease in the transcript levels of RhoA, a small GTPase, was also observed in the amisyn KO hippocampus. RhoA is responsible for inhibiting spine/synapse formation (Tolias et al., 2011) and is known to be negatively regulated by tomosyn (Shen et al., 2020). Opposed to tomosyn, amisyn

might positively regulate RhoA, which might explain why ASD might be associated with a decrease in PSD95 and an increase in spine formation at the same time. This data might indicate that amisyn plays a regulatory role in the spine/synapse formation process.

After we found differences in PSD95 and RhoA, it was tested if a lack of amisyn had any influence in the transcript and protein levels of LTP associated proteins. It was found that only the transcript levels of CAMK4 showed a significant decrease in the amisyn KO mice. This protein kinase is predominantly localized in the nucleus of the cell, being a mediator of the communication between the synapse and the nucleus (Zech et al., 2018). CAMK4 phosphorylates transiently CREB and CBP (CREB binding protein), being required for transcriptional readout (Wayman et al., 2008). However, neither CREB nor phospho-CREB appear to be significantly changed in our experiments, which might indicate that CREB phosphorylation is being mediated by other kinases to compensate for the decrease in CAMK4 levels. This possible compensation might signify that the alteration of CAMK4 transcript levels, caused by amisyn absence, does not have an influence regarding CREB phosphorylation in the synaptic transmission process.

Proteins related to the active zone, calcium channels, Q-SNARE, and other regulatory proteins were not found changed in the amisyn KO mice, which might be an indicator that amisyn does not influence such processes.

5. Conclusion and future perspectives

In conclusion, amisyn seems to play a role in the exocytic process of synaptic vesicles. This protein might be involved in the negative regulation of the number of vesicles that are docked and ready to be released when an action potential arrives, but it might also have a positive regulatory role in the postsynaptic site where some proteins were decreased in amisyn KO mice. This regulatory role might be regulated by phosphorylation upon its binding to $PI(4,5)P_2$.

In the future, it would be interesting to express vectors with mutations of the phosphorylated site, to see if this site is a real phosphorylation site and if the lack of phosphorylation has any consequences in the mammal cells. It would also be of interest to do electron microscopy of brain slices of amisyn mutant mice and analyze synaptic vesicle number and distribution and the synapses, to confirm some of the hypotheses present in this work.

6. References

Ackerman, S. (1992). Major Structures and Functions of the Brain. In *Discovering the Brain*. National Academies Press (US). https://www.ncbi.nlm.nih.gov/books/NBK234157/

AddGene. (n.d.). *pGEX-HCF-1rep1wt*. Retrieved May 18, 2020, from https://www.addgene.org/84606/

Ashery, U., Bielopolski, N., Barak, B., & Yizhar, O. (2009). Friends and foes in synaptic transmission: the role of tomosyn in vesicle priming. In *Trends in Neurosciences*. https://doi.org/10.1016/j.tins.2009.01.004

Bean, B. P., & McDonough, S. I. (2010). Calcium Channels. In *Encyclopedia of Life Sciences*. John Wiley & Sons, Ltd. https://doi.org/10.1002/9780470015902.a0000028.pub2

Blom, N., Gammeltoft, S., & Brunak, S. (1999). Sequence and structure-based prediction of eukaryotic protein phosphorylation sites. *Journal of Molecular Biology*. https://doi.org/10.1006/jmbi.1999.3310

Boeckers, T. M. (2006). The postsynaptic density. *Cell and Tissue Research*, *326*(2), 409–422. https://doi.org/10.1007/s00441-006-0274-5

Brady, S. T., Siegel, G. J., Albers, R. W., & Price, D. L. (2012a). Glutamate and Glutamate Receptors. In *Basic Neurochemistry: Principles of Molecular, Cellular and Medical Neurobiology* (8th ed.). Elsevier Academic Press.

Brady, S. T., Siegel, G. J., Albers, R. W., & Price, D. L. (2012b). Intracellular Trafficking. In *Basic Neurochemistry: Principles of Molecular, Cellular and Medical Neurobiology* (8th ed.). Elsevier Academic Press.

Brady, S. T., Siegel, G. J., Albers, R. W., & Price, D. L. (2012c). Learning and Memory. In *Basic Neurochemistry: Principles of Molecular, Cellular and Medical Neurobiology* (8th ed.). Elsevier Academic Press.

Brady, S. T., Siegel, G. J., Albers, R. W., & Price, D. L. (2012d). Membrane Transport. In *Basic Neurochemistry: Principles of Molecular, Cellular and Medical Neurobiology* (8th ed.). Elsevier Academic Press.

Brady, S. T., Siegel, G. J., Albers, R. W., & Price, D. L. (2012e). Serine and Threonine Phosphorylation. In *Basic Neurochemistry: Principles of Molecular, Cellular and Medical Neurobiology* (8th ed.). Elsevier Academic Press.

Burré, J. (2015). The Synaptic Function of α-Synuclein. *Journal of Parkinson's Disease*, *5*(4), 699–713. https://doi.org/10.3233/JPD-150642

Castermans, D., Volders, K., Crepel, A., Backx, L., de Vos, R., Freson, K., Meulemans, S., Vermeesch, J. R., Schrander-Stumpel, C. T. R. M., de Rijk, P., del-Favero, J., van Geet, C., van de Ven, W. J. M., Steyaert, J. G., Devriendt, K., & Creemers, J. W. M. (2010). SCAMP5, NBEA and AMISYN: Three candidate genes for autism involved in secretion of large dense-core vesicles. *Human Molecular Genetics*. https://doi.org/10.1093/hmg/ddq013

Cazares, V. A., Njus, M. M., Manly, A., Saldate, J. J., Subramani, A., Ben-Simon, Y., Sutton, M. A., Ashery, U., & Stuenkel, E. L. (2016). Dynamic Partitioning of Synaptic Vesicle Pools by the SNARE-Binding Protein Tomosyn. *The Journal of Neuroscience*, *36*(44), 11208–11222. https://doi.org/10.1523/JNEUROSCI.1297-16.2016

Chen, Y., Gan, B. Q., & Tang, B. L. (2010). Syntaxin 16: Unraveling cellular physiology through a ubiquitous SNARE molecule. *Journal of Cellular Physiology*, *225*(2), 326–332. https://doi.org/10.1002/jcp.22286

Cipriano, D. J., Jung, J., Vivona, S., Fenn, T. D., Brunger, A. T., & Bryant, Z. (2013). Processive ATP-driven Substrate Disassembly by the N -Ethylmaleimide-sensitive Factor (NSF) Molecular Machine. *Journal of Biological Chemistry*, *288*(32), 23436–23445. https://doi.org/10.1074/jbc.M113.476705

Clifton, N. E., Cameron, D., Trent, S., Sykes, L. H., Thomas, K. L., & Hall, J. (2017). Hippocampal Regulation of Postsynaptic Density Homer1 by Associative Learning. *Neural Plasticity*, *2017*, 1–11. https://doi.org/10.1155/2017/5959182

Coley, A. A., & Gao, W.-J. (2018). PSD95: A synaptic protein implicated in schizophrenia or autism? *Progress in Neuro-Psychopharmacology and Biological Psychiatry*, *82*, 187–194. https://doi.org/10.1016/j.pnpbp.2017.11.016

Coley, A. A., & Gao, W.-J. (2019). PSD-95 deficiency disrupts PFC-associated function and behavior during neurodevelopment. *Scientific Reports*, *9*(1), 9486. https://doi.org/10.1038/s41598-019-45971-w

Collins, S. C., Do, H. W., Hastoy, B., Hugill, A., Adam, J., Chibalina, M. V., Galvanovskis, J., Godazgar, M., Lee, S., Goldsworthy, M., Salehi, A., Tarasov, A. I., Rosengren, A. H., Cox, R., & Rorsman, P. (2016). Increased expression of the diabetes gene SOX4 reduces insulin secretion by impaired fusion pore expansion. *Diabetes*. https://doi.org/10.2337/db15-1489

Courtney, N. A., Bao, H., Briguglio, J. S., & Chapman, E. R. (2019). Synaptotagmin 1 clamps synaptic vesicle fusion in mammalian neurons independent of complexin. *Nature Communications*, *10*(1), 4076. https://doi.org/10.1038/s41467-019-12015-w

Cryan, J. F., & Holmes, A. (2005). Model organisms: The ascent of mouse: Advances in modelling human depression and anxiety. In *Nature Reviews Drug Discovery*. https://doi.org/10.1038/nrd1825

Dannemann, N., Hart, J. R., Ueno, L., & Vogt, P. K. (2010). Phosphatidylinositol 4,5-bisphosphate-specific AKT1 is oncogenic. *International Journal of Cancer*, *127*(1), 239–244. https://doi.org/10.1002/ijc.25012

Daubner, S. C., Le, T., & Wang, S. (2011). Tyrosine hydroxylase and regulation of dopamine synthesis. *Archives of Biochemistry and Biophysics*, *508*(1), 1–12. https://doi.org/10.1016/j.abb.2010.12.017

Emanuele, M., & Chieregatti, E. (2015). Mechanisms of Alpha-Synuclein Action on Neurotransmission: Cell-Autonomous and Non-Cell Autonomous Role. *Biomolecules*, *5*(2), 865–892. https://doi.org/10.3390/biom5020865

Fasshauer, D., Sutton, R. B., Brunger, A. T., & Jahn, R. (1998). Conserved structural features of the synaptic fusion complex: SNARE proteins reclassified as Q- and R-SNAREs. *Proceedings of the National Academy of Sciences of the United States of America*. https://doi.org/10.1073/pnas.95.26.15781

Fenoy, E., Izarzugaza, J. M. G., Jurtz, V., Brunak, S., & Nielsen, M. (2019). A generic deep convolutional neural network framework for prediction of receptor-ligand interactions-NetPhosPan: Application to kinase phosphorylation prediction. *Bioinformatics*.

https://doi.org/10.1093/bioinformatics/bty715

Ferdaoussi, M., Fu, J., Dai, X., Manning Fox, J. E., Suzuki, K., Smith, N., Plummer, G., & MacDonald, P. E. (2017). SUMOylation and calcium control syntaxin-1A and secretagogin sequestration by tomosyn to regulate insulin exocytosis in human ß cells. *Scientific Reports*, *7*(1), 248. https://doi.org/10.1038/s41598-017-00344-z

Ferguson, S. M., & De Camilli, P. (2012). Dynamin, a membrane-remodelling GTPase. *Nature Reviews Molecular Cell Biology*, *13*(2), 75–88. https://doi.org/10.1038/nrm3266

Ferrer-Orta, C., Pérez-Sánchez, M. D., Coronado-Parra, T., Silva, C., López-Martínez, D., Baltanás-Copado, J., Gómez-Fernández, J. C., Corbalán-García, S., & Verdaguer, N. (2017). Structural characterization of the Rabphilin-3A–SNAP25 interaction. *Proceedings of the National Academy of Sciences*, *114*(27), E5343–E5351. https://doi.org/10.1073/pnas.1702542114

Feyder, M., Karlsson, R.-M., Mathur, P., Lyman, M., Bock, R., Momenan, R., Munasinghe, J., Scattoni, M. L., Ihne, J., Camp, M., Graybeal, C., Strathdee, D., Begg, A., Alvarez, V. A., Kirsch, P., Rietschel, M., Cichon, S., Walter, H., Meyer-Lindenberg, A., … Holmes, A. (2010). Association of Mouse Dlg4 (PSD-95) Gene Deletion and Human DLG4 Gene Variation With Phenotypes Relevant to Autism Spectrum Disorders and Williams' Syndrome. *American Journal of Psychiatry*, *167*(12), 1508–1517. https://doi.org/10.1176/appi.ajp.2010.10040484

Fujita, Y., Shirataki, H., Sakisaka, T., Asakura, T., Ohya, T., Kotani, H., Yokoyama, S., Nishioka, H., Matsuura, Y., Mizoguchi, A., Scheller, R. H., & Takai, Y. (1998). Tomosyn: A syntaxin-1-binding protein that forms a novel complex in the neurotransmitter release process. *Neuron*. https://doi.org/10.1016/S0896-6273(00)80472-9

Gao, J., Hirata, M., Mizokami, A., Zhao, J., Takahashi, I., Takeuchi, H., & Hirata, M. (2016). Differential role of SNAP-25 phosphorylation by protein kinases A and C in the regulation of SNARE complex formation and exocytosis in PC12 cells. *Cellular Signalling*, *28*(5), 425–437. https://doi.org/10.1016/j.cellsig.2015.12.014

GE Healthcare. (n.d.). *Glutathione S-transferase (GST) Gene Fusion System*. Retrieved May 18, 2020, from https://www.cytivalifesciences.co.jp/catalog/pdf/DF_28962284AA_GST_Gene_Fusion_System.pdf

Geerts, C. J., Mancini, R., Chen, N., Koopmans, F. T. W., Li, K. W., Smit, A. B., Van Weering, J. R. T., Verhage, M., & Groffen, A. J. A. (2017). Tomosyn associates with secretory vesicles in neurons through its N- and C-terminal domains. *PLoS ONE*. https://doi.org/10.1371/journal.pone.0180912

Geppert, M., Bolshakov, V. Y., Siegelbaum, S. A., Takei, K., De Camilli, P., Hammer, R. E., & Südhof, T. C. (1994). The role of Rab3A in neurotransmitter release. *Nature*, *369*(6480), 493–497. https://doi.org/10.1038/369493a0

Gobé, C., Elzaiat, M., Meunier, N., André, M., Sellem, E., Congar, P., Jouneau, L., Allais-Bonnet, A., Naciri, I., Passet, B., Pailhoux, E., & Pannetier, M. (2019). Dual role of DMXL2 in olfactory information transmission and the first wave of spermatogenesis. *PLOS Genetics*, *15*(2), e1007909. https://doi.org/10.1371/journal.pgen.1007909

Gordon, S. L., Harper, C. B., Smillie, K. J., & Cousin, M. A. (2016). A Fine Balance of Synaptophysin Levels Underlies Efficient Retrieval of Synaptobrevin II to Synaptic Vesicles. *PLOS ONE*, *11*(2), e0149457. https://doi.org/10.1371/journal.pone.0149457

Guang, S., Pang, N., Deng, X., Yang, L., He, F., Wu, L., Chen, C., Yin, F., & Peng, J. (2018). Synaptopathology Involved in Autism Spectrum Disorder. *Frontiers in Cellular Neuroscience*, *12*. https://doi.org/10.3389/fncel.2018.00470

Guček, A., Gandasi, N. R., Omar-Hmeadi, M., Bakke, M., Døskeland, S. O., Tengholm, A., & Barg, S. (2019). Fusion pore regulation by cAMP/Epac2 controls cargo release during insulin exocytosis. *ELife*, *8*. https://doi.org/10.7554/eLife.41711

Guimaraes, J. C., Rocha, M., & Arkin, A. P. (2014). Transcript level and sequence determinants of protein abundance and noise in Escherichia coli. *Nucleic Acids Research*, *42*(8), 4791–4799. https://doi.org/10.1093/nar/gku126

Hall, B., Limaye, A., & Kulkarni, A. B. (2009). Overview: Generation of Gene Knockout Mice. *Current Protocols in Cell Biology*, *44*(1), 19.12.1-19.12.17. https://doi.org/10.1002/0471143030.cb1912s44

Haucke, V., & Kozlov, M. M. (2018). Membrane remodeling in clathrin-mediated endocytosis. *Journal of Cell Science*, *131*(17), jcs216812. https://doi.org/10.1242/jcs.216812

Hodge, R. D., Bakken, T. E., Miller, J. A., Smith, K. A., Barkan, E. R., Graybuck, L. T., Close, J. L., Long, B., Johansen, N., Penn, O., Yao, Z., Eggermont, J., Höllt, T., Levi, B. P., Shehata, S. I., Aevermann, B., Beller, A., Bertagnolli, D., Brouner, K., … Lein, E. S. (2019). Conserved cell types with divergent features in human versus mouse cortex. *Nature*. https://doi.org/10.1038/s41586-019-1506-7

Huang, M., Wang, B., Li, X., Fu, C., Wang, C., & Kang, X. (2019). α-Synuclein: A Multifunctional Player in Exocytosis, Endocytosis, and Vesicle Recycling. *Frontiers in Neuroscience*, *13*. https://doi.org/10.3389/fnins.2019.00028

Huotari, J., & Helenius, A. (2011). Endosome maturation. *The EMBO Journal*, *30*(17), 3481–3500. https://doi.org/10.1038/emboj.2011.286

Jahn, R., & Fasshauer, D. (2012). Molecular machines governing exocytosis of synaptic vesicles. *Nature*, *490*(7419), 201–207. https://doi.org/10.1038/nature11320

Jung, J.-J., Inamdar, S. M., Tiwari, A., & Choudhury, A. (2012). Regulation of intracellular membrane trafficking and cell dynamics by syntaxin-6. *Bioscience Reports*, *32*(4), 383–391. https://doi.org/10.1042/BSR20120006

Kádková, A., Radecke, J., & Sørensen, J. B. (2019). The SNAP-25 Protein Family. *Neuroscience*, *420*, 50–71. https://doi.org/10.1016/j.neuroscience.2018.09.020

Kandel, E. R., Schwartz, J. H., Jessell, H. M., Siegelbaum, S. A., & Hudspeth, A. J. (2013a). Modulation of Synaptic Transmission: Second Messengers. In *Principles of Neural Science* (5th ed.). McGraw-Hill Medical.

Kandel, E. R., Schwartz, J. H., Jessell, H. M., Siegelbaum, S. A., & Hudspeth, A. J. (2013b). Transmitter Release. In *Priciples of Neural Science* (5th ed.). McGraw-Hill Medical.

Khelashvili, G., Galli, A., & Weinstein, H. (2012). Phosphatidylinositol 4,5-Biphosphate (PIP 2) Lipids Regulate the Phosphorylation of Syntaxin N-Terminus by Modulating Both Its Position and Local Structure. *Biochemistry*, *51*(39), 7685–7698. https://doi.org/10.1021/bi300833z

KOMP Allele Types. (n.d.). Retrieved May 18, 2020, from https://www.komp.org/alleles.php

Kondratiuk, I., Jakhanwal, S., Jin, J., Sathyanarayanan, U., Kroppen, B., Pobbati, A. V., Krisko, A.,

Ashery, U., Meinecke, M., Jahn, R., Fasshauer, D., & Milosevic, I. (2020). PI(4,5)P 2 - dependent regulation of exocytosis by amisyn, the vertebrate-specific competitor of synaptobrevin 2. *Proceedings of the National Academy of Sciences*, 201908232. https://doi.org/10.1073/pnas.1908232117

Kozasa, T., Hajicek, N., Chow, C. R., & Suzuki, N. (2011). Signalling mechanisms of RhoGTPase regulation by the heterotrimeric G proteins G12 and G13. In *Journal of Biochemistry*. https://doi.org/10.1093/jb/mvr105

Lamouroux, A., Vigny, A., Faucon Biguet, N., Darmon, M. C., Franck, R., Henry, J. P., & Mallet, J. (1987). The primary structure of human dopamine-beta-hydroxylase: insights into the relationship between the soluble and the membrane-bound forms of the enzyme. *The EMBO Journal*, *6*(13), 3931–3937. http://www.ncbi.nlm.nih.gov/pubmed/3443096

Lemmon, M. A. (2007). Pleckstrin homology (PH) domains and phosphoinositides. *Biochemical Society Symposium*, *74*(1), 81. https://doi.org/10.1042/BSS0740081

Lenka, G., Tsai, M. H., Lin, H. C., Hsiao, J. H., Lee, Y. C., Lu, T. P., Lee, J. M., Hsu, C. P., Lai, L. C., & Chuang, E. Y. (2017). Identification of methylation-driven, differentially expressed STXBP6 as a novel biomarker in lung adenocarcinoma. *Scientific Reports*. https://doi.org/10.1038/srep42573

Lodish, H., Berk, A., Zipursky, S. L., Matsudaira, P., Baltimore, D., & Darnell, J. (2000a). Neurotransmitters, Synapses, and Impulse Transmission. In *Molecular Cell Biology* (4th ed.). W. H. Freeman. https://www.ncbi.nlm.nih.gov/books/NBK21521/

Lodish, H., Berk, A., Zipursky, S. L., Matsudaira, P., Baltimore, D., & Darnell, J. (2000b). Overview of the Neuron Structure and Function. In *Molecular Cell Biology* (4th ed.). W. H. Freeman. https://www.ncbi.nlm.nih.gov/books/NBK21535/

Lonart, G. (2002). RIM1: an edge for presynaptic plasticity. *Trends in Neurosciences*, *25*(7), 329–332. https://doi.org/10.1016/S0166-2236(02)02193-8

Lowery, L. A., & Sive, H. (2009). Totally tubular: the mystery behind function and origin of the brain ventricular system. *BioEssays*, *31*(4), 446–458. https://doi.org/10.1002/bies.200800207

Ludwig, P. E., & Varacallo, M. (2020). *Neuroanatomy, Central Nervous System (CNS)*. StatPearls Publishing. https://www.ncbi.nlm.nih.gov/books/NBK442010/

Madeo, M., Kovács, A. D., & Pearce, D. A. (2014). The Human Synaptic Vesicle Protein, SV2A, Functions as a Galactose Transporter in Saccharomyces cerevisiae. *Journal of Biological Chemistry*, *289*(48), 33066–33071. https://doi.org/10.1074/jbc.C114.584516

Madera-Salcedo, I. K., Danelli, L., Tiwari, N., Dema, B., Pacreau, E., Vibhushan, S., Birnbaum, J., Agabriel, C., Liabeuf, V., Klingebiel, C., Menasche, G., Macias-Silva, M., Benhamou, M., Charles, N., González-Espinosa, C., Vitte, J., & Blank, U. (2018). Tomosyn functions as a PKCδ-regulated fusion clamp in mast cell degranulation. *Science Signaling*, *11*(537), eaan4350. https://doi.org/10.1126/scisignal.aan4350

Mason, P. (2017a). Neurotransmitter Release. In *Medical Neurobiology* (2nd ed.). Oxford University Press. http://oxfordmedicine.com/view/10.1093/med/9780190237493.001.0001/med-9780190237493-chapter-11

Mason, P. (2017b). Receiving the Synaptic Message. In *Medical Neurobiology* (2nd ed.). Oxford University Press. http://oxfordmedicine.com/view/10.1093/med/9780190237493.001.0001/med-9780190237493-chapter-13

Mason, P. (2017c). Synthesis, Packaging, and Termination of Neurotransmitters. In *Medical Neurobiology* (2nd ed.). Oxford University Press. https://doi.org/10.1093/med/9780190237493.003.0012

Matta, S., Van Kolen, K., da Cunha, R., van den Bogaart, G., Mandemakers, W., Miskiewicz, K., De Bock, P.-J., Morais, V. A., Vilain, S., Haddad, D., Delbroek, L., Swerts, J., Chávez-Gutiérrez, L., Esposito, G., Daneels, G., Karran, E., Holt, M., Gevaert, K., Moechars, D. W., … Verstreken, P. (2012). LRRK2 Controls an EndoA Phosphorylation Cycle in Synaptic Endocytosis. *Neuron*, *75*(6), 1008–1021. https://doi.org/10.1016/j.neuron.2012.08.022

Mayorga, A. J., & Lucki, I. (2001). Limitations on the use of the C57BL/6 mouse in the tail suspension test. *Psychopharmacology*, *155*(1), 110–112. https://doi.org/10.1007/s002130100687

McCain, J. (2013). The MAPK (ERK) Pathway: Investigational Combinations for the Treatment Of BRAF-Mutated Metastatic Melanoma. *P & T : A Peer-Reviewed Journal for Formulary Management*, *38*(2), 96–108. http://www.ncbi.nlm.nih.gov/pubmed/23599677

Merck. (2014). *pGEX Vectors*. https://www.sigmaaldrich.com/technical-documents/protocols/biology/gst-gene-fusion-system/pgex-vectors.html

Meyers, R. A. (1995). Expression Systems for DNA Processes. In *Molecular Biology and Biotechnology: A Comprehensive Desk Reference*. Wiley-VCH.

Milosevic, I., Giovedi, S., Lou, X., Raimondi, A., Collesi, C., Shen, H., Paradise, S., O'Toole, E., Ferguson, S., Cremona, O., & De Camilli, P. (2011). Recruitment of Endophilin to Clathrin-Coated Pit Necks Is Required for Efficient Vesicle Uncoating after Fission. *Neuron*, *72*(4), 587–601. https://doi.org/10.1016/j.neuron.2011.08.029

Mochida, S. (2015). Regulatory Role of Tomosyn in Synaptic Vesicle Fusion. In *Presynaptic Terminals*. Springer Japan. https://doi.org/10.1007/978-4-431-55166-9

Mohanasundaram, P., & Shanmugam, M. M. (2010). Role of Syntaxin 4 in Activity-Dependent Exocytosis and Synaptic Plasticity in Hippocampal Neurons. *Science Signaling*, *3*(144), jc7–jc7. https://doi.org/10.1126/scisignal.3144jc7

Müsch, A. (2014). Vesicular Transport in the Secretory and Endocytic Pathways. *Colloquium Series on Building Blocks of the Cell: Cell Structure and Function*, *2*(3), 1–125. https://doi.org/10.4199/C0011ED1V01Y201407BBC008

National Institutes of Health (US), & Biological Sciences Curriculum Study. (2007). Information about the Brain. In *NIH Curriculum Supplement Series*. National Institutes of Health (US). https://www.ncbi.nlm.nih.gov/books/NBK20367/

Nora, L. C., Westmann, C. A., Martins-Santana, L., Alves, L. de F., Monteiro, L. M. O., Guazzaroni, M.-E., & Silva-Rocha, R. (2019). The art of vector engineering: towards the construction of next-generation genetic tools. *Microbial Biotechnology*, *12*(1), 125–147. https://doi.org/10.1111/1751-7915.13318

Okashah, N., Wan, Q., Ghosh, S., Sandhu, M., Inoue, A., Vaidehi, N., & Lambert, N. A. (2019).

Variable G protein determinants of GPCR coupling selectivity. *Proceedings of the National Academy of Sciences*, 201905993. https://doi.org/10.1073/pnas.1905993116

Park, S., Bin, N.-R., Yu, B., Wong, R., Sitarska, E., Sugita, K., Ma, K., Xu, J., Tien, C.-W., Algouneh, A., Turlova, E., Wang, S., Siriya, P., Shahid, W., Kalia, L., Feng, Z.-P., Monnier, P. P., Sun, H.-S., Zhen, M., … Sugita, S. (2017). UNC-18 and Tomosyn Antagonistically Control Synaptic Vesicle Priming Downstream of UNC-13 in Caenorhabditis elegans. *The Journal of Neuroscience*, *37*(36), 8797–8815. https://doi.org/10.1523/JNEUROSCI.0338-17.2017

Pettitt, S. J., Liang, Q., Rairdan, X. Y., Moran, J. L., Prosser, H. M., Beier, D. R., Lloyd, K. C., Bradley, A., & Skarnes, W. C. (2009). Agouti C57BL/6N embryonic stem cells for mouse genetic resources. *Nature Methods*, *6*(7), 493–495. https://doi.org/10.1038/nmeth.1342

Purves, D., Augustine, G. J., Fitzpatrick, D., Hall, W. C., Mooney, A.-S. L. R. D., Platt, M. L., & White, L. E. (2018a). Molecular Signaling within Neurons. In *Neuroscience* (6th ed.). Sinauer Associates.

Purves, D., Augustine, G. J., Fitzpatrick, D., Hall, W. C., Mooney, A.-S. L. R. D., Platt, M. L., & White, L. E. (2018b). Neurotransmitters and Their Receptors. In *Neuroscience* (6th ed.). Sinauer Associates.

Purves, D., Augustine, G. J., Fitzpatrick, D., Hall, W. C., Mooney, A.-S. L. R. D., Platt, M. L., & White, L. E. (2018c). Synaptic Plasticity. In *Neuroscience* (6th ed.). Sinauer Associates.

Purves, D., Augustine, G. J., Fitzpatrick, D., Hall, W. C., Mooney, A.-S. L. R. D., Platt, M. L., & White, L. E. (2018d). Synaptic Transmission. In *Neuroscience* (6th ed.). Sinauer Associates.

Purves, D., Augustine, G. J., Fitzpatrick, D., Katz, L. C., LaMantia, A.-S., McNamara, J. O., & Williams, S. M. (2001). Electrical Synapses. In *Neuroscience* (2nd ed.). Sinauer Associates. https://www.ncbi.nlm.nih.gov/books/NBK11164/

Ramamoorthy, P., & Whim, M. D. (2008). Trafficking and Fusion of Neuropeptide Y-Containing Dense-Core Granules in Astrocytes. *Journal of Neuroscience*, *28*(51), 13815–13827. https://doi.org/10.1523/JNEUROSCI.5361-07.2008

Rizzoli, S. O. (2014). Synaptic vesicle recycling: Steps and principles. In *EMBO Journal*. https://doi.org/10.1002/embj.201386357

Rosano, G. L., & Ceccarelli, E. A. (2014). Recombinant protein expression in Escherichia coli: advances and challenges. *Frontiers in Microbiology*, *5*. https://doi.org/10.3389/fmicb.2014.00172

Salpietro, V., Dixon, C. L., Guo, H., Bello, O. D., Vandrovcova, J., Efthymiou, S., Maroofian, R., Heimer, G., Burglen, L., Valence, S., Torti, E., Hacke, M., Rankin, J., Tariq, H., Colin, E., Procaccio, V., Striano, P., Mankad, K., Lieb, A., … Houlden, H. (2019). AMPA receptor GluA2 subunit defects are a cause of neurodevelopmental disorders. *Nature Communications*, *10*(1), 3094. https://doi.org/10.1038/s41467-019-10910-w

Salpietro, V., Malintan, N. T., Llano-Rivas, I., Spaeth, C. G., Efthymiou, S., Striano, P., Vandrovcova, J., Cutrupi, M. C., Chimenz, R., David, E., Di Rosa, G., Marce-Grau, A., Raspall-Chaure, M., Martin-Hernandez, E., Zara, F., Minetti, C., Bello, O. D., De Zorzi, R., Fortuna, S., … Houlden, H. (2019). Mutations in the Neuronal Vesicular SNARE VAMP2 Affect Synaptic Membrane Fusion and Impair Human Neurodevelopment. *The American Journal of Human Genetics*, *104*(4), 721–730. https://doi.org/10.1016/j.ajhg.2019.02.016

Scales, S. J., Hesser, B. A., Masuda, E. S., & Scheller, R. H. (2002). Amisyn, a novel syntaxin-binding protein that may regulate SNARE complex assembly. *Journal of Biological Chemistry*. https://doi.org/10.1074/jbc.M204929200

Schonn, J.-S., Van Weering, J. R. T., Mohrmann, R., Schlüter, O. M., Südhof, T. C., De Wit, H., Verhage, M., & Sørensen, J. B. (2010). Rab3 Proteins Involved in Vesicle Biogenesis and Priming in Embryonic Mouse Chromaffin Cells. *Traffic*, *11*(11), 1415–1428. https://doi.org/10.1111/j.1600-0854.2010.01107.x

Schrödinger LLC. (n.d.). *The PyMOL Molecular Graphics System*.

Scott, C. C., Vacca, F., & Gruenberg, J. (2014). Endosome maturation, transport and functions. *Seminars in Cell & Developmental Biology*, *31*, 2–10. https://doi.org/10.1016/j.semcdb.2014.03.034

Shen, W., Kilander, M. B. C., Bridi, M. S., Frei, J. A., Niescier, R. F., Huang, S., & Lin, Y. C. (2020). Tomosyn regulates the small RhoA GTPase to control the dendritic stability of neurons and the surface expression of AMPA receptors. *Journal of Neuroscience Research*. https://doi.org/10.1002/jnr.24608

Shin, O.-H. (2014). Exocytosis and Synaptic Vesicle Function. In *Comprehensive Physiology* (pp. 149–175). John Wiley & Sons, Inc. https://doi.org/10.1002/cphy.c130021

Skarnes, W. C., Rosen, B., West, A. P., Koutsourakis, M., Bushell, W., Iyer, V., Mujica, A. O., Thomas, M., Harrow, J., Cox, T., Jackson, D., Severin, J., Biggs, P., Fu, J., Nefedov, M., de Jong, P. J., Stewart, A. F., & Bradley, A. (2011). A conditional knockout resource for the genome-wide study of mouse gene function. *Nature*, *474*(7351), 337–342. https://doi.org/10.1038/nature10163

Snyder, D. A., Kelly, M. L., & Woodbury, D. J. (2006). SNARE Complex Regulation by Phosphorylation. *Cell Biochemistry and Biophysics*, *45*(1), 111–124. https://doi.org/10.1385/CBB:45:1:111

Sorond, F. A., & Gorelick, P. B. (2019). Brain White Matter: A Substrate for Resilience and a Substance for Subcortical Small Vessel Disease. *Brain Sciences*, *9*(8), 193. https://doi.org/10.3390/brainsci9080193

Stankiewicz, T. R., & Linseman, D. A. (2014). Rho family GTPases: key players in neuronal development, neuronal survival, and neurodegeneration. *Frontiers in Cellular Neuroscience*, *8*. https://doi.org/10.3389/fncel.2014.00314

Südhof, T. C. (2012). The presynaptic active zone. In *Neuron*. https://doi.org/10.1016/j.neuron.2012.06.012

Sultan, F. (2013). Dissection of Different Areas from Mouse Hippocampus. *BIO-PROTOCOL*, *3*(21). https://doi.org/10.21769/BioProtoc.955

Sun, M., Luong, G., Plastikwala, F., & Sun, Y. (2020). Control of Rab7a activity and localization through endosomal type Igamma PIP 5-kinase is required for endosome maturation and lysosome function. *The FASEB Journal*, *34*(2), 2730–2748. https://doi.org/10.1096/fj.201901830R

Takahashi, M., & Ohnishi, H. (2002). Negative regulation of exocytosis at the nerve terminal. *Molecular Psychiatry*, *7*(6), 536–537. https://doi.org/10.1038/sj.mp.4001050

Takahashi, N., Hamada-Nakahara, S., Itoh, Y., Takemura, K., Shimada, A., Ueda, Y., Kitamata, M., Matsuoka, R., Hanawa-Suetsugu, K., Senju, Y., Mori, M. X., Kiyonaka, S., Kohda, D., Kitao, A., Mori, Y., & Suetsugu, S. (2014). TRPV4 channel activity is modulated by direct interaction of the ankyrin domain to PI(4,5)P2. *Nature Communications*, *5*(1), 4994. https://doi.org/10.1038/ncomms5994

Tan, T. C., Valova, V. A., Malladi, C. S., Graham, M. E., Berven, L. A., Jupp, O. J., Hansra, G., McClure, S. J., Sarcevic, B., Boadle, R. A., Larsen, M. R., Cousin, M. A., & Robinson, P. J. (2003). Cdk5 is essential for synaptic vesicle endocytosis. *Nature Cell Biology*, *5*(8), 701–710. https://doi.org/10.1038/ncb1020

Tao-Cheng, J.-H., Thein, S., Yang, Y., Reese, T. S., & Gallant, P. E. (2014). Homer is concentrated at the postsynaptic density and does not redistribute after acute synaptic stimulation. *Neuroscience*, *266*, 80–90. https://doi.org/10.1016/j.neuroscience.2014.01.066

The UniProt Consortium. (2019). UniProt: a worldwide hub of protein knowledge The UniProt Consortium. *Nucleic Acids Research*. https://doi.org/10.1093/nar/gky1049

Tolias, K. F., Duman, J. G., & Um, K. (2011). Control of synapse development and plasticity by Rho GTPase regulatory proteins. *Progress in Neurobiology*, *94*(2), 133–148. https://doi.org/10.1016/j.pneurobio.2011.04.011

Tortora, G. J., & Derrickson, B. (2017). Nervous Tissue. In *Principles of Anatomy & Physiology* (15th ed.). Wiley.

Trexler, A. J., Sochacki, K. A., & Taraska, J. W. (2016). Imaging the recruitment and loss of proteins and lipids at single sites of calcium-triggered exocytosis. *Molecular Biology of the Cell*, *27*(15), 2423–2434. https://doi.org/10.1091/mbc.e16-01-0057

van den Bogaart, G., Lang, T., & Jahn, R. (2013). Microdomains of SNARE Proteins in the Plasma Membrane. In *Functional Organization of Vertebrate Plasma Membrane* (pp. 193–230). https://doi.org/10.1016/B978-0-12-417027-8.00006-4

Vanlandingham, P. A., & Ceresa, B. P. (2009). Rab7 regulates late endocytic trafficking downstream of multivesicular body biogenesis and cargo sequestration. *The Journal of Biological Chemistry*, *284*(18), 12110–12124. https://doi.org/10.1074/jbc.M809277200

Vyas, Y., & Montgomery, J. (2016). The role of postsynaptic density proteins in neural degeneration and regeneration. *Neural Regeneration Research*, *11*(6). https://doi.org/10.4103/1673-5374.184481

Wang, H., Xu, J., Lazarovici, P., Quirion, R., & Zheng, W. (2018). cAMP Response Element-Binding Protein (CREB): A Possible Signaling Molecule Link in the Pathophysiology of Schizophrenia. *Frontiers in Molecular Neuroscience*, *11*. https://doi.org/10.3389/fnmol.2018.00255

Wang, Z.-W. (2008). Roles of SNARE Proteins in Synaptic Vesicle Fusion. In *Molecular Mechanisms of Neurotransmitter Release*. Humana Press. https://doi.org/10.1007/978-1-59745-481-0

Wayman, G. A., Lee, Y.-S., Tokumitsu, H., Silva, A., & Soderling, T. R. (2008). Calmodulin-Kinases: Modulators of Neuronal Development and Plasticity. *Neuron*, *59*(6), 914–931. https://doi.org/10.1016/j.neuron.2008.08.021

Won, H., Mah, W., & Kim, E. (2013). Autism spectrum disorder causes, mechanisms, and treatments: focus on neuronal synapses. *Frontiers in Molecular Neuroscience*, *6*. https://doi.org/10.3389/fnmol.2013.00019

Xue, Y., Liu, Z., Cao, J., Ma, Q., Gao, X., Wang, Q., Jin, C., Zhou, Y., Wen, L., & Ren, J. (2011). GPS 2.1: Enhanced prediction of kinase-specific phosphorylation sites with an algorithm of motif length selection. *Protein Engineering, Design and Selection*. https://doi.org/10.1093/protein/gzq094

Yuan, W., & Song, C. (2020). The Emerging Role of Rab5 in Membrane Receptor Trafficking and Signaling Pathways. *Biochemistry Research International*, *2020*, 1–10. https://doi.org/10.1155/2020/4186308

Zech, M., Lam, D. D., Weber, S., Berutti, R., Poláková, K., Havránková, P., Fečíková, A., Strom, T. M., Růžička, E., Jech, R., & Winkelmann, J. (2018). A unique de novo gain-of-function variant in CAMK4 associated with intellectual disability and hyperkinetic movement disorder. *Molecular Case Studies*, *4*(6), a003293. https://doi.org/10.1101/mcs.a003293